

NF-1583.02
NONPROPRIETARY VERSION

METHODS OF RECORD
AN LWR FUEL ASSEMBLY BURNUP CODE
TOPICAL REPORT

FEBRUARY 1983

CP&L
Carolina Power & Light Company

8303160418 830310
PDR ADOCK 05000324
P PDR

R E C O R D

AN LWR FUEL ASSEMBLY BURNUP CODE

H.K. Næss
T. Skardhamar*

*Institute for Energy Technology, Kjeller, Norway

NONPROPRIETARY VERSION

TOPICAL REPORT

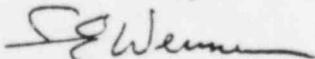
Prepared by

SCANDPOWER INC

4853 Cordell Avenue
Bethesda, Maryland 20814

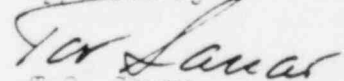
20 January 1983

Reviewed by :



S.E. Wennemo

Approved by :



T.O. Saur

DISCLAIMER OF RESPONSIBILITY

This document was prepared by SCANDPOWER Incorporated on behalf of Carolina Power & Light Company. This document is believed to be completely true and accurate to the best of our knowledge and information. It is authorized for use specifically by Carolina Power & Light Company, SCANDPOWER Incorporated, and/or the appropriate subdivisions within the Nuclear Regulatory Commission only.

With regard to any unauthorized use whatsoever, Carolina Power & Light Company, SCANDPOWER Incorporated, and their officers, directors, agents, and employees assume no liability nor make any warranty or representation with regard to the contents of this document or its accuracy or completeness.

Proprietary information of SCANDPOWER Incorporated is indicated by "bars" drawn in the margin of the text of this report.

ABSTRACT

This report describes the methods of the RECORD computer code, the basis for fundamental models selected, and a review of code qualification against measured data. RECORD is a detailed reactor physics code for performing efficient LWR fuel assembly calculations, taking into account most of the features found in BWR and PWR fuel designs. The code calculates neutron spectrum, reaction rates and reactivity as a function of fuel burnup, and generates the few-group data required by full scale core simulators.

METHODS OF RECORD
AN LWR FUEL ASSEMBLY BURNUP CODE

C O N T E N T S

	<u>Page</u>
ABSTRACT	
1. INTRODUCTION	1-1
2. SUMMARY DESCRIPTION AND MAIN FEATURES OF RECORD	2-1
2.1 Nature of Physical Problem Solved	2-1
2.2 Method of Solution	2-2
2.3 Nuclear Data Library	2-6
2.4 Main Features of Code	2-8
2.5 Data Generation Unit of FMS	2-12
2.6 Computer Requirements	2-15
3. THERMAL SPECTRUM AND FEW-GROUP DATA	3-1
3.1 Fundamental Equations	3-2
3.2 Flux Disadvantage Factor Calculation	3-4
3.3 Spectrum Calculation	3-7
3.4 Scattering Models	3-9
3.5 Point Energy Approach	3-10
3.6 Macrogroup Data	3-13

	<u>Page</u>
4. EPITHERMAL SPECTRUM AND FEW-GROUP DATA	4-1
4.1 Fundamental Equations	4-1
4.2 Treatment of Resonance Absorption and Fission	4-6
4.3 Fast Advantage Factor	4-15
4.4 Macrogroup Data	4-17
5. TREATMENT OF BURNABLE POISON	5-1
5.1 The THERMOS - GADPOL Method	5-1
5.2 Gadolinium Treatment	5-2
5.3 Shim Rod (Boron glass) Treatment	5-4
6. CONTROL ABSORBES	6-1
6.1 Control Blades - BWR Option	6-1
6.2 Rod Cluster Control - PWR Option	6-6
7. TWO-DIMENSIONAL FLUX AND POWER DISTRIBUTION	7-1
7.1 Multigroup Diffusion Equation	7-1
7.2 Geometry and Mesh Descriptions	7-2
7.3 Difference Equations	7-3
7.4 Method of Solution	7-4
8. BURNUP CALCULATIONS	8-1
8.1 Fuel Burnup Chains	8-1
8.2 Fission Product Representation	8-2
8.3 Solution of Burnup Equations	8-3
9. OTHER FEATURES OF RECORD	9-1
9.1 TIP Instrumentation Factors	9-1
9.2 Delayed Neutron Parameters	9-2

	<u>Page</u>
10. CODE QUALIFICATION	10-1
10.1 Analysis of Clean Critical UO_2 and UO_2/PuO_2 Lattices	10-2
10.2 Fuel Depletion Isotopic Analysis Comparisons . . .	10-5
10.3 Gamma Scan Comparisons of BWR Assembly Pin-Power Distributions	10-5
10.4 Historical Review of LWR Analyses with RECORD - PRESTO	10-8
11. REFERENCES	11-1

APPENDICES :

- A Breit-Wigner Formula for Cross-Section Calculations
- B Output Options in the Record Code
- C Excerpts from RECORD Output

1. INTRODUCTION

In the design and operation of a Light Water Reactor (LWR), there exists a need for performing, in a routine way, the complicated reactor physics calculations necessary for the accurate analysis of LWR fuel assemblies, and to generate directly the few-group data required for use in reactor simulation and fuel management calculations. Answers to reactor operation or design problems should be obtained quickly and efficiently from basic geometric and material specification of fuel assembly and control system, together with operating conditions and burnup requirements, and with a minimum of time consuming work in data preparation and data transfer between different codes.

The code RECORD has been developed to meet the requirements of performing efficient LWR calculations, taking into account most of the complex features which arise in BWR and PWR fuel designs, and treating these with sufficient detail to ensure necessary accuracy. RECORD calculates neutron spectra, group data and reactivity as function of fuel burnup in LWR fuel assemblies. Reaction rates, power and burnup distributions in two dimensions are calculated with individual treatment of each fuel pin, and taking into account effects of control absorbers, burnable poison rods, soluble poison, voids, and other heterogeneities which may be present. Of importance also are flexible restart options which enable straight-forward calculations to be performed at low-power conditions, and of differential effects during burnup. More over, RECORD is a User-oriented code, with an easily applied input, and provides clear and precise output listings in accordance with flexible output options.

The development of the RECORD code is intimately connected with the development of Scandpower's Fuel Management System (FMS), an integrated code system for fuel management and core performance calculations in Light Water Reactors (Ref. 1). The basic units of this system are shown in

Figure 1.0.1. RECORD represents the data generation unit supplying, through a data bank, the necessary reactor physics data to the macroscopic codes of FMS. In particular, RECORD generates the few-group data and coefficients to the PRESTO Code (Refs. 2, 3), which is the 3-dimensional reactor simulator of FMS.

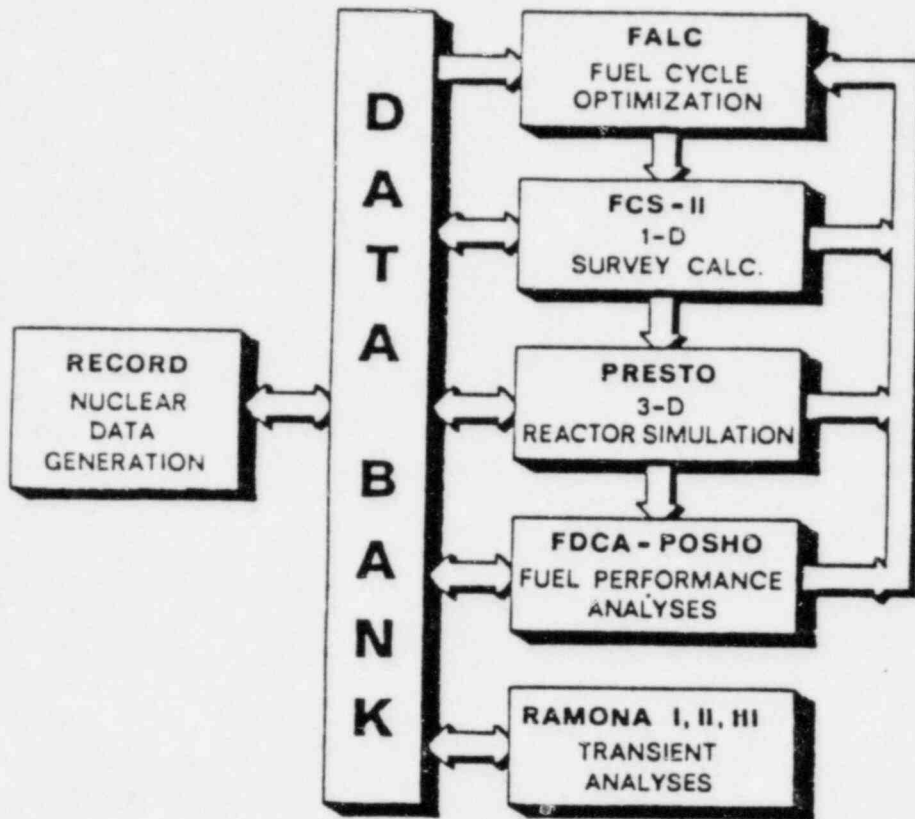
The RECORD Code and FMS have been under development since about 1969, with first commercial applications in 1972. The code has been in routine use since then. Through the years, RECORD has been subject to continuous revisions and extensions, with the introduction of model improvements to increase code accuracy and effectiveness, and incorporation of new options and features as needs have arisen. Users of RECORD have been Utilities and consultants in Europe and USA. Of particular importance in the development of RECORD and FMS, has been the active cooperation of reactor operators in providing feedback of information from actual reactor operating data from many different LWRs. The exchange of results and experiences between code developers and code Users has been of utmost importance in bringing the RECORD code to its present high level of accuracy and performance.

The basic assumptions and theoretical models on which the code is based have been validated through extensive applications of the code by many Users through the years in evaluation calculations, in project calculations, and data bank generation for PRESTO and other FMS codes. Reference 4 gives a review of some of the experiences accumulated through these years, using RECORD and PRESTO in the simulation of LWR cores. Experiences in using RECORD-generated cross-section data base in BWR transient analysis with the RAMONA codes are discussed in some detail in Reference 5. In such analyses, it is of particular importance to be able to model correctly during burnup, the coolant density (void) dependence of cross-sections, as well as effects due to fuel and moderator temperature variations.

This report provides a description of the main features of RECORD, and the physical assumptions on which the code is based. The basic physical models can be regarded as being well established and are not expected to be changed radically within the present concept of the code. In any large code system like RECORD, however, there will always be room for further refinements and

improvements, or introduction of new desirable features, as needs become defined through the accumulated experience of past and future applications of the code. Unless stated otherwise, the description of RECORD in this report applies to the 1981 production version of the code. A detailed program description, including description of input and output of the code, is otherwise given in the FMS Documentation System (Ref. 6), available to Users, and in various internal reports (e.g., Refs. 7 and 8).

After a summary description of the code and its main features, the report describes in detail the distinct models for the thermal and epithermal neutron spectra and group data calculation. A satisfactory model for the treatment of burnable poison is very essential for present LWR designs, and a chapter is devoted to the description of the THERMOS-GADPOL model used in RECORD. The treatment of control absorbers, and calculation of flux/power distributions and fuel burnup are described in subsequent chapters. Also described are the methods of RECORD in calculating TIP instrumentation factors, and delayed neutron parameters for application in neutron kinetic codes. A review of some of the analyses on which the code qualification is based is given in Chapter 10.



FMS

SCP'S FUEL MANAGEMENT SYSTEM

FIGURE 1.0.1 The FMS Code System for Light Water Reactor Calculations

2. SUMMARY DESCRIPTION AND MAIN FEATURES OF RECORD

RECORD performs reactor physics calculations on BWR and PWR fuel assemblies, and generates data banks containing required few-group data, isotopic densities and other nuclear data for use by core simulators, such as PRESTO and other codes of the Fuel Management System, FMS. It is a production code, implying that these calculations can be performed directly and efficiently, and where system efficiency is viewed both in terms of computer resources as well as manpower needed to prepare input data and to digest the output.

This chapter summarizes the basic physical principles and features of the RECORD code. The physical models are described in more detail in the ensuing chapters of the report.

2.1 Nature of Physical Problem Solved

RECORD determines reactivity, reaction rates, power and burnup distributions in two dimensions across an LWR fuel assembly. Typical BWR and PWR configurations are indicated in excerpts of code printouts, as shown in Figures 2.1.1 and 2.1.2. The code can also treat internal water-cross fuel with geometry as indicated in Figure 2.1.3. The solution area on which calculations are performed is the fuel assembly, together with the associated surrounding water gaps. The fuel is composed of cylindrical rods in a square regular array embedded in the water moderator. In BWRs, the lattice cells are surrounded by a flow box region, where the code always treats the whole assembly geometry. In PWRs, 1/4-assembly symmetry option must be assumed in most real cases.

Each lattice position defines, in general, a fuel pin cell composed of one fuel rod and its surrounding moderator. Some positions may be empty (water holes) or, in PWRs, may be occupied by rod cluster control rod fingers or burnable poison shim rods. RECORD thus takes into account perturbations due to control absorbers within the assembly, as well as those which may be inserted in the surrounding water gaps. The code is specifically designed to handle directly the heterogeneities which arise in LWR designs, such as variable fuel enrichments and dimensions, burnable poison (gadolinium) pins,

burnable absorber (boron) shim rods, water holes, and soluble poison and voids in the moderator.

An example of a typical BWR configuration treated directly by RECORD is given in Figure 2.1.4. The Figure shows the solution area on which calculations are performed, and typical region divisions within that area.

2.2 Method of Solution

In development of RECORD, the aim has been, at all times, to achieve as far as possible a balanced system with respect to the detail adopted in describing the physical processes occurring in an LWR fuel assembly. The degree of sophistication adopted for the different models depends on the importance of physical events occurring, and their sensitivity to the accuracy aimed at in the final results. The modelling, in turn, has to be balanced against computer costs (running times, core storage, etc.), to be within limits acceptable for an efficient production code for extensive use in a wide range of calculations.

This section outlines the method of solution made in the RECORD code for solving the physical problems of determining group data and other characteristics of LWR fuel assemblies as function of fuel burnup. The modelling has been critically appraised in relation to the usage of the code, and required accuracies. Systematic validation of methods against experimental data from lattice experiments, from reactor operating data, and from comparisons with more detailed codes, form the basis of confidence in the physical models adopted in RECORD. The descriptions given here are brief summaries only, and the different models are described in more detail in the following chapters.

2.2.1 Neutron Spectrum Calculation

The thermal energy range in RECORD is taken to extend up to 1.84 eV (thus including the large resonances in Pu²³⁹ and Pu²⁴⁰), where neutron thermalization is treated by a transport theory approach with point energy representation (Refs. 9, 10), and where the Nelkin scattering model is applied

(Ref. 11). The thermal spectrum for fuel, clad and moderator regions are determined for each fuel pin cell in the assembly lattice, and are recalculated after given burnup intervals, being functions of the isotopic concentrations reached at any given time in each fuel pin. These spectra are obtained from energy-dependent flux disadvantage factors calculated for each pin cell, using a modified Amouyal-Benoist method (Ref. 12), together with a homogeneous pin cell spectrum, calculated for an average pin cell representative of the spectrum region where the given pin cell is situated. The fuel pins are grouped into a number of thermal spectrum regions, depending on their spectral environment.

In the epithermal energy region, the neutron spectrum is calculated, using a multigroup B-1 or P-1 approximation with extended Greuling-Goertzel slowing down (Ref. 13). The epithermal spectrum is calculated for an average pin cell representative of the whole assembly cell, and is assumed to be space-independent over the fuel assembly. This spectrum is generally recalculated during burnup at the same states at which the thermal spectrum calculation is performed. Resonance absorbers are treated by means of lattice resonance integrals, calculated from total single-pin resonance integrals and modified by resonance distribution functions for each energy group, and by shielding factors taking into account the influence of the lattice on the resonance absorption in each fuel pin.

2.2.2 Burnable Poison

Highly absorbing cells, such as burnable poison (gadolinium) fuel pins or burnable absorber (boron) shim rods, require more detailed transport theory calculations for correct predictions of reaction rates. Such cells are treated by the THERMOS - GADPOL System, two auxiliary codes to RECORD, which include a burnup version of the THERMOS code (Refs. 14, 15). These generate required effective thermal group data, which are read into RECORD as function of void (or boron concentration), plutonium content and time integrated thermal flux (Ref. 16). The data transfer between THERMOS, GADPOL and RECORD is automated via disc files.

2.2.3 Cell Homogenization

The code identifies as distinct diffusion subregions, each fuel pin cell in the assembly, each water hole or shim rod cell, and water gaps and flow box regions. The lattice cell (unit cell) areas are defined by the lattice pitch, being equal to the square of the pitch for most cells of a given fuel assembly. The flow area within the flow box not included in this way in the lattice cell areas in a BWR assembly (i.e., eventual inner water gap), is generally added to the moderator area associated with the edge lattice cells. Similarly, the area of the very narrow water gap, usually present in PWR geometry, is generally included in the edge lattice cell moderator areas. The other region divisions in the assembly cell depend on the configuration geometry (e.g., Fig. 2.1.4). In usual applications of RECORD, the code lays out the mesh spacings and region divisions automatically, depending on the case data.

Macroscopic five-group data (two thermal and three epithermal groups) are calculated for each region from the isotopic concentrations, and by effectively integrating the isotopic cross-sections over the spectrum calculated for each region. These data are then used in the diffusion calculation over the fuel assembly, and in the subsequent assembly homogenization calculations. Pinwise microscopic five-group cross-sections for all fuel isotopes used in the calculations of fuel burnup are also determined for the lattice cells.

2.2.4 Control Rods

Cruciform control rods, either solid blade or rodded blade design, or cluster control rods (RCC), are treated as nondiffusion subregions and are defined by boundary conditions applied at the absorber surfaces. These boundary conditions are current-to-flux ratios, calculated from transport theory reflection and transmission probabilities of isotropic and linearly anisotropic flux components (Ref. 17), together with special treatment of high resonance isotopes (Ref. 18). Both boron based and Ag-In-Cd based control elements can be treated directly by the code.

2.2.5 Spatial Calculations

The flux distribution across fuel assembly and adjacent water gaps, and eigenvalue or k_{eff} of the system, are obtained by solving the five-group, two-dimensional diffusion equations in x-y geometry, using a fast overrelaxation iterative procedure, combined with a periodic use of coarse-mesh-group rebalancing (Ref. 19). A modified Wielandt technique is used to give fast convergence. Five-group diffusion theory with two thermal and three epithermal groups, and with up-scattering in the lowest thermal group, is found to be a minimum for adequate spatial representation of a fuel assembly.

The mesh grid, imposed on the solution area, defines the mesh points at which the macrogroup diffusion fluxes are determined. The diffusion calculations utilize the regionwise group data from the neutron spectrum and cell homogenization calculations, and the boundary conditions from the control rod calculations. From the mesh point fluxes are derived normalized average group fluxes for all regions used in the subsequent assembly homogenization calculations, and in the calculation of power distributions and fuel burnup.

2.2.6 Assembly Homogenization

Assembly averaged five- and two-group data are obtained by further averaging the regionwise group data over volume and group fluxes from the spatial calculation. This gives assembly-averaged, few-group fission and removal cross-sections, as well as diffusion coefficients. The assembly-averaged absorption cross-sections are subsequently obtained from the neutron balance equations and the eigenvalue of the diffusion calculation. Here the assembly unit is considered as the fuel assembly, together with the associated surrounding water gap.

2.2.7 Burnup Model

The fuel burnup chains assumed in RECORD are the chains starting at U^{235} and U^{238} , and where the main trans-plutonium isotopes americium and curium are explicitly represented. These chains are shown in Figure 8.1.1. The fission

products are treated by a scheme consisting of 12 fission products in six chains, and four pseudo fission products (Ref. 20), as shown in Figure 8.2.1. Calculation of fuel burnup is based on an analytical solution of the burnup differential equations for each fuel pin in an assembly. After each burnup interval, new spectrum calculation, cell-homogenization, spatial calculation, and assembly homogenization are made.

2.2.8 Assembly Environment Problems, Four-Assembly Calculations

The solution area in a RECORD calculation is a two-dimensional representation of an LWR fuel assembly and surrounding water gap. Effect of assembly environment is obtained by defining appropriate boundary conditions at the outer edges of the solution area. When control absorbers are present in the water gap, the required boundary conditions are usually determined directly by the code. Zero current boundaries are otherwise generally assumed, but for some calculations, different sets of five-group current-to-flux ratios at each outer edge may be defined. Axial leakage is represented by an input buckling parameter.

RECORD may be coupled to a large, two-dimensional diffusion code, MD2 (Ref. 19), such that five-group, four-assembly calculations, with explicit representation of all lattice cells at any burnup state for each assembly, can be performed when required and with a minimum of manual data preparation.

2.3 Nuclear Data Library

The Nuclear Data Library contains the microscopic cross-sections and resonance integral data for nuclides which may be needed in the spectrum and group data calculation by RECORD. These data have been processed mainly from the basic ENDF/B-III data files. Other data contained in the library include neutron production parameters for the fissile nuclides, normalized fission spectrum, inelastic scattering matrix data, and delayed neutron data. The library consists of two parts: a library for the thermal data, and one for the epithermal data, respectively.

2.3.1 Thermal Cross-Sections

In RECORD, the thermal energy range extends up to 1.84 eV, and the thermal absorption and fission cross-sections for non- $1/v$ nuclides are represented in the library at 180 energy points (equidistant in velocity units). The cross-sections at these points for nuclides showing non- $1/v$ behavior are obtained either by linear interpolation of the energy-dependent cross-sections, or calculated directly from the resonance parameters in ENDF/B-III, applying the single-level Breit-Wigner formula. Details of the methods used in these calculations are given in Reference 20 and in Appendix A. For nuclides with a $1/v$ -dependent cross-section, only the 2200 m/s value is required in the RECORD library. These values were obtained from ENDF/B-III whenever possible; otherwise, for some fission products, from Reference 21. The elastic scattering cross-sections are generally assumed to be constant in the thermal energy region but may, where resonance parameters are given in the ENDF/B-III file, also be calculated from the single-level Breit-Wigner formula, and are tabulated in the library at 60 equidistant velocity (energy) points.

The point energy model in RECORD uses 15 fixed energy points (Table 3.5.1), and the required cross-section data for each needed nuclide are interpolated by the code from the data on the library file.

2.3.2 Epithermal Cross-Sections

In RECORD, 35 energy groups are used to describe the epithermal region, which is defined in the energy range 10 MeV to 1.84 eV. The absorption, fission and scattering cross-sections for these groups, are primarily evaluated from resonance parameters and/or smooth cross-sections given in ENDF/B-III, using single or multi-level Breit-Wigner formalism, applying the Finnish processing code ETOF (Ref. 22). The ETOF code, which is based on ETOM-1 (Ref. 23), but with several modifications, derives point cross-sections for absorption, fission and scattering, and the group-averaged cross-sections are then calculated assuming a $1/E$ spectrum in the epithermal energy region. Also calculated for each energy group, are the averaged anisotropic elastic scattering cross-section, the slowing down cross-

section, and inelastic scattering cross-section for each nuclide. Where fission product data are not available in ENDF/B, the group cross-sections are obtained from Reference 21 by linear interpolation.

The epithermal group structure in RECORD is fixed (Table 4.1.1), and the 35-group data are tabulated for each nuclide for direct application by RECORD, depending on the nuclides present in any given case.

2.3.3 Resonance Integral Data

The Nuclear Data Library also contains data for use in the treatment of resonance capture in uranium and plutonium isotopes. This comprises data for evaluating the single-pin total resonance absorption and fission integrals, as well as resonance distribution functions, giving the fraction of the resonance integral which is contained in the different epithermal groups. The distribution functions take into account the variation in resonance absorption and fission distribution for different lattices, and have been precalculated as function of pin-cell geometry, isotopic composition and fuel temperature, depending on the different isotopes. In running a case, RECORD will select from the library those functions which are most appropriate for a given lattice.

2.4 Main Features of Code

Some of the more important, general features of RECORD, as distinct from solution methods, are outlined in this section.

2.4.1 Integrated Code System

RECORD is an integrated code system, consisting of component codes which operate efficiently together via a processing and steering system, and which reads and generates data files and calls upon and transfers data between the different units of the code, depending upon the case under consideration. The processing and steering system is automatic and depends only upon case input data. Efficiency and accuracy in using the code is

ensured through a minimum of manual data transfer and computer time. A simplified schematic outline of RECORD is given in Figure 2.4.1.

2.4.2 User-Oriented Features

Considerable effort has gone into making RECORD a User-oriented code, with respect to input specification and output listings. This is of importance, not only for ease in using the code, but also in connection with Quality Assurance in performing the necessary reactor physics calculations. High standard in input description and other code documentation, and clear, readable output listings greatly facilitate avoidance, as well as detection, of invalid calculations due to input errors. Erroneous runs not only increase calculation costs, but may have potentially large economic consequences if faulty results form the basis for decision making in reactor operation and fuel reload strategies. If errors enter design calculations, safety implications may also be involved. The input and output of a production code used for these calculations must be clearly auditable and verifiable.

2.4.3 Input Specification

The input data to RECORD is designed such that the User, as far as possible, need only specify his problem in usual engineering terms, as regards geometry, material composition, operation data, etc., together with a number of option parameters determining the extent of calculations and output required. The subsequent processing of this information into a form whereby the reactor physics calculations can be performed is done automatically by the code, together with reading of necessary cross-sections and other data from the data libraries.

The input data is supplied to the code on cards and/or card images read from a file. Each card is identified by an identification number in the first columns of the card, which define the input variables given in the remaining columns (specified in free format). The input card images can thus, in principle, be read into the code in any order. The identification number on

each card also enables easy specification of sub-cases. Several cases can be run in succession, where one need only to specify those cards which differ from that of the previous case.

The card images of all data cards are listed by the code at the beginning of the printed output. In addition, the code supplies what may be called an interpreted listing of the input data set. All quantities, dimensions and options, either defined in the input data or implied, are printed with clear, explanatory texts, and with units given for all numerical values printed.

The code also performs tests for elementary errors in the input data, or if some input data exceed given limitations in the code. If some errors are found, error messages will be printed and the calculation stopped. A "Check Input" option helps the User in checking that his input data are correct, and to detect errors at an early stage before much computing time is used.

A detailed description of input and output of RECORD is given in the FMS Documentation (Ref. 6).

2.4.4 Output of RECORD

The output of the RECORD code consists essentially of two parts:

- a) the output listing obtained from the line printer, and
- b) the data files (disc files) generated by the code.

The output listing of RECORD is designed to give, in a precise form, the input to the code and the essential results of calculations. The data in the output are grouped together in a number of parts and, wherever possible, each part is listed on the same page with all quantities defined with a clear text. The listing pages are of A4 format for easy copying or other handling by User. All output pages are numbered sequentially and, at each

page top, the Code Version Number, Case Number, and the Case Identification Card text is printed.

A one-page output is always obtained at each calculation state, giving the main results of calculations. These include k_{∞} and k_{eff} values, homogenized few-group data for the assembly cell, average fuel composition, power peaking factors, etc. Flexible output options otherwise enable the User to obtain additional and more detailed calculation results to be listed at any particular burnup state. Typical outputs often requested are power maps and pinwise burnup distributions in a fuel assembly. Detailed fuel inventory (weight per cent of the main uranium and plutonium isotopes, and/or isotopic concentrations of all fuel isotopes present) in each fuel pin can be listed as function of fuel burnup. Another useful output group that may be requested is the neutron balance, showing, in a two-group scheme, the relative contributions to the neutron reaction rates from the most important isotopes and regions of an LWR fuel assembly. The output option groups presently available in RECORD are given in Appendix B. Excerpts from RECORD output listings are shown in Appendix C.

Discussion of the data files is deferred to Section 2.5 of this report.

2.4.5 Restart Options

In performing reactor physics calculations on reactor fuel, the need often arises to be able to initiate calculations on a fuel which has been depleted to a given burnup state. Restart options are available in RECORD, enabling such calculations to be performed for depleted LWR fuel assemblies by making use of a fuel burnup file, or so-called BFILE, generated in a previous RECORD calculation. Application of restart options enable, e.g., burnup calculations to be continued after given burnup states, either with same or new operating conditions, and makes possible the generation of "cold" data banks as function of burnup. Depleted fuel pins may also be replaced by pins with fresh fuel or new densities. Restart calculations with RECORD can be performed all in one run, or at some later time, by using files generated and saved in a previous run.

2.4.6 Limitations of RECORD

Some of the limitations of RECORD should be noted. These limitations or restrictions relate to the physical problems which can be handled, the geometries which can be treated, the solution methods adopted, and limitations due to computer requirements.

The RECORD code has been designed to handle light water lattices only, as represented by the LWR fuel assemblies described in Section 2.1. The fuel must be UO_2 or PuO_2 , but specific enrichment and dimensions can be specified for each fuel pin. The moderator is H_2O , but may also contain soluble poison and other isotopes. Uniform or non-uniform void distributions can also be defined for the moderator regions. Burnable poison and control absorber types usual to present commercial LWR fuel assembly designs, can be treated directly by the code.

The main limitations of RECORD are summarized in Tables 2.4.1 and 2.4.2.

2.5 Data Generation Unit of FMS

RECORD is the data generation unit of FMS. The results of the reactor physics calculations over an LWR fuel assembly and associated, surrounding water gaps, are condensed in a systematic manner to supply the few-group data required by the macroscopic codes of FMS. The code generates a number of files (Fig. 2.4.1), containing the required few-group data, isotopic concentrations, and other data, which are later activated by PRESTO and other codes of FMS or by RECORD, itself, in later runs. These files essentially constitute the Data Bank, being the basis for subsequent fuel management and transient calculations on Light Water Reactors with FMS (Fig. 1.0.1).

Most of the data written on the files can also be listed in the RECORD output listing, from which is additionally obtained certain coefficients and other data also needed by the macroscopic codes. The contents of the main files generated will now be described.

2.5.1 RECFILE

This is the main data bank file generated by RECORD, and contains assembly cell-averaged, two-group data, assembly-averaged fuel isotopic concentrations, and k_{∞} -values, for use by PRESTO and the other FMS codes. Optionally, the file may also contain normalized pin-powers for given fuel assembly. These data are stored as function of average fuel burnup, and either exposure-weighted void (BWR) or ppm boron (PWR). The file is built up on the basis of a previously generated RECFILE, such that the file produced will contain the new data generated, added to that contained in the previous RECFILE.

2.5.2 Σ -file

This file contains detailed specification of mesh point divisions, region boundaries, composition identification, and macroscopic five-group data for all material compositions in the different regions of a given fuel assembly cell. The group data are generated and stored on the file as function of average fuel burnup. The original purpose of this file was to transfer data to the larger, two-dimensional diffusion code, MD2, for eventual detailed four-assembly calculations (Section 2.2.8). The file is now more often used to couple the GADPOL code to RECORD when performing burnable poison calculations. As will be explained in Chapter 5, the GADPOL code is a link between the THERMOS code and RECORD, making adjustments to the THERMOS-calculated cross-sections, so as to preserve the burnable poison lattice cell reaction rates in going from the cylindrical geometry of THERMOS to the x-y diffusion calculation in RECORD. By introducing the Σ -file from RECORD, the GADPOL code will extract from the file the required mesh point distribution for a given burnable poison cell configuration.

2.5.3 Restart File (BFILE)

This file is generated for use in subsequent restart calculations (see also Section 2.4.5). The file contains all required data for the fuel, enabling restart calculations to be initiated on a fuel assembly at some given burnup state. Specifically, the file contains case parameters, isotope identification, densities and enrichments of initial fuel, and pinwise burnups and fuel isotopic concentrations, as function of average fuel burnup. The file also contains, as function of burnup, necessary gadolinium data, isotopic concentrations in eventual shim rods, and concentration of boron absorber in eventual curtains. In particular, the file is much applied when generating "cold" data banks for describing low power conditions during burnup.

2.5.4 FILEED File

Also of some importance when performing project calculations involving a large number of calculations, is the construction of an input data bank, providing a systematic way of storing case input data, together with logical assignment of identification numbers to each data set. This enables easy retrieval of particular case data, and the construction of new input data sets. A subroutine, FILEED, is included in RECORD as an input pre-processor to the code, and performs the following main functions:

- Generates a file (FILEED file), containing the case data sets for a given run, and which are added to the input case data bank contained in an existing FILEED file
- Builds new data sets on the basis of data from an existing file, and adds this new data set to that file
- Assigns identification numbers to each new case data set given to or generated by the FILEED routine
- Lists prescribed parts of the input data file.

In general, the FILEED file is generated whenever the FILEED input pre-processor is used in specifying case input data to RECORD. The FILEED function may also be bypassed if unwanted, in which case the User must always present complete input case specification for main case of run, and also where the User must provide his own case identification numbers.

2.6 Computer Requirements

The RECORD code has been developed using the CDC CYBER-74 computer at Kjeller, Norway, and is operative also on other CDC machines. The code is programmed in FORTRAN IV (CDC Extended). With a few exceptions, the statement types conform to ANSI Standards. The code has one main program, and is then structured into seven overlays which are called by the main program. Some of the overlays are further divided into segments. In order to keep the central memory requirements at a reasonable level, the code makes use of a number of disc files to store and transfer data between the overlays. The data transfer between the central memory and these disc files is generally made via BUFFER IN/OUT statements. These are the main non-ANSI statements of the code, but make possible a very efficient data transfer on CDC computers. For the library files and the data bank files generated by the code, the data transfer is made via READ/WRITE statements.

The memory requirements and computing times are machine-dependent. For the CDC CYBER-74 computer, the code's central memory requirement is, at present, 45000 (or 130000 octal) CDC words, and typical computing time for an 8 x 8 BWR assembly (using 20 x 20 mesh points) is about 30 CPU seconds for an initial calculation, including all the initial processing. Each subsequent burnup interval, with new spectrum and diffusion calculation and where use is made of previous flux, will require about 20 CPU seconds. In the standard data bank generation procedure with RECORD, a complete burnup calculation to 35000 MWD/TU for one fuel assembly at a given void, will require about 300 CPU seconds. The main computer requirements for RECORD are summarized in Table 2.6.1.

TABLE 2.4.1 Main Limitations to Physical Problems Treated by RECORD

GEOMETRY	General	:	2-Dimensional x - y geometry
	Fuel Assembly Type	:	BWR, PWR, or single-pin cell
	Lattice Positions	:	Square array, max. no. 9 x 9
FUEL	No. of Fuel Rods	:	Maximum 81
	Composition	:	UO ₂ -PuO ₂ , initial enrichment specified in input for all rods
	Geometry	:	Cylindrical rods, dimensions may be specified individually for all rods
	Fuel Rod Types	:	Max. 81 (i.e., of different compositions and dimensions)
BURNABLE POISON	Composition	:	Gadolinium (Gd ₂ O ₃) + UO ₂ /PuO ₂
	Type and Number	:	Max. 10 rods, max. four types
	Thermal Group Data	:	From THERMOS-GADPOL, or from Gadolinium Library
CLAD	Composition	:	Specified in input (max. five isotopes)
	Geometry	:	Cylindrical, dimensions may be specified individually for all rods
MODERATOR	Composition	:	H ₂ O + soluble poison and eventual other (≤5) isotopes
	Voids	:	Uniform, or specific void fractions can be specified for each lattice cell
FLOW BOX	Composition	:	Specified in input (max. five isotopes)
	Geometry	:	Rectangular regions of given thickness surrounding lattice area of BWR assembly
CONTROL ABSORBERS	Geometry	:	Solid blade, rodged blade, or rod cluster
	Absorber	:	B ₄ C, boron steel, boral or Ag-In-Cd
	Clad	:	Zircaloy, stainless steel or aluminium
	Other Types	:	Boundary conditions calculated externally and specified in input
SHIM RODS	Geometry	:	Cylindrical, max. 10 rods, max. four types
	Absorber	:	Specified in input (max. 10 isotopes); of these, max. five burnable isotopes)
	Clad	:	Specified in input (max. five isotopes)
	Thermal Group Data	:	From THERMOS-GADPOL

TABLE 2.4.2 Main Limitations in Solution Methods and Other Details in RECORD

NEUTRON GROUPS	Thermal Spectrum	: 15 energy points
	Epithermal Spectrum	: 35 energy groups
	Diffusion Calculations	: 5 macrogroups (3 epithermal & 2 thermal)
	Output Data Bank	: 2 macrogroups (1 thermal & 1 fast)
	Thermal Cutoff	: 1.84 eV
MESH	Mesh Points in Diffusion Calculation	: Max. 30 x 30 (mesh point numbers and spacings generally determined by code itself)
REGIONS	Lattice Region	: Maximum 81
	Total No. of Regions	: Max. 100 (i.e., lattice + water gaps and other regions)
ISOTOPES	No. of Isotopes in Fuel	: Max. 40 (heavy isotopes and fission products accounted for in each fuel pin)
	No. of Isotopes in Lattice	: Max. 48 (fuel, clad and moderator regions)
BURNUP	No. of Burnup States (at which spectrum recalculation and output generation occurs)	: Max. 50, in general; Max. 20, when generating RECFILE (main data bank file)

TABLE 2.6.1 Main Computer Requirements for RECORD

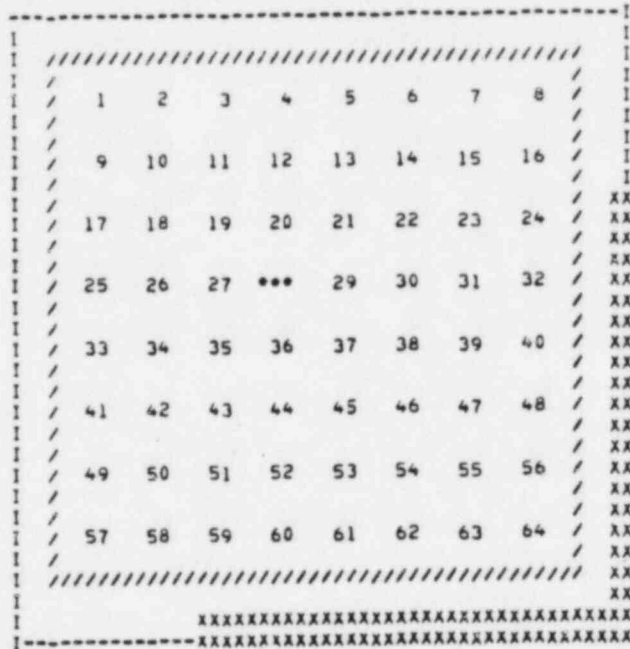
COMPUTER TYPE	:	CDC CYBER-74, -75, -76 CDC-6500, -6600 CDC CYBER-170
PROGRAMMING LANGUAGE	:	FORTRAN, CDC Extended (ANSI Standards mostly)
CORE STORAGE	:	130 K (octal) words
PERIPHERAL DEVICES NEEDED	:	Disc storage device
CODE STRUCTURE	:	Overlay
NO. OF SOURCE CARDS	:	Approximately 28,000
TYPICAL RUNNING TIME	:	On CYBER-74, about 30 CPU sec. initially, and about 20 CPU sec. per subsequent burnup step for typical BWR assembly configuration

1. CASE IDENT. RE-SA 1 0 BWR SAMPLE PROBLEM.

2. FUEL ASSEMBLY GEOMETRY

B W R

SYMMETRY SPECIFIED



NUMBER OF LATTICE POSITIONS = 64
 PITCH = 1.6256 CM

OUTER DIMENSIONS OF ASSEMBLY CELL = 15.2400 CM
 WIDTH OF NARROW WATER GAP = .4750 CM
 (WIDTH OF WIDE WATER GAP = .9530 CM)

RUCKLING = .6842E-04 CM**2

///// = FLOW BOX, OUTER DIMENSIONS = 13.8120 CM
 WALL THICKNESS = .2030 CM

XXXXXX = CONTROL PLATE, EFF. HALF SPAN = 12.2950 CM
 HALF THICKNESS = .3960 CM
 CENTRE PIECE HALF SPAN = 1.9840 CM

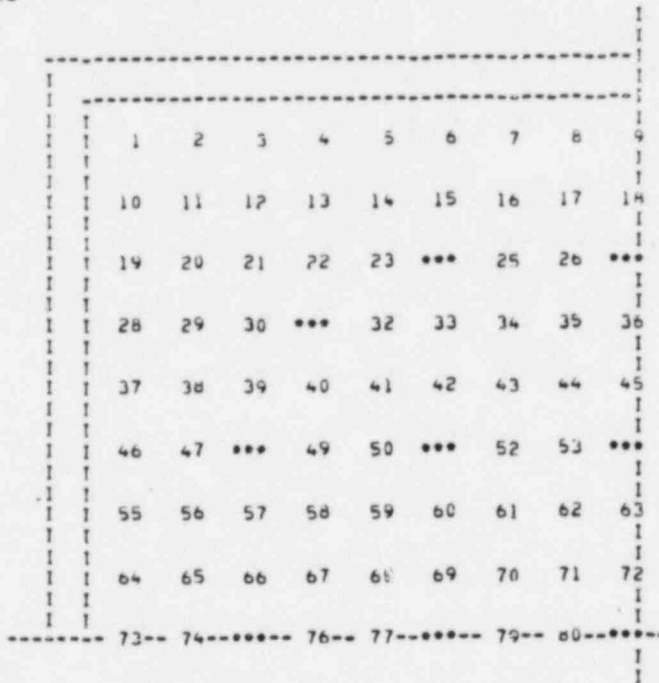
FIGURE 2.1.1 Example of BWR Configuration in RECORD

1. CASE IDENT. RE-SA 4 0 PWR SAMPLE PROBLEM.

2. FUEL ASSEMBLY GEOMETRY

P W R 1/4 ASSEMBLY

SYMMETRY SPECIFIED



NO. OF LATTICE POSITIONS IN 1/4 ASSEMBLY = 81 (THIS INCLUDES THOSE ON SYMMETRY AXIS)
PITCH = 1.2600 CM

OUTER DIMENSIONS OF 1/4 ASSEMBLY CELL = 10.7600 CM
WIDTH OF WATER GAP = .0500 CM

HUCKLING = .6844E-04 CM**2

FIGURE 2.1.2 Example of PWR Configuration in RECORD

1. CASE IDENT. RE-SV 1 0 SVEA INTERNAL WATER CROSS FUEL. TFST CASE.

2. FUEL ASSEMBLY GEOMETRY B W R SVEA INTERNAL WATER CROSS FUEL SYMMETRY SPECIFIED

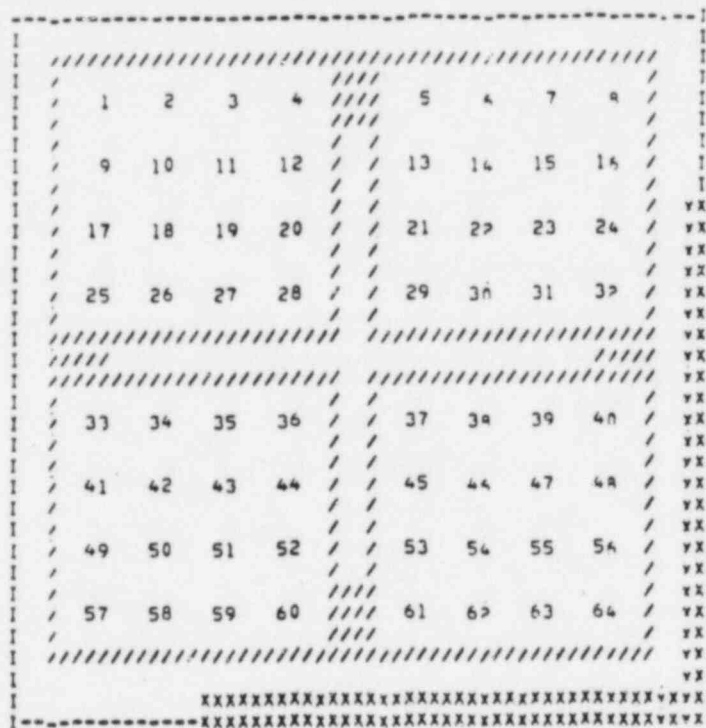
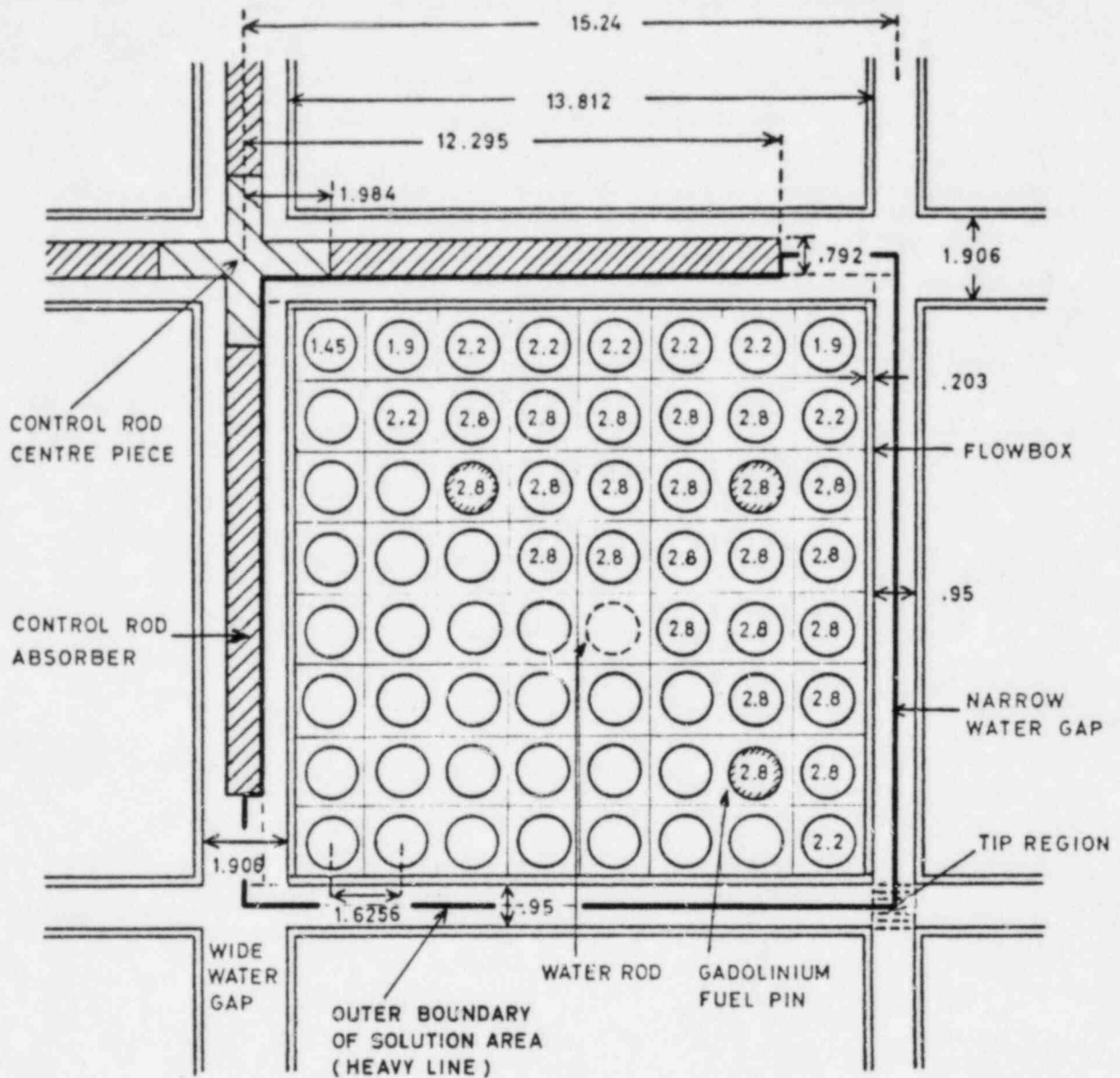


FIGURE 2.1.3 Example of Internal Water Cross Fuel in RECORD



All dimensions are in cm.

- Fuel UO_2 , radius 0.54 cm, initial enrichment as above in wt% U^{235} to total U. 4 pins containing gadolinium with given wt% Gd_2O_3 .
- Clad Zircaloy-2.
Inner/outer radius = 0.54/0.626 cm.
- Floibox Zircaloy-2.
- Control Rod Rodded blade type, B_4C absorber.
Absorber radius 0.175 cm, clad thickness 0.0635 cm, pitch of pins 0.4884 cm. Clad and centerpiece are of stainless steel, SS-304.

FIGURE 2.1.4 Example of Typical BWR Configuration Treated by RECORD, Showing Region Division and Solution Area

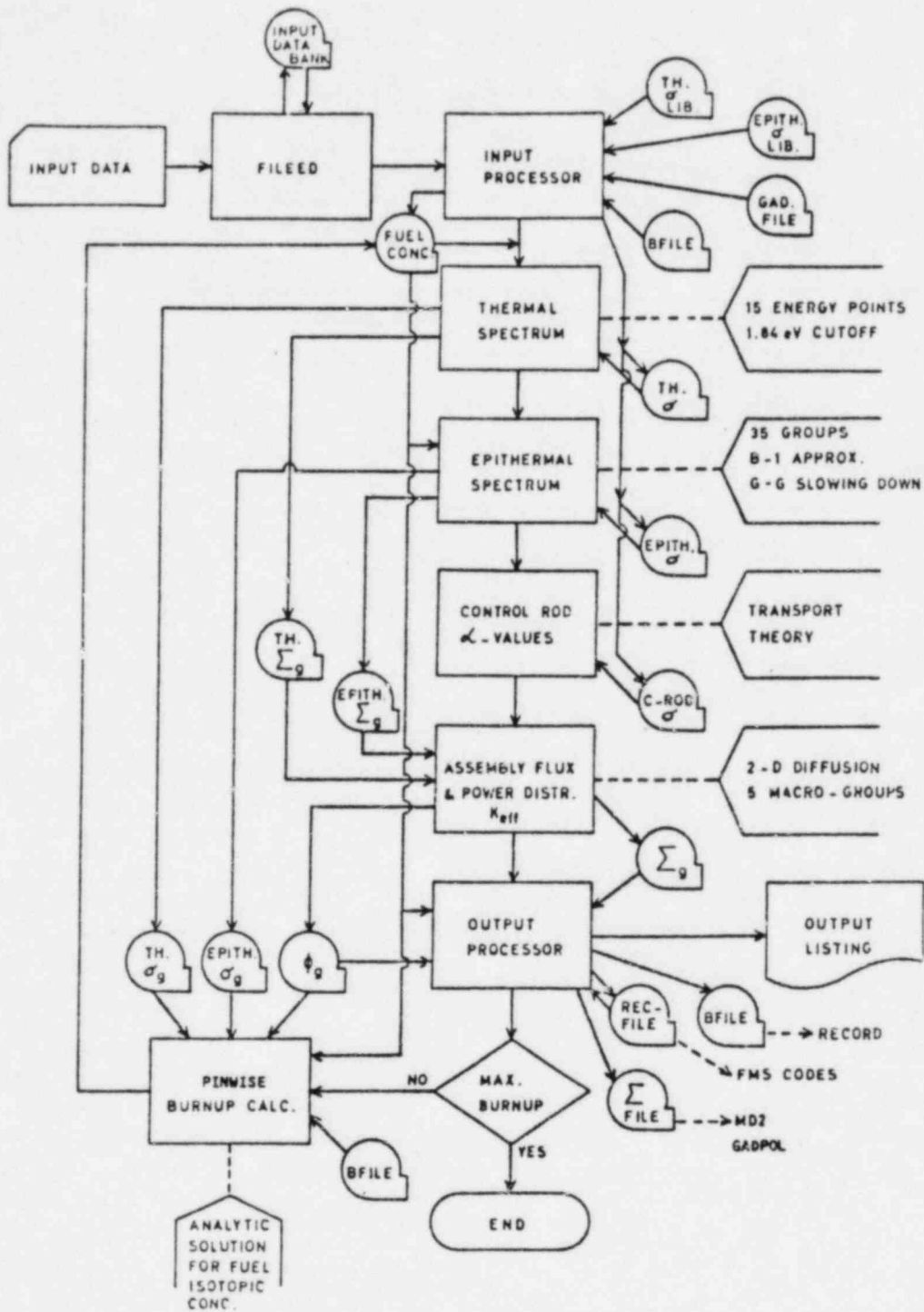


FIGURE 2.4.1 Schematic Flow Diagram for RECORD Code, with Indication of Main Data Files Used and Generated

3. THERMAL SPECTRUM AND FEW-GROUP DATA

This chapter describes the method used in RECORD for determining the neutron spectrum in the thermal energy range and derivation of macrogroup parameters for use in subsequent diffusion and burnup calculations over a fuel assembly.

The thermal energy range in RECORD extends to 1.84 eV and, in this interval, the neutron spectrum is determined by solving the transport equation applied to the basic Wigner-Seitz unit cell of the fuel assembly lattice, i.e., the circular cell of the same area as the square cross-section of the unit lattice cell. The transport equation is solved using a development (Ref. 9) of the point energy approach (Ref. 10). The Nelkin scattering model (Ref. 11) is applied for hydrogen bound in water, and the Brown-St. John model (Ref. 24) is applied for oxygen.

The philosophy in RECORD is to calculate the neutron spectrum in the thermal energy range for a so-called "average pin cell", using three space regions (fuel, clad and moderator). This average pin cell is representative of specific spectrum regions, and it is defined as that cell having the amount of each isotope as found from averaging over all pin cells in the spectrum region. The pin cells of a fuel assembly are grouped into a number of thermal spectrum regions, depending on their spectral environment, (an example of thermal spectrum region division is shown in Fig. 3.0.1).

Having obtained the homogeneous pin cell spectrum, the procedure is then to calculate the energy-dependent flux ratios for each pin cell, using a modified Amouyal-Benoist method (Refs. 12, 25). These are the ratios between the flux in a certain region (fuel, clad or moderator) to the homogeneous pin cell flux. Assuming that the homogeneous pin cell spectrum is constant and equal for all fuel pin cells in a given spectrum region, and using this spectrum from the average pin cell calculation, regionwise neutron spectra is obtained for each pin cell in the fuel assembly.

From these regionwise microgroup neutron spectra for each pin cell, thermal macrogroup cross-sections and constants are determined for all isotopes present in all pin cells in the fuel assembly. Summation over all isotopes present in a certain pin cell gives effective macrogroup cross-sections and constants for use in the two-dimensional diffusion calculation over the fuel assembly. The procedure for calculating the spectrum and group constants in the thermal energy range is repeated at specified burnup intervals given in the input.

The following sections contain some of the basic equations and discussions of some essential points involved in the treatment of the thermal energy range in RECORD. For more details in the derivation of these equations and discussion of the assumptions, the reader is referred to the References.

3.1 Fundamental Equations

The thermal neutron flux spectrum, over which the above mentioned averaging must be done, is the solution of the time-independent Boltzmann integral neutron transport equation. With the assumption of isotropic scattering and no up-scattering above thermal cut-off E^* , this equation can be written in usual notation.

$$\hat{\Sigma}_t(\vec{r}, E) \phi(\vec{r}, E) = \int_V d\vec{r}' T(\vec{r}' \rightarrow \vec{r}, E) \left[S(\vec{r}', E) + \int_0^{E^*} dE' \hat{\Sigma}_s(\vec{r}', E' \rightarrow E) \phi(\vec{r}', E') \right] \quad (3.1.1)$$

In RECORD, Equation (3.1.1) is solved by starting with an integration over the cell volume V , which yields

$$\hat{\Sigma}_t(E) \psi(E) = \int_0^{E^*} dE' \hat{\Sigma}_s(E' \rightarrow E) \psi(E') + \hat{S}(E) \quad (3.1.2)$$

where $\psi(E)$ and $\hat{S}(E)$ are the volume-averaged cell spectrum and source, respectively, while the $\hat{\Sigma}$'s are volume and flux weighted cross-sections. Here the property has been used that, irrespective of the energy, the transport kernel $T(\vec{r}' \rightarrow \vec{r}, E)$ integrates to unity

$$\int d\vec{r} T(\vec{r}' \rightarrow \vec{r}, E) = 1$$

and where:

$$\psi(E) = \frac{1}{V} \int d\vec{r} \phi(\vec{r}, E) = \sum_i \frac{V_i}{V} F_i(E) \psi(E) \quad (3.1.3a)$$

$$\hat{S}(E) = \frac{1}{V} \int d\vec{r} S(\vec{r}, E) = \sum_i \frac{V_i}{V} S_i(E) \quad (3.1.3b)$$

$$\hat{\Sigma}_t(E) = \frac{1}{V\psi(E)} \int d\vec{r} \Sigma_t(\vec{r}, E) \phi(\vec{r}, E) = \sum_i \frac{V_i}{V} F_i(E) \Sigma_{t,i}(E) \quad (3.1.3c)$$

$$\hat{\Sigma}_s(E' \rightarrow E) = \frac{1}{V\psi(E)} \int d\vec{r} \Sigma_s(\vec{r}, E' \rightarrow E) \phi(\vec{r}, E) = \sum_i \frac{V_i}{V} F_i(E') \Sigma_{s,i}(E' \rightarrow E) \quad (3.1.3d)$$

with $F_i(E)$ being the ratio of the neutron flux in region i at energy E , to that of the whole cell.

$$F_i(E) = \frac{\psi_i(E)}{\psi(E)} \quad i = 1, 2, 3 \quad (3.1.4)$$

where

$i = 1, 2, 3$ refers to the three regions:
fuel, clad and moderator.

The solution of the problem then proceeds in two steps. First, spatial calculations using the modified Amouyal-Benoist method is performed, generating the flux ratios $F_i(E)$ in the different thermal microgroups. Next, these flux ratios are used to weight cross-sections, Equation (3.1.3), that enter the homogeneous medium spectrum, Equation (3.1.2). This equation is solved by a multigroup method (Refs. 12, 14).

From the cell spectrum $\psi(E)$, obtained in this way, and the flux ratios for each energy group $F_i(E)$, the average thermal neutron spectrum for region i is obtained.

$$\psi_i(E) = F_i(E) \cdot \psi(E) \quad (3.1.5)$$

3.2 Flux Disadvantage-Factor Calculations

The Amouyal-Benoist method is employed in RECORD to calculate the flux disadvantage-factors

$$\delta_i(E) = \frac{\psi_i(E)}{\psi_1(E)} \quad i = 1, 2, 3 \quad (3.2.1)$$

which are the ratios between flux in region i to the flux in the fuel region.

As seen in the previous section, we need the ratio between the flux in region i to that of the whole cell. But it is easily seen that this ratio is given by:

$$F_i(E) = \frac{\psi_i(E)}{\psi(E)} = \frac{\delta_i(E)}{\sum_i V_i \delta_i(E)/V} \quad (3.2.2)$$

The specific method used for calculation of flux disadvantage-factors in RECORD is by Z.J. Weiss. For details in the derivation of the equations and on discussions of principles and assumptions on which the theory is based, see Reference 12.

If one defines the probabilities Γ_0 and Γ_1 as the probability that a neutron entering the cladding from the moderator will be absorbed in the fuel or cladding, respectively, the disadvantage-factor can be written as:

$$\delta_2 = \frac{\Sigma_{a1} V_1 \Gamma_1}{\Sigma_{a2} V_2 \Gamma_0} \quad (3.2.3)$$

$$\delta_3 = 2R_2 \Sigma_{a1} \left(\frac{R_1}{R_2}\right)^2 \left(\frac{1-\Gamma_1-\Gamma_2}{\Gamma_0} + \left(1 + \frac{\Gamma_1}{\Gamma_0}\right) \left(\frac{3x}{8} \cdot \frac{F(R_3/R_2)}{1-(R_2/R_3)^2} + \frac{3}{4}\lambda_\infty(x)\right) \right) \quad (3.2.4)$$

where

$$F(Z) = \frac{\ln(Z^2)}{1-1/Z^2} + \frac{1}{2Z^2} - \frac{3}{2} \quad (3.2.5)$$

and

$$x = \Sigma_{t3} R_2$$

and where

Σ_{t3} = the total cross-section in the moderator,

R_2 = the outer radius of cladding material, and

$\lambda_{\infty}(x)$ = effective linear extrapolation length for a black cylinder embedded into a nonabsorbing, infinite medium.

$$\lambda_{\infty}(x) = \begin{cases} \frac{0.2442}{0.4316+x} + 0.7675 & 0 \leq x \leq 1 \\ \frac{0.292}{0.28+x} + 0.7104 & x > 1 \end{cases} \quad (3.2.6)$$

The problem has then been reduced to the evaluation of the probabilities Γ_0 and Γ_1 . They can be expressed in terms of first collision probabilities, as follows :

$$\Gamma_0 = (1 - c_1)\alpha \quad (3.2.7a)$$

$$\Gamma_1 = (1 - c_2)\beta \quad (3.2.7b)$$

where

$$\alpha = \frac{P_1(1 - c_2 P_{22}) + c_2 P_2 P_{21}}{(1 - c_1 P_{11})(1 - c_2 P_{22}) - c_1 c_2 P_{12} P_{21}} \quad (3.2.7c)$$

$$\beta = \frac{P_2(1 - c_1 P_{11}) + c_1 P_1 P_{12}}{(1 - c_1 P_{11})(1 - c_2 P_{22}) - c_1 c_2 P_{12} P_{21}} \quad (3.2.7d)$$

$$c_{1,2} = \Sigma_{s1,2} / \Sigma_{t1,2} \quad (3.2.7e)$$

P_1 and P_2 are the first collision probabilities in fuel and cladding due to an isotropic incident flux on the cladding. The remaining four probabilities are defined as: P_{ij} is the probability that a neutron, born uniformly and isotropically in region i , will suffer its first collision in region j .

These collision probabilities can be expressed by third order Bickley functions, and Bessel functions of the first and second kind.

The calculation of Bickley and Bessel functions are relatively time consuming. In RECORD, these disadvantage-factors are calculated for each microgroup and for each fuel pin in the fuel assembly. In order to reduce computer cost, some further approximations are introduced. These are by Van der Kamp (Ref. 25), and based on considerations of Nordheim and Sauer. This leads to much simpler expressions for the actual collision probabilities, avoids the time consuming Bickley and Bessel functions, and reduces

the computer time by a factor of ca. 40. This original method has been tested on numerous occasions against exact, one-group transport calculations (Ref. 26). Errors of more than 1% were observed only very rarely. The new, fast version of the method not involving the Bickley and Bessel functions has been tested against the original one. Results showed (Ref. 25) that the discrepancy was always less than 1% in the one-group case, while the difference in the disadvantage factors in the multigroup case is negligible.

3.3 Spectrum Calculations

The homogeneous medium spectrum equation (3.1.2)

$$\hat{\Sigma}_t(E)\psi(E) = \int_0^{E^*} dE' \hat{\Sigma}_s(E'+E) \psi(E') + \hat{S}(E) \quad (3.3.1)$$

will be reduced to a set of N algebraic equations by dividing the thermal energy range from 0 to E^* into a number of intervals. These equations are solved by an over-relaxed, normalized, Gauss-Seidel (Liebmann) technique, as described in Reference 15. The over-relaxation factor is taken as 1.2, and normalization is achieved by requiring from each iterant that it satisfies the condition of neutron conservation

$$\int \hat{\Sigma}_a(E) \psi(E) dE = \int \hat{S}(E) dE \quad (3.3.2)$$

where $S(E)$ is the slowing down source per unit energy.

Before the numerical solution of Equation (3.3.1) is sought, the energy variable will be replaced by the velocity, because the scattering kernel is a smoother function of velocity than of energy. The following relation exists :

$$E = 0.0253 v^2 \quad (3.3.3)$$

with the velocity (v) in units of 2200 m/s and the energy in eV.

With $\psi(E)dE = \psi(v)dv$, $\psi(v) = vN(v)$ and $\Sigma_S(E' \rightarrow E)dE = \Sigma_S(v' \rightarrow v)dv$ Equation (3.3.1) will be expressed as

$$\hat{\Sigma}_t(v) N(v) = \int_0^{v^*} dv' \hat{\Sigma}_s(v' \rightarrow v) v' N(v')/v + \hat{S}(v)/v \quad (3.3.4)$$

This equation may be written as

$$\hat{\Sigma}_{tj} N_j = \sum_i P_{ij} N_i + \hat{S}_j \quad (3.3.5)$$

where

$$P_{ij} = \hat{\Sigma}_s(v_i \rightarrow v_j) v_i \Delta v_i / v_j \quad (3.3.6)$$

This is the set of algebraic equations which is solved in the code. The subscripts j and i denote j 'th and i 'th velocity group. The scattering kernel will be mentioned in the next section.

The source is calculated assuming a spatially flat $1/v^2$ epithermal flux, no upward scattering in the epithermal range, and by use of the free-gas scattering model (Ref. 12). With the velocity (v) as the independent variable, the source of thermal neutrons slowed down from the epithermal interval can be expressed as

$$\hat{S}(v)/v = \sum_S (1/v^{*2} - \alpha^2/v^2) / (1 - \alpha^2)$$

with

$$\alpha = (M - 1)/(M + 1),$$

i.e., the maximum fractional velocity loss possible upon collision between a neutron and a moderating atom with free atomic mass M .

3.4 Scattering Models

The calculation of the scattering kernel P_{ij} above, is given in detail in Reference (12). Consequently, only some comments will be given here.

A derivation of the scattering kernel in the thermal range must take into account the Maxwellian motion of the moderator atoms and the variation of the scattering cross-section with the relative velocity between neutron and scattering nucleus.

In RECORD, two scattering models are used. The first one is the free-gas model by Brown-St. John (Refs. 24, 12), and the second one is the molecular model for water, proposed by Nelkin (Refs. 11, 12).

The main assumption of the Brown-St. John (BSJ) model considers the moderator to be composed of free particles with a Maxwellian velocity distribution. For neutron energies below 1 eV, this picture is not quite correct, as the neutrons do not collide with individual atoms but rather with the molecule (H_2O) as a whole. However, the chemical binding can be accounted for by replacing the actual proton mass by an effective rotational mass. The oxygen atoms can still be treated as free-gas particles with their own mass. The effective mass of proton is calculated on the assumption that the neutron energy is small compared with the quanta of molecular vibration, but large compared to the energy differences between the rotational levels of the molecules, so that rotations can be treated as classical.

A further refinement of the scattering model considers the entire molecule, rather than the individual scattering atom, as the basic dynamical unit. Translation of the molecule as a whole, as well as rotations and vibrations of its nuclei about their equilibrium positions, have to be considered. The molecular model for water proposed by Nelkin (Refs. 11, 12) was chosen for use in RECORD. Its basic assumptions are :

- 1) The translation of the molecule is free and described by the center of mass motion with weight $\lambda = 1/m_o$, where m_o is the mass of the molecule.

- 2) The rotation of the molecule is hindered by neighboring water molecules and the hindered rotation has been replaced by a single oscillation with energy $w_r = 0.06$ eV and weight $\lambda_r = 1/m_r$. Here m_r is the effective rotational mass.
- 3) The three degrees of freedom of the OH bond have been described by isotropic vibrational modes of energies $w_1 = 0.205$ eV, $w_2 = w_3 = 0.481$ eV with equal weights $\lambda_1 = \lambda_2 = \lambda_3$. Here $\lambda_i = 1/m_i$ where m_i is the vibrational mass of the i'th mode. Their values have been obtained from the condition that, for large energy transfer, the free-gas scattering kernel obtains $\lambda_1 = \lambda_2 = \lambda_3 = 0.1712$.

In the Nelkin model for H_2O , the contribution from oxygen was calculated by treating it in the free-gas (BSJ) approximation.

Detailed formulae and a discussion of the numerical methods used to evaluate these kernels may also be found in an IAEA Report (Ref. 27).

3.5 Point Energy Approach

The production of plutonium isotopes during burnup of uranium fuel requires some changes, either in a theoretical view of our problem or in a numerical treatment of the transport equation. These changes are necessary because of the large thermal resonances in Pu^{239} and Pu^{240} at 0.297 eV and 1.055 eV, respectively.

The reactor core design may also contain other elements with resonances inside or closely above the pure thermal energy range. It may be in burnable poisons, such as europium, dysprosium, and samarium, or in control rods of silver, indium and cadmium.

One possibility for eliminating the problems introduced by these resonances is to increase the number of thermal microgroups. In RECORD, however,

microgroup calculations of the flux disadvantage-factors are performed for each fuel pin cell. An increase in number of microgroups will greatly increase computer costs.

These considerations led to the adoption of the point energy method (Ref. 10), where the necessary number of energy points treated is about one half of the number of groups which otherwise had been necessary.

The method generally comprises an improvement of all numerical integrations that occur during the solution of the problem, e.g., energy transfer integral, reaction rates, etc.

Fredin (Ref. 10) showed that a numerical integration scheme based on the Gaussian type quadrature formula, being developed for an accurate evaluation of the thermal reaction rates in U/Pu systems, can be successfully used even in a solution to the problem of thermal neutron spectra.

The whole thermal energy range (0 to 1.84 eV) is divided into N subintervals. Before the Gaussian quadrature formula is used in each interval, appropriate variable transformations, $E = \tau_k(z)$, are applied, which cluster the integration points towards the range of the resonance influence.

$$\int_0^{E^*} \Sigma(E) \psi(E) dE = \sum_{k=1}^N \int_{z_{k,1}}^{z_{k,2}} \Sigma(\tau_k(z)) \psi(\tau_k(z)) \frac{d\tau_k(z)}{dz} dz$$

$$= \sum_{i=1}^k w_i \Sigma(E_i) \psi(E_i)$$
(3.5.1)

where

- E_i = the energy points,
- w_i = corresponding weights, and
- k = total number of the points.

Other symbols have their usual meaning.

A similar scheme (Ref. 9) is used in RECORD for calculation of thermal neutron data for light water moderated lattices during burnup.

Having chosen a suitable, numerical integration scheme for evaluation of the reaction rates, a new problem arises in determining the value of the neutron spectrum in the given set of velocity points. Going back to the homogeneous medium spectrum equations, (3.3.6), we have

$$\hat{\Sigma}_{tj} N_j = \sum_{i=1}^k P_{ij} N_j + \hat{S}_j \quad (3.5.2)$$

The main trouble with a direct application of the numerical integration scheme in the calculation of neutron spectrum is due to the undesirable behavior of the scattering kernel. To improve the accuracy of Equation (3.5.2), the behavior of the scattering kernel, as well as that of the neutron spectrum in the vicinity of the point, have been taken into account. The construction of the scattering matrix is based on a method (Ref. 28) utilizing straight-forward interpolation of the spectrum between two integration points by the Lagrange formula, taking into account the spectrum values in two additional nearest points. A procedure for the construction of the scattering matrix based on this idea has been used in RECORD.

One may suppose that the main contribution to the value of the integral in Equation (3.3.4) or the discretization in Equation (3.5.2) is due to the interval containing the diagonal element of the scattering matrix. Since the scattering kernel has a sharp maximum there, a great deal of attention was paid to that interval. The rest of the scattering matrix was left almost uncorrected.

It has been shown (Ref. 9) that the described version of the multipoint method, which is used in RECORD, gives approximately the same accuracy as the multigroup approach, with about one-half of the number of velocity intervals. The number of energy points in RECORD are fixed at 15, and are listed in Table 3.5.1.

3.6 Macrogroup Data

The macrogroup data for all lattice cells are calculated from the thermal microgroup neutron spectrum.

An effective macroscopic cross-section for the thermal energy interval may be expressed as:

$$\Sigma_{\text{eff}}^k = \frac{\int_V d\vec{r} \int_0^{E^*} dE \phi(\vec{r}, E) \sigma^k(E) N^k(\vec{r})}{\int_V d\vec{r} \int_0^{E^*} dE \phi(\vec{r}, E)} \quad (3.6.1)$$

where the index k denotes element (or isotope) k , and v the volume of the fuel pin cell.

We consider homogeneous composition in the individual regions and with N_i^k denoting the number density of element k in region no. i we get

$$\Sigma_{\text{eff}}^k = N^k \sigma^k(2200) \cdot \bar{g}^k \cdot \bar{F}^k \quad (3.6.2)$$

where

$$\left. \begin{aligned} \bar{N}^k &= \sum_i N_i^k V_i / \sum_i V_i \\ \bar{g}^k &= \sum_i N_i^k V_i \bar{g}_i^k F_i / (\sum_i N_i^k V_i F_i) \\ \bar{F}^k &= \sum_i N_i^k V_i F_i / (\sum_i N_i^k V_i) \end{aligned} \right\} \quad (3.6.3)$$

and where

$$\begin{aligned}
 \bar{\psi}_i &= \int_0^E dE \psi_i(E) \quad , \quad \psi_i(E) = \frac{1}{V_i} \int_{V_i} d\vec{r} \phi(\vec{r}, E) \\
 F_i &= \bar{\psi}_i / \bar{\psi} \quad , \quad \bar{\psi} = \sum_i V_i \bar{\psi}_i / V \\
 \bar{\sigma}_i^k &= \bar{\sigma}_i^k / \sigma^k(2200), \quad \bar{\sigma}_i^k = \int_0^{E^*} dE \sigma^k(E) \psi_i(E) / \int_0^E dE \psi_i(E)
 \end{aligned}
 \tag{3.6.4}$$

In RECORD, as described in Section 3.1, the regionwise neutron spectrum $\psi_i(E)$ is calculated, where $i = 1, 2, 3$ denotes the three regions: fuel, clad and moderator, respectively. With this neutron flux $\psi_i(E)$ known, the absorption, scattering and fission cross-section are calculated according to the formulae above. A summation over all isotopes k present in a given fuel pin cell give effective data for this pin cell. This procedure is repeated for all pin cells in the fuel assembly.

Two thermal macrogroups are always used in standard usage of RECORD. Optionally, it may be specified in the input to the code that only one thermal macrogroup is to be used. In the two-group case, RECORD calculates the scattering removal cross/section from :

$$\int_{G_1} dv' \int_{G_2} \psi(v') \hat{\Sigma}_S(v'+v) dv \equiv \Sigma_{RG1, G2} \psi_1 \tag{3.6.5}$$

$$\Sigma_{RI, J} = \frac{\sum_{i=1}^I \Delta v_i v_i N_i \sum_{j=1}^J \hat{\Sigma}_S(v_i+v_j) \Delta v_j}{\sum_{i=1}^I \Delta v_i v_i N_i} \tag{3.6.6}$$

where

$$N_i = \text{neutron density at velocity } v = v_i.$$

From Equation (3.3.6), we have the following relation for the scattering kernel

$$P_{ij} = \hat{\Sigma}_s(v_i \rightarrow v_j) v_i \Delta v_i / v_j \quad (3.6.7)$$

With Equation (3.6.7) into Equation (3.6.6), we get

$$\Sigma_{rI,J} = \sum_{i=1}^I N_i \sum_{j=1}^J P_{ij} v_j \Delta v_j / \left(\sum_{i=1}^I \Delta v_i v_i N_i \right) \quad (3.6.8)$$

which is the expression used in RECORD for calculating the scattering removal cross-section.

The calculation of this scattering removal cross-section is performed with the neutron density $N_i = N(v_i)$ from the "average pin cell" calculation representative for a specific spectrum region. Afterward, this removal cross-section is assumed to be constant and equal for all the fuel pin cells in this spectrum region.

The thermal diffusion coefficient for a region R is calculated from the following expression

$$D^R = \sum_{k \text{ in } R} \frac{\Sigma_S^R}{3(\Sigma_S^R + \Sigma_A^R)(\Sigma_A^R + \Sigma_{tr}^R)} \quad (3.6.9)$$

with

$$\left. \begin{aligned} \Sigma_S^R &= \bar{N}^k \hat{g}_S^k \sigma_S^k(2200) \hat{F}^k \\ \Sigma_A^R &= \bar{N}^k \hat{g}_A^k \sigma_A^k(2200) \hat{F}^k \\ \Sigma_{tr}^R &= \bar{N}^k \hat{g}_{tr}^k \sigma_S^k(2200) \hat{F}^k \end{aligned} \right\} \quad (3.6.10)$$

where the summation is made over all isotopes k present in the region R . Σ_S , Σ_A and Σ_{tr} is the scattering, absorption and transport cross-section, respectively.

The transport cross-section is calculated in the following way. For all materials (isotopes), except hydrogen, we use

$$\sigma_{tr}(v) = (1 - 2/3M) \sigma_S(v) \quad (3.6.11)$$

where M is atomic mass of the material. For hydrogen in water Radkowsky's (Refs. 29, 12) prescription is used.

$$\sigma_{tr}(v) = (1 - \bar{\mu}(v)) \sigma_S(v) \quad (3.6.12)$$

where

$$\bar{\mu}(v) = \frac{4}{3} \sqrt{\frac{\sigma_0}{\sigma_S(v)}} - \frac{2}{3}, \quad \sigma_0 = 20.4 \text{ barn} \quad (3.6.13)$$

This procedure for calculation of transport cross-sections and diffusion coefficients is made for all regions in the fuel assembly.

Effective thermal macrogroup microscopic absorption and fission cross-sections for all isotopes k are also calculated for each fuel pin cell in the lattice. These cross-sections are needed in the burnup routine, and are obtained from Equation (3.6.2).

$$\sigma_{eff}^k = \sigma^k(2200) \frac{g^k}{g} \frac{F^k}{F} \quad (3.6.14)$$

The thermal water gap spectrum is obtained from a single-pin calculation on a water hole cell, using a fission spectrum as source. The group data for the water gap are calculated using that water cell spectrum and the formulas in Equations (3.6.2) - (3.6.4).

The group data describing the flowbox wall are calculated using the water cell spectrum. Optionally, other group data describing water gap and flowbox may be introduced into RECORD through special input data.

TABLE 3.5.1 Thermal Energy Point (Group) Structure in RECORD

ENERGY POINT I	VELOCITY POINT I (in units of 2200 m/s)	ENERGY POINT I (in eV)	UPPER BOUNDARY OF ENERGY "GROUP" I (in eV)
1	.1607	.0006556	.004181
2	.7906	.01587	.03814
3	1.7131	.07448	.1229
4	2.6358	.1763	.2315
5	3.2655	.2706	.2979
6	3.4936	.3098	.3299
7	3.8069	.3678	.4333
8	4.5374	.5225	.6270
9	5.4723	.7600	.8909
10	6.1798	.9693	1.0033
11	6.3067	1.0095	1.0337
12	6.4384	1.0521	1.0645
13	6.5425	1.0864	1.1148
14	6.7428	1.1539	1.2608
15	7.7425	1.5214	1.8400

RECORD 91-4 INPUT RE-HA 7 1 ,MATCH FT2 ,7DB2.34-4G6.0 ,0-35G4D/T,BURN,HOT,40%VOID

THERMAL SPECTRUM REGIONS IN LATTICE CELL POSITIONS (DEFAULT VALUES)

I	////////////////////////////////////								I	
I	/								/	I
I	/	5	5	3	3	3	5	6	/	I
I	/								/	I
I	/	5	1	1	1	GAD	1	5	/	I
I	/								/	I
I	/								/	XX
I	/	3	1	GAD	2	2	1	4	/	XX
I	/								/	XX
I	/	3	1	2	2	2	1	4	/	XX
I	/								/	XX
I	/	3	GAD	2	2	GAD	5	4	/	XX
I	/								/	XX
I	/	5	1	1	1	5	5	6	/	XX
I	/								/	XX
I	/	6	5	4	4	4	6	6	/	XX
I	/								/	XX
I	////////////////////////////////////								XX	
I									XX	
I									XX	
I									XX	

1 TO 6 DENOTE FUEL PIN CELL REGIONS
 GAD DENOTES GADOLINIUM CONTAINING FUEL PIN CELLS

FIGURE 3.0.1 Example of Thermal Spectrum Region Division in BWR Fuel Assembly, as Applied in RECORD

4. EPITHERMAL SPECTRUM AND FEW-GROUP DATA

This chapter describes the theoretical basis used in RECORD in determining the spectrum and few-group data in the epithermal energy region. The description includes the main assumptions and equations involved in treating the neutron slowing down, and those for treating resonance absorption and fission. For detailed derivations of equations and discussion of assumptions, the reader is referred to the reports listed in References, Chapter 11.

While the energy spectrum and group data calculation in the thermal energy range is based on rather detailed pinwise treatment of the thermal spectrum over a fuel assembly, a more approximate treatment, based on an average spectrum, can be applied for the epithermal energy range. The mean free path of epithermal neutrons is large, compared to lattice cell dimensions, and the spatial variation of the epithermal spectrum across typical LWR assemblies is small. This allows, with acceptable accuracy, the use of an average cell spectrum concept in determining the epithermal few-group data.

4.1 Fundamental Equations

The neutron spectrum and group constants in the epithermal region is calculated using the method of the BIGG-II code (Ref. 13). This is a multigroup Fourier transform neutron spectrum code, whose fundamental equations are derived by applying a Greuling-Goertzel slowing-down model to a B-1 or P-1 approximation of the one-dimensional Boltzmann equation.

The following set of equations are solved (for formal derivation, see Ref. 13) :

$$(\Sigma^T(u) - G_0^0) \phi(u) + B(u)J(u) + \sum_{f=0}^{f_0} \frac{dq_f}{du} + \frac{dq_F}{du} = S(u) \quad (4.1.1)$$

$$-\frac{1}{3} B(u) \phi(u) + [h(u)\Sigma^T(u) - G_1^0(u)] J(u) + \sum_{f=0}^{f_0} \frac{dp_f}{du} = 0 \quad (4.1.2)$$

$$G_{0,f}^1(u) \left(1 - \frac{d\lambda_{0,f}}{du}\right) \phi(u) + q_f(u) + \lambda_{0,f}(u) \frac{dq_f}{du} = 0 \quad (4.1.3)$$

$$q_F(u) = \sum_F \xi_F \Sigma_F^S(u) \phi(u) \quad (4.1.4)$$

$$G_{1,f}^1(u) \left(1 - \frac{d\lambda_{1,f}}{du}\right) J(u) + p_f(u) + \lambda_{1,f} \frac{dp_f}{du} = 0 \quad (4.1.5)$$

where

- u = lethargy variable
- $\phi(u)$ = neutron flux
- $J(u)$ = neutron current
- f_0 = no. of light elements treated by the Greuling-Goertzel slowing down model
- $q_f(u)$ = slowing down density from the f 'th light element
- $q_F(u)$ = total slowing down density from heavy (or "Fermi age") elements
- $p_f(u)$ = anisotropic slowing down density from the f 'th light element
- $S(u)$ = neutron fission source
- $I(u)$ = source from inelastic scattering

$\Sigma^T(u)$ = total macroscopic cross-section

$\bar{\xi}_F \Sigma_F^S(u)$ = average slowing down density for
F'th heavy element

$B(u)$ = buckling

$$h(u) = \frac{1}{3} \frac{B}{\Sigma^T(u)} \frac{\tan^{-1}(B/\Sigma^T(u))}{1 - \tan^{-1}(B/\Sigma^T(u))}$$

$$\lambda_{i,f}(u) = - \frac{G_{i,f}^2(u)}{G_{i,f}^1(u)}$$

$G_{i,f}^n(u)$ = coefficients in Greuling-Goertzel
expansion (as defined in Ref. 30).

The P-1 approximation is obtained by entering $h(u) = 1$.

In the numerical solution of the above equation set, the $3 + 2f_0$ equations are approximated by a finite difference scheme, in which the epithermal region is divided into a number of energy groups, in accordance with a lethargy mesh chosen as suitable. The equations are integrated over the lethargy interval $\Delta u = u_j - u_{j-1}$ where u_j is the upper lethargy boundary of microgroup j , and in these intervals cross-sections and slowing down constants are replaced by average values of the type

$$\bar{\Sigma}_j = \frac{\int_{\Delta u_j} \Sigma(u) \phi(u) du}{\phi_j} \quad (4.1.6)$$

where ϕ_j is the total flux in group j , given by

$$\phi_j = \int_{\Delta u_j} \phi(u) du \quad (4.1.7)$$

Inelastic slowing down in the system is treated using an inelastic slowing down matrix a_{ij} , which gives the probability that a neutron inelastically scattered in microgroup j shall be transferred to group i . The probability that a neutron inelastically scattered in microgroup j shall be transported out of that group will then be given by

$$A_j = \sum_{i=j+1}^{j_{in}} a_{i,j} \quad (4.1.8)$$

where j_{in} denotes the "inelastic cutoff".

We then have for the inelastic removal term

$$\int_{\Delta u_j} \Sigma^I(u) \phi(u) du = A_j \Sigma_j^I \phi_j \quad (4.1.9)$$

and source term

$$I_j = \sum_{i=1}^{j-1} a_{j,i} \Sigma_i^I \phi_i \quad (4.1.10)$$

where Σ_i^I is the total inelastic scattering cross-section and ϕ_i is the group flux in microgroup i .

RECORD is designed for uranium fueled systems, where most of the inelastic scattering takes place in the U^{238} isotopes. The approximation is therefore presently made by using only one inelastic matrix, that of U^{238} , in the inelastic slowing down calculations.

The above fundamental equations are valid for a homogeneous one-dimensional system. Before these equations can be applied to a heterogeneous lattice, such as a light water fuel assembly, the real system must first be homogenized to an equivalent fictitious, homogeneous system. In RECORD, the procedure is to calculate the epithermal spectrum for an average pin cell having

geometric dimensions and material properties, defined from averaging over all lattice cells containing fuel and moderator, also including the moderator in the associated water gap surrounding the fuel assembly. This average pin cell, consisting of fuel, clad and moderator is, in turn, homogenized to the required equivalent homogeneous system. During this latter homogenization procedure, proper account has to be taken of resonance absorption in the fuel.

The epithermal group structure in RECORD is fixed at 35 energy groups, defined in the range 10 MeV to 1.84 eV, and is listed in Table 4.1.1. The solution of the equations then determine the 35-group neutron spectrum for the so-called average pin cell. The philosophy in RECORD is now to assume this spectrum to be space-independent over the fuel assembly and, to apply the spectrum to all individual lattice cells to calculate effective average absorption, fission and removal cross-sections in each cell at any given time. This spectrum is used also in calculating the effective epithermal group data in the water gap.

In RECORD, the number of epithermal few-groups are fixed at 3 (a fast fission, an intermediate, and a resonance group) having the following energy division:

Macrogroup 1	10 - 0.821 MeV (microgroups 1 - 8)
Macrogroup 2	821 - 5.560 keV (microgroups 9 - 17)
Macrogroup 3	5560 - 1.840 eV (microgroups 18 - 35)

The effective few-group data for all lattice cells, as well as assembly-averaged data, are recalculated during burnup, being functions of the fuel isotopic concentrations at any given time. Even though the epithermal spectrum will not change as markedly during burnup as the thermal spectrum, it will also be influenced by the change in uranium, plutonium and fission product concentrations, and is therefore generally recalculated at the same burnup states at which the thermal spectrum calculation is performed. (An option in the code allows one, if desired, to keep the epithermal spectrum constant at that calculated for the initial state.)

4.2 Treatment of Resonance Absorption and Fission

The method in RECORD for treating resonance absorption reactions is based on calculation of resonance integrals and the determination of resonance distribution functions for the fuel resonance isotopes. The resonance reactions are dependent on isotopic compositions of resonance isotopes in a fuel and will therefore, in general, show both spatial and burnup dependence over an LWR fuel assembly. Resonance integrals and distribution functions are determined in RECORD for all fuel pin cells of an assembly, and are modified by Dancoff factors, which take into account the different resonance shielding effects for fuel pins at different positions in the fuel assembly lattice.

4.2.1 Resonance Absorption

Under the assumption of spatially flat source in the moderator, and where the resonance absorption at a given lethargy can be considered normalized to the moderator source (Ref. 13), the total resonance absorption in a micro-group j can be expressed by

$$R_j = (1 - p_j)q_{j-1} \quad (4.2.1)$$

where

$$q_{j-1} = \sum_{f=0}^{f_0} q_{f,j-1} + q_{F,j-1} \quad (4.2.2)$$

$$p_j = \exp \left[- \frac{\phi_j'}{q_{j-1}} \sum_{\ell=0}^{\ell_0} N_{\ell} \Delta R_{\ell,j}^A \right] \quad (4.2.3)$$

and where

- ϕ_j' = asymptotic flux at lower lethargy boundary of microgroup j
- ℓ_0 = no. of resonance absorption isotopes
- N_ℓ = homogenized number density of resonance isotope ℓ
- $\Delta R_{\ell,j}^A$ = resonance absorption integral for isotope ℓ in microgroup j
- q_f and q_F are slowing down densities (defined in Section 4.1.)

The lattice resonance integral is evaluated from

$$\Delta R_{\ell,j}^A = \alpha_\ell^A R_{SP,\ell}^A \psi_{\ell,j}^A \quad (4.2.4)$$

where

- $R_{SP,\ell}^A$ = total single-pin resonance absorption integral of isotopes ℓ
- $\psi_{\ell,j}^A$ = resonance distribution function, giving fraction of resonance absorption integral which is contained in microgroup j
- α_ℓ^A = mutual shielding factor

The calculation of lattice resonance integral for microgroup j is therefore based on a total single-pin resonance integral, which is modified by (a) the mutual shielding factor taking into account the influence of the lattice on

the resonance absorption in a given pin, and (b) the resonance distribution functions. See Sections 4.2.4 and 4.2.5 below.

For resonance absorption isotope ℓ , the resonance absorption in micro-group j is then calculated as

$$(\text{Res. abs})_j^\ell = \frac{N_\ell \Delta R_{\ell,j}^A}{\sum_{\ell=1}^{\ell_0} N_\ell \Delta R_{\ell,j}^A} R_j \quad (4.2.5)$$

The resonance absorption isotopes considered by RECORD are the fuel isotopes ^{235}U , ^{238}U , ^{239}Pu , ^{240}Pu and ^{241}Pu . For calculation of total resonance integrals, see Section 4.2.3.

4.2.2 Resonance Fission

For the resonance fission isotopes m , we assume that the ratio between fission and absorption in the microgroup is not influenced by energy variation of the moderator source or the shielding effect due to the presence of resonances in other isotopes. The resonance fission is then given by

$$(\text{Res. fis})_j^m = \frac{\Delta R_{m,j}^F}{\Delta R_{m,j}^A} (\text{Res. abs.})_j^m = \frac{N_m \Delta R_{m,j}^F}{\sum_{\ell=1}^{\ell_0} N_\ell \Delta R_{\ell,j}^A} R_j \quad (4.2.6)$$

where $\Delta R_{m,j}^F$ is the fraction of resonance fission integral contained in micro-group j . This lattice resonance fission integral is evaluated similar to the resonance absorption integral:

$$\Delta R_{m,j}^F = \alpha_m^F R_{SP,m}^F \psi_{m,j}^F \quad (4.2.7)$$

where

$R_{SP,m}^F$ = total single-pin resonance
fission integral of isotope m

$\psi_{m,j}^F$ = fraction of resonance fission
integral contained in microgroup j

α_m^F = mutual shielding factor.

4.2.3 Resonance Integrals

The procedure in RECORD for determining resonance reaction rates is based on representing the resolved resonance integrals as functions of composition and geometry of the fuel lattice. Together with energy distribution functions extracted from the code library, this enables very fast computation of resonance absorption and fission within required degree of accuracy. The method thus depends on using single-pin resonance integrals which have been determined for a wide range of lattices, and representing these in a suitable way in RECORD. The resonance integrals are based either on experiments, or have been calculated from more basic data.

The temperature-dependent, single-pin resonance integral for U^{238} is calculated from an empirical expression (Ref. 31), normalized to the well-known Hellstrand's formula (Ref. 32) for UO_2 fuel:

$$RI_{U^{238}} = RI_0 \exp[\alpha(\sqrt{T} - \sqrt{T_0})] + C \quad (4.2.8)$$

where

$$RI_0 = 30\sqrt{\frac{S}{M} + 0.077} \quad (4.2.9)$$

$$\alpha = 0.0696 - 0.000262 * \frac{M}{S} \quad (4.2.10)$$

T = effective fuel temperature ($^{\circ}\text{K}$)

T_0 = 300°

S/M = effective surface-to-mass ratio
for fuel rod (cm^2/gm), and

C = the normalization factor to the
Hellstrand formula at $T = T_0$:

$$C = \left[4.15 + 26.6 \sqrt{\frac{S}{M}} \right] * W - RI_0 \quad (4.2.11)$$

In this expression $W = 0.97$. Extensive evaluation calculations with RECORD on different lattices and using the present cross-section libraries, have shown the need for a reduction of the basic resonance integral by about 3% to obtain good agreement between calculated and measured reactivities.

Experimental values for lumped fission or absorption resonance integrals for other isotopes are not readily available, but can be calculated from resonance parameters using multi-level Breit-Wigner formalism. For the isotopes U^{235} , Pu^{239} , Pu^{240} , and Pu^{241} ; the single-pin resonance integrals in the resolved resonance energy region are represented in RECORD by the following function :

$$RI_{SP,\ell}^x = a_0 + \frac{a_1}{\sqrt{R_0 \epsilon_{\ell}}} + \frac{a_2}{R_0 \epsilon_{\ell}} \quad (4.2.12)$$

where

R_0 = fuel rod radius (cm)

ϵ_{ℓ} = isotopic enrichment (wt %) of isotope

and a_0 , a_1 and a_2 are fitted constants for isotope ℓ and reaction x (absorption or fission). These constants have been determined from resonance integrals calculated for a broad range of isotopic enrichments and fuel pin radii, and fitting the data to the function (Eq. 4.2.12), using a least square procedure. An example of such a fitting is given in Figure 4.2.1. The error due to the fitting is of the order 1 - 2%, depending on the isotope and reaction type for a broad interval of $R_0 \epsilon_\ell$, which is substantially less than the errors in the resonance integrals themselves being of the order of 5%. The contribution to the total resonance integral from the unresolved resonance energy region is obtained by adding the appropriate parts of the infinite dilution resonance integral to Equation 4.2.12. It should also be noted that the function (Eq. 4.2.12) is valid only for enrichments higher than some limiting value for ϵ_ℓ . If the isotopic enrichments are below this limiting value, then the resonance integrals are redefined by linear interpolation in the range from lower limiting value to infinite dilution value.

As is seen from the above, with the exception of U^{238} , the temperature dependence of the resonance integrals is neglected, being small compared to other effects. The reader is reminded that the resonance integrals apply for energies above 1.84 eV. The by far dominant resonance absorption in plutonium nuclides, are in the large resonances at 0.296 and 1.056 eV of Pu^{239} and Pu^{240} , respectively, and these are treated with the point energy approach in the thermal energy region. The temperature-dependent Doppler broadening is important for these resonances, and is taken into account using the Doppler functions of the single-level formalism in the calculation of capture and fission thermal cross-sections for these nuclides.

In the pinwise treatment of resonance reactions, RECORD calculates the single-pin resonance integrals using Equations (4.2.8) and (4.2.12), or using linear interpolation for low ϵ_ℓ , for each fuel pin in a given fuel assembly, as well as for the "average pin cell" in the epithermal spectrum calculation. In addition, for each fuel pin cell the code may also read the epithermal library and extract, if necessary, new distribution functions appropriate for given fuel rod radius and isotopic enrichments. Furthermore, as the isotopic compositions change during burnup, the code recalculates the

pinwise lattice resonance integrals, and new distribution functions are read from the library when necessary.

4.2.4 Mutual Shielding Factor

The expressions for resonance integrals given in the previous section apply for an isolated rod, and the calculation of resonance reactions must include a correction term, the so-called mutual shielding factor, which takes into account that the fuel rods in a lattice are not isolated from each other.

For U^{238} RECORD uses the method of Levine (Ref. 29), who has shown that the total lattice resonance integral for UO_2 rods, with dimensions of practical interest, can be expressed by the following equation :

$$R_L^{U^{238}} = 2.619 \sqrt{1.102 \sigma_S^O + \frac{1}{2NR_O} \cdot \frac{D}{1 + 0.1(1-D)}} + 0.89 \quad (4.2.13)$$

where

$\sigma_S^O = 3.7$ is the approximate constant epithermal scattering cross-section for oxygen

N = number density of the U^{238} absorber

R_O = fuel rod radius, and

D = the usual Dancoff Factor, expressing the probability that a neutron entering the moderator isotropically, will suffer a moderator collision before reaching another fuel rod.

The derivation of Equation (4.2.13) includes straight-line fits to Monte Carlo results of calculated resolved and unresolved resonance integrals. For further discussion of Equation (4.2.13) see Reference 12.

The single-pin resonance integral for ^{238}U , R_{SP}^{238} is obtained from Equation (4.2.13) by putting $D = 1$, and the mutual shielding factor is then given by

$$\alpha = R_{\text{L}}^{238} / R_{\text{SP}}^{238} \quad (4.2.14)$$

For ^{235}U and plutonium isotopes, another procedure is used. The resonance integral for a pin in a lattice, $RI_{\text{L},\ell}^{\times}$, is calculated using Equation (4.2.12), but with an effective fuel pin radius given by

$$R_{\text{eff}} = R_o / D \quad (4.2.15)$$

where R_o is the fuel rod radius and D is the Dancoff factor for the lattice. The effective mutual shielding factor for isotope ℓ and reaction \times is then calculated by

$$\alpha_{\ell}^{\times} = RI_{\text{L},\ell}^{\times} / RI_{\text{SP},\ell}^{\times} \quad (4.2.16)$$

The mutual shielding factor is thus a function of the Dancoff factor for a given pin. RECORD performs very fast calculation of this factor, by making use of the method of Sauer (Ref. 33), assuming a homogeneous mixture of clad and water as effective "moderator" outside the fuel pin:

$$D = 1 - \frac{e^{-\tau \Sigma_m \bar{\ell}_m}}{1 + (1-\tau) \Sigma_m \bar{\ell}_m} \quad (4.2.17)$$

where

$$\bar{\ell}_m = \frac{4 V_m}{S_f} = \text{average chord length in "moderator"}$$

$$\Sigma_m = \text{total epithermal cross-section in "moderator"}$$

V_m = volume of "moderator" (including clad volume)

S_f = surface area of fuel rod

τ = a "geometric index" which is given by

$$\tau = T/\bar{\ell}_m - 0.08 = (P - 2R_o)/\bar{\ell}_m - C \quad (4.2.18)$$

where

T = shortest chord length in "moderator"

P = lattice pitch

R_o = fuel rod radius

$C = \begin{cases} 0.08, & \text{square lattice} \\ 0.12, & \text{hexagonal lattice, (single-pin} \\ & \text{case only in RECORD)} \end{cases}$

Equation (4.2.17) assumes a fuel pin embedded in a uniform lattice. This will not be the case for the corner and edge pins in a fuel assembly, nor those pins adjacent to empty positions in a lattice, and the Dancoff factor has to be modified accordingly. In the square lattice geometry assumed in RECORD, the screening factors 1-D for the corner and edge pins are at present approximated by multiplying by 3/8 and 5/8, respectively, together with a semi-empirical correction due to shielding effects from neighboring fuel assemblies, which will be dependent on the water gap thickness. Corresponding corrections to 1-D are made also for those pins in the vicinity of water holes within the lattice.

4.2.5 Resonance Distribution Functions

Normalized distribution functions for resonance absorption, $\psi_{\ell,j}^A$, and for resonance fission, $\psi_{\ell,j}^F$, are used in the lattice resonance integral calculations for a resonance isotope ℓ , to determine the fraction of the resonance integral which is contained in a microgroup j . The normalization condition is

$$\sum_j \psi_{\ell,j} \Delta u_j = 1 \quad (4.2.19)$$

where the summation is taken over all microgroups and Δu_j is the lethargy width of group j . $\psi_{\ell,j}$ is equal to zero outside the defined region, so that the normalization condition corresponds to normalization in the resonance region. The defined resonance region will vary from element to element.

The ψ -functions will depend on lattice geometry, and composition or fuel temperature. The method in RECORD is to use precalculated ψ -values which have been obtained for a broad range of lattices covering the variations in typical lattices to be expected when applying RECORD to LWR analysis. The ψ -functions are stored in the code epithermal library as functions of rod radius and isotopic enrichments for U²³⁵ and the plutonium isotopes. For U²³⁸ the ψ -functions have been calculated and stored in the library as function of rod radius and fuel temperature.

For a given case, RECORD will select from the library those ψ -functions most appropriate to the lattice to be treated. As has been mentioned in Section 4.2.3, the code selects ψ -functions for each fuel pin in the lattice depending on enrichment, dimensions or temperature, and will redefine these during burnup, if necessary, as the isotopic concentrations change.

4.3 Fast Advantage Factor

At high energies, due to the fission source in fuel, the average flux in the fuel will be higher than the average flux in clad and moderator. In the

epithermal calculations, the spectrum calculated is a space-average of the real flux in the moderator and clad regions of the average pin cell, and a correction must be introduced to obtain correct calculation of the reaction rates at the high energies. This is accounted for by the introduction of a "fast advantage factor", defined as the ratio of the average flux in fuel to the average flux in clad and moderator. From the balance equations for the fuel and moderator at lethargies where we have only slowing-down of neutrons, we obtain the general expression for the fast advantage factor:

$$\xi = \frac{\bar{\phi}_f(u)}{\bar{\phi}_m(u)} = (1-\beta) \frac{V_m}{V_f} \cdot \frac{\Sigma_m}{\Sigma_f} \cdot \frac{1-P_0^*}{P_0^*} + \beta \quad (4.3.1)$$

where

P_0^* = escape probability from fuel to moderator

β = normalized scattering source in moderator

V_m = volume of moderator

V_f = volume of fuel

Σ_m = total epithermal cross-section in
moderator

Σ_f = total epithermal cross-section in fuel

Basically, the fast advantage factor is a function of neutron energy. However, the absorption, fission and scattering cross-sections for the main fuel isotopes show only small variations in the high energy range (lethargy range $0 < u < 2.4$), and it can be shown that, to a first approximation, an energy-independent fast advantage factor may be applied for the high energy range under consideration. The main fuel isotopic cross-sections are therefore multiplied by a constant fast advantage factor in the specified energy

range, to give approximate correct absorption, fission and scattering rates in the fuel.

More detailed discussion of the assumptions involved, and expressions for evaluating the terms in Equation (4.3.1), are given in Reference 12.

For those energy groups below the range where the fast advantage factor is applied, the flux is assumed to be the same in the moderator, cladding and fuel. The flux in the fictitious homogeneous system for which the epithermal equations are solved, will then be equal to the assumed flux in the heterogeneous system.

4.4 Macrogroup Data

When the epithermal neutron energy spectrum has been calculated using the theory described in the previous sections, the next stage in the calculations is the determination of effective epithermal few-group data for all lattice cells and other regions of the fuel assembly cell. As has been explained in Section 4.1, the number of epithermal few-groups in RECORD is fixed at three, and the effective cross-sections for these macrogroups are obtained in principle by integrating the microgroup cross-sections over the neutron spectrum, and where proper account is taken also of the resonance absorption and fission in the relevant isotopes.

4.4.1 Macrogroup Absorption and Fission Cross-Sections

For a given neutron energy spectrum $\phi(u)$, an effective microscopic cross-section for reaction x is defined by

$$\bar{\sigma}_x = \frac{\int \sigma_x(u) \phi(u) du}{\int \phi(u) du} \quad (4.4.1)$$

Integrating over a macrogroup M , and replacing the integration by summation, the effective cross-section of isotope i in that macrogroup is given by

$$\bar{\sigma}_{x,M}^i = \frac{1}{\phi_M} \sum_{j \text{ in } M} \sigma_{x,j}^i \phi_j \quad (4.4.2)$$

where

$$\phi_M = \sum_{j \text{ in } M} \phi_j \quad \text{is the group flux in macrogroup } M, \text{ and}$$

$$\sigma_{x,j}^i \quad \text{is the effective microgroup cross-section for isotope } i, \text{ reaction } x, \text{ in microgroup } j$$

For a resonance absorption isotope, the absorption in macrogroup M can be expressed as

$$(\text{Abs})_M^\ell = N_\ell \bar{\sigma}_{a,M}^\ell \phi_M + (\text{Res. abs.})_M^\ell \quad (4.4.3)$$

where N_ℓ is the homogenized number density of isotope ℓ .

The resonance absorption is calculated from

$$(\text{Res. abs.})_M^\ell = N_\ell \sum_{j \text{ in } M} A_{\ell,j} \quad (4.4.4)$$

where

$$A_{\ell,j} = \frac{\Delta R_{\ell,j}^A}{\sum_{\ell=1}^{\ell_0} N_\ell \Delta R_{\ell,j}^A} R_j \quad (4.4.5)$$

R_j = total resonance absorption in microgroup j
(Eq. 4.2.1)

$\Delta R_{\ell,j}^A$ = lattice resonance absorption integral
(Eq. 4.2.4)

ℓ_0 = no. of resonance absorption isotopes

The total absorption in macrogroup M is then given by

$$(\text{Abs.})_M^T = \sum_{i=1}^{k_0} N_i \bar{\sigma}_{a,M} \phi_M + \sum_{\ell=1}^{\ell_0} (\text{Res. abs.})_M^{\ell} \quad (4.4.6)$$

where k_0 = total no. of isotopes in system.

The last term reduces to

$$\sum_{j \text{ in } M} R_j$$

The average macroscopic absorption cross-section for group M is defined from the total absorption according to

$$\Sigma_{a,M} \phi_M = (\text{Abs.})_M^T \quad (4.4.7)$$

giving

$$\Sigma_{a,M} = \sum_{i=1}^{k_0} N_i \bar{\sigma}_{a,M}^i + \frac{1}{\phi_M} \sum_{j \text{ in } M} R_j \quad (4.4.8)$$

From the total fissions in macrogroup M is derived, in a similar way, the macroscopic fission cross-section

$$\Sigma_{f,M} = \sum_{\ell=1}^{\ell_0} N_{\ell} \bar{\sigma}_{f,M}^{\ell} + \frac{1}{\phi_M} \sum_{m=1}^{m_0} N_m \sum_{j \text{ in } M} F_{m,j} \quad (4.4.9)$$

where

$$F_{m,j} = \frac{\Delta R_{m,j}^F}{\sum_{\ell=1}^{\ell_0} N_{\ell} \Delta R_{\ell,j}^A} R_j \quad (4.4.10)$$

$\Delta R_{m,j}^F$ = lattice resonance fission integral
(Eq. 4.2.7)

N_m = homogenized number density of resonance
fission isotope m

s_o = no. of resonance fission isotopes

4.4.2 Macroscopic Removal Cross-Section

In the calculation of the removal cross-section in a macrogroup M, considered separately, is the removal of neutrons due to elastic scattering in light "Greuling-Goertzel" isotopes, and that due to scattering in the more heavy "Fermi age" isotopes. In addition comes the contribution from inelastic scattering.

Let u_{M-1} and u_M be the lethargy boundaries for a macrogroup M, and let

$$u_{M-1} < u' < u_M$$

(a) "Greuling-Goertzel" Isotope :

Total number of neutrons scattered out of macrogroup M due to a "light" isotope f is given by

$$Q_{f,M}^R = \frac{1}{1 - \alpha_f} \int_{u_{M-1}}^{u_M} \Sigma_f^S(u') \phi(u') (e^{u' - u_M} - \alpha_f) du' \quad (4.4.11)$$

Assuming "flat" flux over microgroup j , we get:

For $u_M - u_{M-1} < -\ln \alpha_f$

$$Q_{f,M}^R = \frac{1}{1 - \alpha_f} \sum_{j \text{ in } M} \Sigma_{f,j}^S \phi_j \left(\frac{1}{\Delta u_j} e^{u_j - u_M} (1 - e^{-\Delta u_j}) - \alpha_f \right) \quad (4.4.12)$$

where

$-\ln \alpha_f$ = maximum lethargy gain per collision

α_f = $(A - 1)^2 / (A + 1)^2$ (A_f is atomic mass)

ϕ_j = flux in microgroup j

Δu_j = lethargy width of microgroup j

$\Sigma_{f,j}^S$ = elastic scattering cross-section of "light" isotope f in microgroup j

For $u_M - u_{M-1} \geq -\ln \alpha_f$

$$Q_{fM}^R = q_f(u_M) \quad (4.4.13)$$

where

$q_f(u_M)$ is the slowing down density at u_M from isotope f .

(b) "Fermi Age" Isotopes :

Since aluminium is the lightest of the isotopes treated by Fermi age theory in RECORD, we will always have

$$u_M - u_{M-1} \geq - \ln \alpha_{Al} \sim 0.16$$

The elastic scattering out of the macrogroup because of the "heavy" isotopes is then given by

$$q_{F,M}^R = q_F(u_M) \quad (4.4.14)$$

where

$q_F(u_M)$ is the total slowing down density at u_M from the "heavy" isotopes.

(c) Inelastic Removal :

The removal of neutrons due to inelastic scattering is given by

$$I_M^R = \sum_{j \text{ in } M} \sum_{i > j_M} a_{i,j} \Sigma_j^I \phi_j \quad \text{for } j_{in} > j_M \quad (4.4.15)$$

$$I_M^R = 0 \quad \text{for } j_{in} \leq j_M$$

where

a_{ij} = element in the inelastic scattering matrix

Σ_j^I = total inelastic scattering cross-section
in microgroup j

j_{in} = inelastic "cut-off"

The total removal of neutrons from macrogroup M, due to both elastic and inelastic slowing down, is thus

$$Q_M^R = \sum_{f=1}^{f_0} Q_{f,M}^R + a_{F,M} + I_M^R \quad (4.4.16)$$

The removal cross-section in macrogroup M is then defined as

$$\Sigma_{r,M} = \frac{Q_M^R}{\phi_M} \quad (4.4.17)$$

4.4.3 Diffusion Coefficient

From the solution of the fundamental one-dimensional B-1 equations, is derived the general expression for the lethargy-dependent diffusion coefficient

$$D(u) = \frac{L_o(u)}{B_o^2 \phi_o(u)} \quad (4.4.18)$$

where

$L_o(u)$ is the net leakage in the middle of the reactor, corresponding to the flux $\phi_o(u)$, and B_o^2 is the buckling.

The effective diffusion coefficient for macrogroup M is calculated as

$$D_M = \frac{\sum_{j \text{ in } M} L_j}{\sum_{j \text{ in } M} B_o^2 \phi_j} \quad (4.4.19)$$

where

$L_j = B_o^2 J_j$ is the microgroup leakage

J_j = microgroup current

TABLE 4.1.1 Energy and Lethargy Structure in the 35-Group Epithermal Cross-Section Library of RECORD

GROUP	LOWER ENERGY BOUNDARY (eV)	UPPER LETHARGY BOUNDARY
1	7.189 · 10 ⁶	0.3300
2	5.169 · "	0.6599
3	3.716 · "	0.9899
4	2.671 · "	1.3201
5	1.920 · "	1.6503
6	1.381 · "	1.9798
7	9.926 · 10 ⁵	2.3100
8	8.210 · "	2.5000
9	5.130 · "	2.9701
10	3.688 · "	3.3001
11	2.652 · "	3.6299
12	1.906 · "	3.9602
13	1.370 · "	4.2904
14	5.572 · 10 ⁴	5.1900
15	2.265 · "	6.0902
16	9.210 · 10 ³	6.9901
17	5.560 · "	7.5000
18	1.522 · "	8.7903
19	6.190 · 10 ²	9.6900
20	2.517 · "	10.5899
21	1.900 · "	10.8711
22	1.350 · "	11.2128
23	1.100 · "	11.4176
24	82.000	11.7114
25	63.000	11.9750
26	45.000	12.3114
27	32.000	12.6524
28	26.000	12.8600
29	20.000	13.1224
30	15.000	13.4100
31	11.000	13.7202
32	8.000	14.0387
33	5.400	14.4317
34	3.150	14.9707
35	1.840	15.5083

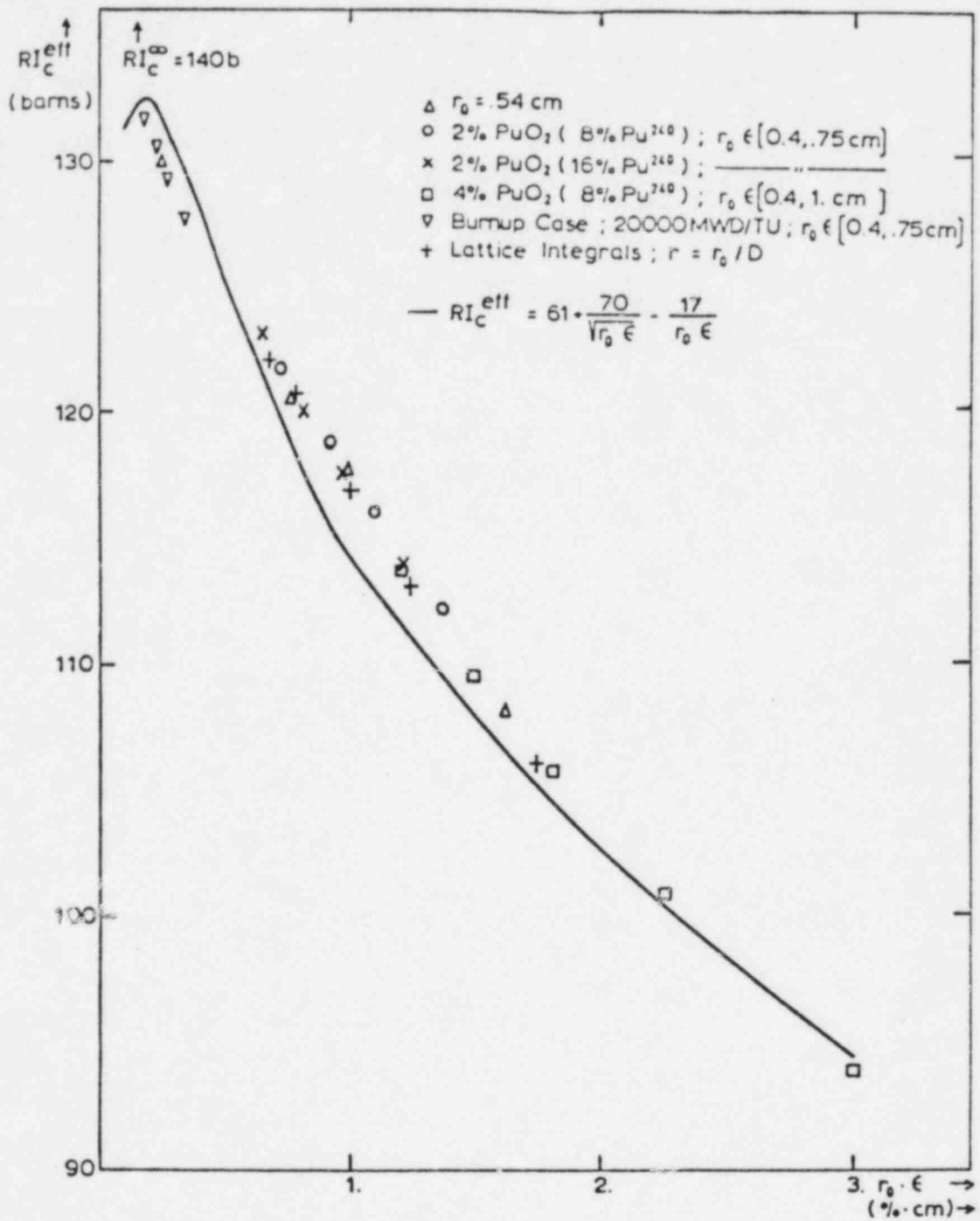


FIGURE 4.2.1 Effective Single-Pin Capture Resonance Integral for Pu^{239} as a Function of Pin Radius and Isotopic Enrichment (1.84-110 eV)

5. TREATMENT OF BURNABLE POISON

Modern LWR fuel assemblies contain highly absorbing cells, such as burnable poison (gadolinium) fuel pins or burnable absorber (boron) shim rods. The presence of such highly absorbing pins requires detailed calculations of neutron distributions in space and energy within these pins as function of burnup for correct prediction of reaction rates and reactivity. In BWR fuel assemblies, the reaction rates in burnable poison pins are sensitive to the void in the surrounding moderator, and the accuracy of the burnable poison model is of importance also for void coefficient calculations.

In the FMS-system, two associated codes, THERMOS and GADPOL, are used in treating burnable poison cells. The results of calculations with these codes are subsequently fed into the RECORD code in the form of effective cross-sections for gadolinium containing pin cells or boron shim rods. Optionally, a precalculated GADOLINIUM LIBRARY is available for gadolinium-containing fuel pins in 8 x 8 assemblies for a certain range of uranium and gadolinium enrichments.

5.1 The THERMOS - GADPOL Method

The method uses a burnup version of the transport theory code, K7-THERMOS (Ref. 15), to treat the burnable poison cell configuration and the depletion of the burnable absorber, while the GADPOL code modifies the THERMOS results to be suited for the later diffusion theory calculations in RECORD.

In THERMOS, a local part of the fuel assembly is described in cylindrical geometry (Fig. 5.1.1). It consists of the burnable poison cell, described explicitly, and its eight closest lattice cells, given as a homogeneous mixture of fuel and moderator. Additional hydrogen is introduced in an outer region to simulate the spectrum softening effect of the water gap surrounding the assembly. Use of fine mesh and several regions inside the poison cell, ensures a detailed description of the thermal flux dip. The maximum number of mesh points is 24, and 17 energy points can be used in the thermal energy range up to 1.84 eV. The point energy approach (Refs. 9, 10)

is applied in THERMOS where 17 energy points is equivalent to about 30 - 35 energy groups.

The THERMOS-calculated cross-sections are normalized to the surface flux of the poisoned pin cell. To ensure the conservation of the reaction rates in this highly absorbing pin cell when using RECORD, the GADPOL Code is applied to modify the THERMOS cross-sections before these are given as input to RECORD. In GADPOL, two-dimensional diffusion calculations in x - y geometry are performed. The calculation extends over the same region of the assembly as defined in THERMOS, while the mesh point distribution is equal to the RECORD distribution in that part of the assembly. Any mesh in RECORD may then be freely chosen, also with mesh points inside the poison cell, and still get the correct reaction rates and burnup distribution.

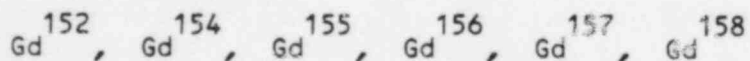
Thus effective shielded thermal cross-sections, representing the highly absorbing pin cell, are provided to RECORD. These cross-sections are functions of time-integrated thermal surface flux for the pin cell, and they are given in tabular form for use in RECORD.

All data transfer between THERMOS / GADPOL / RECORD is automated on disc files.

The description given assumes, in principle, a single burnable poison cell surrounded by lattice cells which do not contain any burnable poison. A modification of the THERMOS/GADPOL model, however, also enables treatment of the problem of two gadolinium-containing fuel pins in adjacent lattice positions, arising in certain BWR fuel assembly designs.

5.2 Gadolinium Treatment

In natural gadolinium, all isotopes from Gd^{152} to Gd^{161} occur (Table 5.2.1). In the FMS modelling of gadolinium burnup, using the THERMOS/GADPOL system, the following Gd-isotopes are included:



The main absorption in gadolinium isotopes occurs in the thermal energy range. The initial epithermal contributions to the total absorption rates are about 10 - 12 % for Gd^{155} and less for the other isotopes.

The effect of epithermal resonance capture on the burnup of Gd-isotopes is included by introduction of an "epithermal group" in the thermal spectrum code THERMOS. This is done by using externally calculated effective resonance integrals. These are calculated by taking into account self-shielding and shielding from other important resonance absorbers (U^{235} , U^{238} , Pu and gadolinium isotopes), and a spatially flat and $1/E$ -dependent epithermal spectrum.

Results from THERMOS consist of microscopic fission and absorption cross-sections for the U and Pu isotopes present, together with macroscopic absorption cross-sections for the poison, and scattering removal cross-sections and diffusion coefficient for the whole pin cell. The cross-sections are given for the two thermal macro energy groups used in RECORD, and at different burnup steps, until the absorption in gadolinium is negligible.

As the highly absorbing isotopes Gd^{155} and Gd^{157} deplete, the total absorption in gadolinium goes into an equilibrium situation, and we have a so-called residual gadolinium effect. It was found that this residual poison is practically constant after a given flux-time, which is chosen as the "switch-over point".

Before this point in time, the cross-sections applied in RECORD for fuel pin cells containing gadolinium, come from the THERMOS/GADPOL codes. After this point, however, RECORD-generated cross-sections are used, and the effect of residual gadolinium is accounted for through the macroscopic rest absorption of the cell, as calculated from THERMOS/GADPOL at this burnup.

5.3 Shim Rod (Boron Glass) Treatment

The FMS modelling of burnup in the PWR burnable absorber shim rods (both the annular, pyrex glass type, and the solid boral type absorber) is performed using the THERMOS/GADPOL system.

The effect of epithermal absorption in B^{10} on boron burnup is taken into account by introduction of an "epithermal group" in THERMOS. This epithermal absorption is calculated based on the assumption of a spatially constant and $1/E$ -dependent epithermal neutron spectrum. It is also assumed that this epithermal absorption does not influence the thermal spectrum.

Because of this artificial epithermal treatment in THERMOS, the depletion of B^{10} is recalculated in RECORD, using the effective thermal microscopic B^{10} cross-sections from THERMOS and the epithermal ones from the RECORD calculation.

The effective quantities calculated by THERMOS/GADPOL and transferred to RECORD are : the effective thermal microscopic cross-sections mentioned above, the shim rod cell diffusion coefficient, macroscopic scattering removal, and rest absorption cross-sections (B^{10} poison excluded).

The THERMOS results are modified by GADPOL, similar to the description given in Section 5.1, and the quantities are given as function of time-integrated thermal surface flux of the shim rod cell.

TABLE 5.2.1 Average Neutron Cross-Sections for the Gd-Isotopes

ISOTOPE	ABND. (%)	Cross-Sections (σ) / Resonance Integrals (RI) (barns)			
		THERMAL		EPITHERMAL	
		$\sigma_{n\gamma}$	σ_{nn}	RI_Y^∞	RI_Y^{eff}
Gd ¹⁵²	0.2	1100±100	6.81 ³⁾	3000±300	2000
Gd ¹⁵³ ²⁾	Unstable (β^+)	97	-	~100	
Gd ¹⁵⁴	2.2	85±12	6.86 ³⁾	215±20	180
Gd ¹⁵⁵ ¹⁾	14.9	61100±500	63.5	1550±50	1110
Gd ¹⁵⁶	20.6	1.5 ±1.2	8.24 ³⁾	95±5	90
Gd ¹⁵⁷ ¹⁾	15.7	254300±2000	1010	730±20	493
Gd ¹⁵⁸	24.7	2.5 ±0.5	5.31 ³⁾	61±6	-
Gd ¹⁵⁹ ²⁾	β -unstable $t_{1/2}$ =18.56 hrs	-	-		
Gd ¹⁶⁰	21.7	0.77±0.02	5.0 ³⁾	7.0±1.0	-
Gd ¹⁶¹ ²⁾	β -unstable $t_{1/2}$ =3.7 min	31000±12000	-		

Ref. : BNL-325, 3. Edition

1) ENDF/B-III

2) Nuklidkarte, 4. Auflage 1974

3) Calculated with RESU-II, based on resonance parameters from BNL-325.

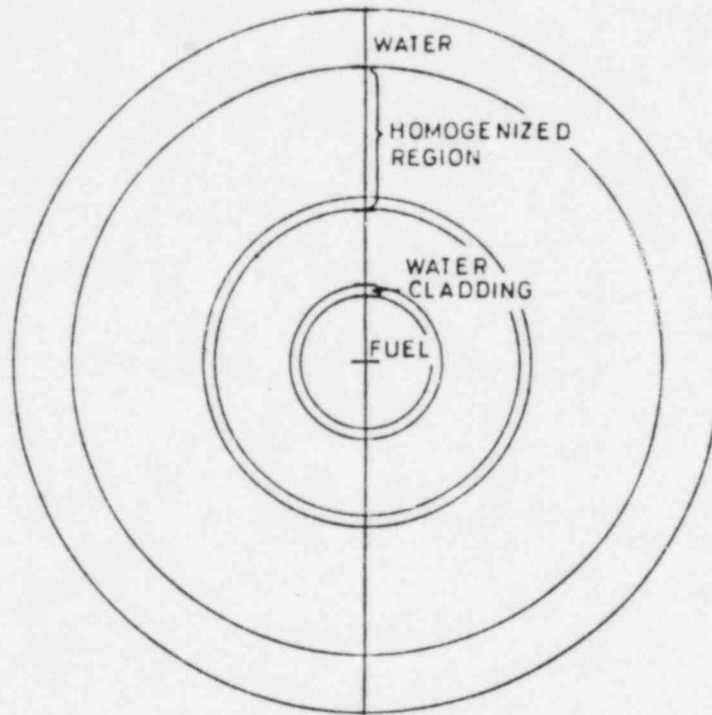


FIGURE 5.1.1 Geometry in THERMOS for Gadolinium Fuel Calculations

6. CONTROL ABSORBERS

Control rod absorbers are treated in RECORD as non-diffusion subregions, defined by boundary conditions applied at the absorber surfaces. The boundary conditions are current-to-flux ratios calculated from transport theory approximations. Both BWR control blades and PWR rod cluster control elements are treated directly by the code.

6.1 Control Blades - BWR Option

Two types of boron-based BWR control absorbers are modelled in RECORD:

- Solid-blade cruciform absorbers
- Rodded-blade cruciform absorbers

The effect of an inserted control blade is accounted for by treating the blade as the boundary for the neutron diffusion region (see Chapter 7). Effective 5-group boundary conditions are obtained, as below described, based on transport theory approximations accounting for detailed, geometrical effects and for the presence of neutron scattering materials in addition to the absorbing material.

6.1.1 Solid Blade Absorbers

The mono-energetic, diffusion theory, current-to-flux ratio, α , is obtained by :

$$\alpha = \frac{1}{2} \cdot \frac{1 - T_i - R_i}{1 + T_{an} + R_{an}} \quad (6.1.1)$$

where

T_i = slab transmission probability,
isotropic angular distribution

R_i = slab reflection probability, isotropic angular distribution

T_{an} = slab transmission probability, linearly anisotropic angular distribution

R_{an} = slab reflection probability, linearly anisotropic angular distribution

The transmission and reflection probabilities are functions of the slab optical thickness and the ratio of scattering-to-total cross-section. A semi-empirical formulation (Ref. 34), yielding very good agreement with tabulated transport theory results (Ref. 35), is used to calculate T_i , R_i , T_{an} and R_{an} .

The diffusion theory current-to-flux ratio is normalized to the transport corrected current-to-flux ratio for a black boundary :

$$\frac{1}{\alpha_{eff}} = \left(\frac{1}{\alpha} - \frac{1}{0.5} \right) + \frac{1}{0.4692} \quad (6.1.2)$$

where

α_{eff} = effective, diffusion theory current-to-flux ratio

α = Equation (6.1.1)

($\alpha_{eff} = 0.4692$ for a black slab)

Effective boundary conditions are obtained for each microgroup, and are subsequently collapsed into the macrogroup (5-group) structure used in RECORD. The lattice flux spectrum, modified with slab flux depression factors, $1/(1 + \sqrt{3}\alpha)$, (Ref. 36), is used as weight factors in calculating the macrogroup average α -values.

Optionally, the macrogroup values are further modified to account for the influence of an outer stainless steel clad on the absorber blade.

6.1.2 Rodded-Blade Absorbers

The blade of a rodDED control absorber typically consists of an array of B_4C -filled, stainless steel tubes contained within a stainless steel sheath. Water is allowed to flow inside the sheath.

Diffusion theory current-to-flux ratios are calculated for the outer surface of the blade sheath or clad. The mono-energetic current-to-flux ratio is obtained by Equation 6.1.1, replacing the slab transmission and reflection coefficients by the corresponding values for cylindrical absorbers. These coefficients are calculated by a formulation (Ref. 37) making use of the corresponding slab values, and applying empirical correction factors to account for the cylindrical geometry. Blackness coefficients as calculated by the method used in RECORD, in comparison with tabulated transport theory results (Ref. 38), are shown in Figure 6.1.1. The blackness coefficient, B , is related to the current-to-flux ratio, α , by :

$$B = \frac{4\alpha}{1 + 2\alpha} \quad (6.1.3)$$

The following formula, as derived in Reference 37, is used to account for the stainless steel tube, regarded as a clad to the B_4C absorber :

$$B = B_0 \left[\frac{1 - 2\Sigma_T \Delta (1 - F_1)}{1 - 2\Sigma_s \Delta F_1 B_0} \right] \cdot \left[(1 - 2\Sigma_T \Delta) F_2 + 2\Sigma_s \Delta F_1 \right] \quad (6.1.4)$$

where

B_0 = albedo (= $1-B$), unclad absorber

B = albedo at clad outer surface

Σ_T, Σ_s = clad total and scattering macroscopic cross-sections

Δ = clad thickness

F_1 = probability that neutrons originating from a uniform, isotropic source in the clad will enter the absorber

F_2 = probability that neutrons with a P_1 angular distribution at the clad outer surface will be directed toward the absorber

The following approximations are used :

$$F_1 \approx \frac{1}{4} \left(\frac{2 R_o + \Delta}{R} \right)$$

where

R_o = absorber outer radius

R = clad outer radius

$$F_{2,i} \approx \frac{R_o}{R}$$

$$F_{2,an} \approx 1.0$$

where subscripts i and an denote the isotropic and linearly anisotropic components of F_2 .

For cylindrical absorbers, transformation to α_{eff} is obtained as follows (Ref. 17) :

$$\alpha_{eff} = \frac{1}{3\lambda_{eff}} \quad (6.1.5)$$

with

$$\lambda_{\text{eff}} = \frac{4}{3} \cdot \frac{1 - B}{B} + \frac{\Sigma_{\text{tr}} \cdot R + 0.7604}{\Sigma_{\text{tr}} \cdot R + 0.4052} \cdot 0.7104 \quad (6.1.6)$$

where

$$\Sigma_{\text{tr}} = \text{transport cross-section of exterior medium} \\ \text{(lattice region)}$$

The single cylinder α_{eff} (Eq. 6.1.5) is calculated for each macrogroup (five groups) after collapsing the microgroup values, as described above, for slab absorbers.

The effective current-to-flux ratio, α_s , on a plane surface tangential to an array of absorbing cylinders is given by

$$\frac{1}{\alpha_s} = \frac{P}{\pi R} \left(\frac{G}{L \Sigma_a} + \frac{1}{\alpha_c} \right) - \frac{1}{L \Sigma_a} \quad (6.1.7)$$

where

P = cylinder pitch

R = cylinder radius

L = exterior medium diffusion length

Σ_a = exterior medium macroscopic absorption
cross-section

α_c = single cylinder α_{eff} (from Eq. 6.1.5)

G = expression containing modified Bessel functions

This formula, derived in Reference 37, is based on an expression for the diffusion theory current into an absorbing cylinder, being a member of an infinite, linear array of equal cylinders given in Reference 39.

Comparisons of α_{eff} -values, calculated with the method described above with reference transport calculations (numerical integration, Ref. 40), are shown in Figure 6.1.2. Results are shown both for typical cold and hot voided exterior medium (Eq. 6.1.7) and for R/P = 0.5 and 0.3. A further discussion of these results is given in Reference 37.

The final step in calculating the rodded-blade current-to-flux ratio is to account for the stainless steel blade sheath. Reflection and transmission coefficients for the sheath, regarded as an absorbing and scattering slab, are obtained by the method described above under Section 6.1.1. These coefficients are used to account for the influence of the blade sheath on the final, macrogroup current-to-flux ratios, as described in Reference 41.

6.2 Rod Cluster Control - PWR Option

Rod cluster control elements, based on either boron or Ag-In-Cd as the absorber material, may be represented in RECORD. The elements are regarded as absorbing cylinders with an optional stainless steel or zircaloy clad.

Effective current-to-flux ratios are calculated as described above (Eq. 6.1.5), based on transport theory approximations for the neutron transmission and reflection coefficients. An exception is made for the resolved resonance region (10 eV to 350 eV) for Ag-In-Cd absorbers. Here, the neutron slowing-down process is described by a modified NRIM approximation. An analytic expression for the resonance integral is obtained, including the Doppler effect on resonance absorption. The method is based on work described in Reference 42, and described in detail in Reference 18.

The cylindrical absorber elements are represented as equivalent square regions in the rectangular mesh of the diffusion routine in RECORD. Trans-

formation of the effective current-to-flux ratios from cylindrical to rectangular geometry is performed following a method described in Reference 17 :

$$\alpha_{x-y} = \gamma \cdot \frac{\sqrt{\pi}}{2} \alpha_{cyl} \quad (6.2.1)$$

The transformation factor γ is unity for the epithermal region and for the highest thermal group. For the lowest thermal group, γ is represented by the following polynomial :

$$\gamma = a_0 + a_1 \alpha_{cyl} + a_2 \alpha_{cyl}^2 \quad (6.2.2)$$

The coefficients a_0 , a_1 and a_2 are found by least square fitting to data reported in Reference 17.

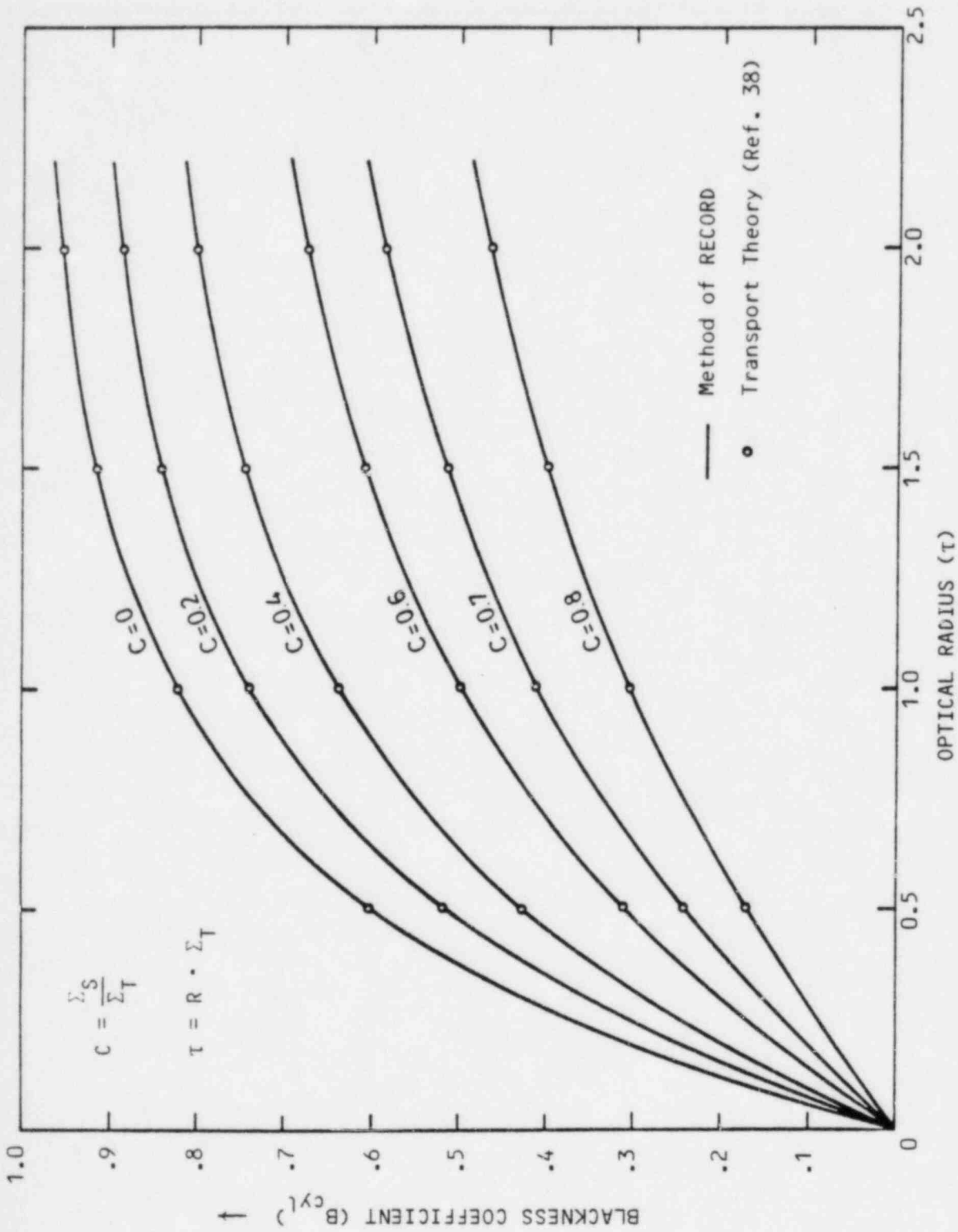


FIGURE 6.1.1 Blackness Coefficient of Cylindrical Absorbers vs. Optical Radius

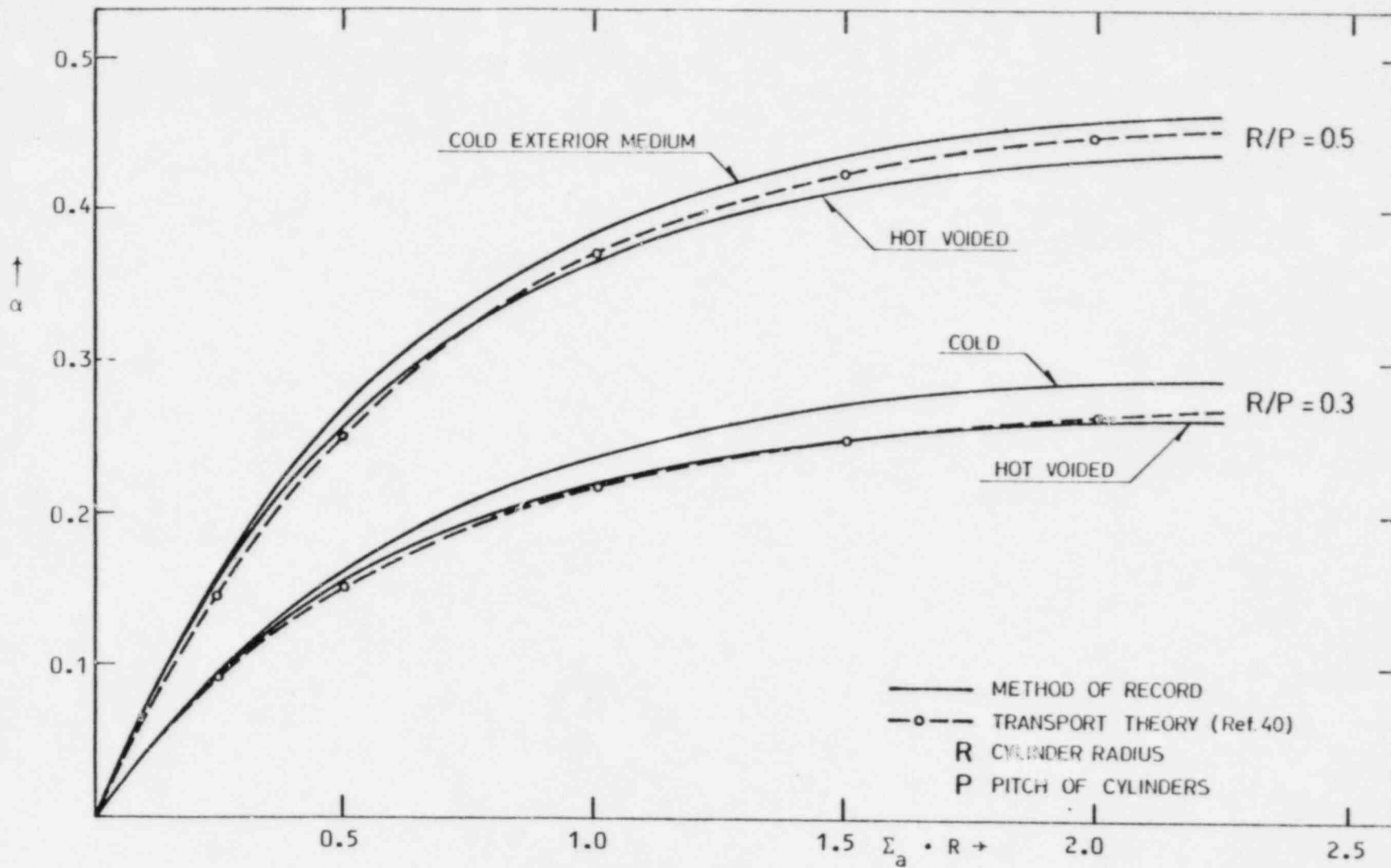


FIGURE 6.1.2 Effective Current-to-Flux Ratios for Array of Cylindrical Absorbers as Calculated with Method used in RECORD, in Comparison with Transport Theory Reference Results

7. TWO-DIMENSIONAL FLUX AND POWER DISTRIBUTION

The multigroup flux calculations across a fuel assembly and adjacent water gaps, and the eigenvalue (k_{eff}) of the system, are determined from two-dimensional five-group diffusion theory, using the methods of the MD-2 code (Ref. 19).

7.1 Multigroup Diffusion Equations

The two-dimensional diffusion equation for group g ($g = 1, 2, \dots, G$) in Cartesian coordinates is written:

$$\begin{aligned}
 & - \frac{\partial}{\partial x} D^g(x,y) \frac{\partial}{\partial x} \phi^g(x,y) - \frac{\partial}{\partial y} D^g(x,y) \frac{\partial}{\partial y} \phi^g(x,y) \\
 & + \sigma^g(x,y) \phi^g(x,y) = s^g(x,y)
 \end{aligned} \tag{7.1.1}$$

where

$$\sigma^g = D^g B^g + \Sigma_a^g + \sum_{\substack{g'=1 \\ g' \neq g}}^G \Sigma_r^{g \rightarrow g'} \tag{7.1.2}$$

$$s^g = \sum_{\substack{g'=1 \\ g' \neq g}}^G \Sigma_r^{g' \rightarrow g} \phi^{g'} + \frac{\chi^g}{\lambda} \sum_{g'=1}^G (\nu \Sigma_f)^{g'} \phi^{g'} \tag{7.1.3}$$

with

D^g = diffusion coefficient, group g

Σ_a^g = macroscopic absorption cross-section,
group g

$\Sigma_r^{g \rightarrow g'}$ = macroscopic removal cross-section from
group g to g'

χ^g = fraction of fission yield in group g

$(\nu \Sigma_f)^g$ = ν times macroscopic fission cross-section,
group g

B^g = transverse buckling, group g

λ = eigenvalue (k_{eff})

ϕ^g = neutron flux, group g

The boundary conditions are:

$$D^g(x,y) \frac{\partial}{\partial n} \phi^g(x,y) + \alpha^g(x,y) \phi^g(x,y) = 0 \quad (7.1.4)$$

$$g = 1, 2, \dots, G$$

where

$\frac{\partial}{\partial n}$ = the normal derivative operator, and

α = the current-to-flux ratio

7.2 Geometry and Mesh Description

The solution is approximated over a rectangular area that is composed of subregions separated by interfaces parallel to the outer boundaries of the rectangular area.

Two types of subregions exist, the diffusion subregions in which all the coefficients for group g in Equation (7.1.1) are constants, and the non-diffusion subregion where the neutron flux is not defined.

Across an interface between two diffusion subregions, the flux and the current are continuous. On the outer boundaries and the interfaces between diffusion and non-diffusion subregions, the boundary conditions (Eq. 7.1.4) must be satisfied.

A nonuniform grid of mesh lines is imposed on the rectangular area. Each line must be parallel to a boundary line and must extend from one boundary to the opposite boundary. The mesh lines must be chosen such that the subregion interfaces coincide exactly with the mesh lines.

7.3 Difference Equations

Equation (7.1.1) is approximated by five-point difference equations at the mesh points (i,j) , $i = 1,2,\dots,I$, $j = 1,2,\dots,J$. The usual box-integrated method is used (Ref. 43).

The equation for mesh point (i,j) and group g is of the form:

$$\begin{aligned} & a_{0,i,j}^g \phi_{i,j}^g - a_{1,i,j}^g \phi_{i-1,j}^g - a_{2,i,j}^g \phi_{i+1,j}^g - a_{3,i,j}^g \phi_{i,j-1}^g \\ & - a_{4,i,j}^g \phi_{i,j+1}^g = \sum_{\substack{g'=1 \\ g' \neq g}}^G \gamma_{i,j}^{g'+g} \phi_{i,j}^{g'} + \frac{\chi^g}{\lambda} \sum_{g'=1}^G \beta_{i,j}^{g'} \phi_{i,j}^{g'} \end{aligned} \quad (7.3.1)$$

where

$$a_{1,i,j}^g = \frac{1}{2 h_{i-1}} (D_{i-1,j}^g k_j + D_{i-1,j-1}^g k_{j-1}) \quad (7.3.2)$$

$$a_{2,i,j}^g = a_{1,i+1,j}^g \quad (7.3.3)$$

$$a_{3,i,j}^g = \frac{1}{2 k_{j-1}} (D_{i-1,j-1}^g h_{i-1} + D_{i,j-1}^g h_i) \quad (7.3.4)$$

$$\alpha_{4,i,j}^g = \alpha_{3,i,j+1}^g \quad (7.3.5)$$

$$\alpha_{0,i,j}^g = \sum_{k=1}^4 \alpha_{k,i,j}^g + F_{i,j}(\sigma^g) + \Delta_{0,i,j}^g \quad (7.3.6)$$

$$\gamma_{i,j}^{\mathcal{E}' \rightarrow \mathcal{E}} = F_{i,j}(\sum_r \mathcal{E}' \rightarrow \mathcal{E}) \quad (7.3.7)$$

$$\beta_{i,j}^g = F_{i,j}((\nu \Sigma_f)^g) \quad (7.3.8)$$

The functional $F_{ij}(n)$ denotes the integration of n around mesh point (i,j) , and

$$F_{i,j}(n) = (n_{i-1,j} k_j + n_{i-1,j-1} k_{j-1}) h_{i-1} + (n_{i,j-1} k_{j-1} + n_{i,j} k_j) h_i \quad (7.3.9)$$

$\Delta_{0,i,j}^g$ is the contribution to $\alpha_{0,i,j}^g$ from the integration of $\alpha^g(x,y)$ along a mesh line at the boundary of a diffusion - nondiffusion interface, h_i and k_j denote the mesh length in x and y direction.

7.4 Method of Solution

A one-line overrelaxation iterative procedure, combined with a periodic use of coarse-mesh-group rebalancing is used to obtain the solution of the difference equations.

One-Line Overrelaxation Procedure

The one-line overrelaxation procedure is written:

$$A_{0_i}^g \hat{\phi}_i^{g(m+1)} = A_{1_{i-1}}^g \hat{\phi}_{i-1}^{g(m+1)} + A_{1_i}^g \hat{\phi}_{i+1}^{g(m)}$$

$$+ \sum_{g'=1}^{g-1} C_i^{g'+g} \hat{\phi}_i^{g'(m+1)} + \sum_{g'=g+1}^G C_i^{g'+g} \hat{\phi}_i^{g'(m)}$$

$$+ \frac{x^g}{\lambda(n)} \left(\sum_{g'=1}^{g-1} B_i^{g'} \hat{\phi}_i^{g'(m+1)} + \sum_{g'=g}^G B_i^{g'} \hat{\phi}_i^{g'(m)} \right),$$

(7.4.1)

$$\hat{\phi}_i^{g(m+1)} = \omega^g \left(\hat{\phi}_i^{g(m+1)} - \hat{\phi}_i^{g(m)} \right) + \hat{\phi}_i^{g(m)} ;$$

$$i = 1, 2, \dots, I \quad ; \quad g = 1, 2, \dots, G$$

where

$$A_{0_i}^g = \begin{bmatrix} \alpha_{0_{i,1}}^g & -\alpha_{4_{i,1}}^g & & & \\ & -\alpha_{0_{i,2}}^g & & & \\ & & -\alpha_{4_{i,j}}^g & & 0 \\ & & & & \\ \text{Symm.} & & & & -\alpha_{4_{i,J-1}}^g \\ & & & & & \alpha_{0_{i,J}}^g \end{bmatrix}$$

(7.4.2)

$$A_{1_i}^g = \text{diag} \{ \alpha_{2_{i,j}}^g \}$$

(7.4.3)

$$B_i^g = \text{diag} \{ \beta_{i,j}^g \}$$

(7.4.4)

$$C_i^{g' \rightarrow g} = \text{diag} \{ \gamma_{i,j}^{g' \rightarrow g} \} \quad (7.4.5)$$

$$\vec{\phi}_i^g = (\phi_{i,1}^g \ \phi_{i,2}^g \ \dots \ \phi_{i,J}^g)^T \quad (7.4.6)$$

The relaxation parameters ω^g ; $g = 1, 2, \dots, G$ are calculated by estimating the spectral radius of the Jacobian iterative matrix for each group, and making use of the matrix possessing the Young's property A (Ref. 44). The iteration index for the overrelaxation is denoted by m , and n has been used to denote the number of rebalancing performed. The eigenvalue is calculated in each rebalancing calculation and is kept constant during the overrelaxation iterations. For each m , g and i , the Equation (7.4.1) is solved by factorization techniques (Ref. 44). Convergence of Equation (7.4.1) is assumed when:

$$\max_{i,j,g} \left| \frac{\phi_{i,j}^g(m+1) - \phi_{i,j}^g(m)}{\phi_{i,j}^g(m)} \right| \leq \epsilon_1 \quad (7.4.7)$$

and

$$\left| \frac{\lambda(n+1) - \lambda(n)}{\lambda(n)} \right| \leq \epsilon_2 \quad (7.4.8)$$

Coarse-Mesh-Group Rebalancing

The equations (Eq. 7.3.1) are written in the following way:

$$A \vec{\phi} = \frac{1}{\lambda} P \vec{\phi} \quad (7.4.9)$$

where the matrices and the vector are of order $I * J * G$.

On the fine-mesh-group system, a number of coarse-mesh-group blocks are imposed. Each block is identified by the set $(\tilde{i}, \tilde{j}, \tilde{g})$ where

$$1 \leq \tilde{i} \leq \tilde{I}; 1 \leq \tilde{j} \leq \tilde{J}; 1 \leq \tilde{g} \leq \tilde{G}.$$

The upper i -line, j -line and g -line in coarse cell $(\tilde{i}, \tilde{j}, \tilde{g})$, is denoted by

$$i_{\tilde{i}}, j_{\tilde{j}} \text{ and } g_{\tilde{g}}$$

Let $\vec{\phi}_a$ be the last iterated flux vector. A corrected flux $\vec{\phi}_c$ with the elements

$$\phi_{c,i,j}^g = d_{i,j}^g \phi_{a,i,j}^g ; \begin{cases} i_{\tilde{i}-1} + 1 \leq i \leq i_{\tilde{i}} \\ j_{\tilde{j},1} + 1 \leq j \leq j_{\tilde{j}} \\ g_{\tilde{g}-1} + 1 \leq g \leq g_{\tilde{g}} \end{cases} \quad (7.4.10)$$

may be found by solving the following equation for the largest in modulus eigenvalue (which is the same as k_{eff}) (Ref. 45):

$$\tilde{A} \vec{d} = \frac{1}{\lambda} \tilde{P} \vec{d} \quad (7.4.11)$$

where the matrices are of order $\tilde{I} * \tilde{J} * \tilde{G}$ with the elements:

$$\tilde{A}_{m,m'} = \langle 1, A \vec{\phi}_{a,m'} \rangle \quad (7.4.12)$$

$$\tilde{P}_{m,m'} = \langle 1, P \vec{\phi}_{a,m'} \rangle \quad (7.4.13)$$

Here $\vec{\phi}_{a,m'}$ denotes a vector of order $\tilde{I} * \tilde{J} * \tilde{G}$ with nonzero elements $\phi_{a,i,j}^g$ only if (i,j,g) is belonging to the coarse cell numbered by m' .

The solution of (7.4.11) is obtained by Wielandt iterations and the inhomogeneous equation is solved by factorization technique (Ref. 44).

8. BURNUP CALCULATIONS

Fuel burnup is determined from the isotopic concentrations in the fuel, their effective cross-sections, and integrated flux-time for a given fuel assembly. The description which follows emphasizes the main assumptions regarding fuel and fission product chains, and the principle of the solution method.

8.1 Fuel Burnup Chains

For enriched fuel where burnup proceeds to high levels, it is important that all nuclides are represented in the burnup chain which contribute significantly to the neutron production and absorption. The fuel burnup chains assumed in RECORD are the chains starting at U^{235} and U^{238} , as shown in Figure 8.1.1.

The U^{235} chain is assumed to terminate with the neutron capture in U^{236} without leading to formation of other nuclides. In reality, absorption in U^{236} leads to formation of U^{237} , which decays rapidly to Np^{237} . The $(n,2n)$ reaction in U^{238} , which is not included in the chain either, also leads to the formation of Np^{237} . Although at present neglected, the absorption in Np^{237} in LWR fuels may become more important at high burnups if, for instance, irradiated U^{235} and associated U^{236} is used in recycled fuel.

The U^{238} chain also includes the trans-plutonium nuclides Am^{241} , Am^{242} , Am^{243} and Cm^{244} . The neutron absorption in some of these nuclides are of significance at high burnups and has to be taken into account. The absorption in Am^{241} leads to Am^{242} , with some fraction being the fissile Am^{242m} . This fraction is spectrum-dependent, and a value of 16% is often used as being representative for thermal reactor systems. The curium isotopes, Cm^{242} and Cm^{244} , have no significance on the neutron absorption from a reactivity point-of-view, but have their importance in their α -decay and spontaneous fissions, which cause problems in the transport of irradiated fuel.

8.2 Fission Product Representation

The fission product model incorporated in RECORD is a result of a general study of the individual nuclide contribution to the total poisoning in a typical BWR reactor. The model consists of a scheme with explicit treatment of 11 fission products in four chains, together with the chains for Xe^{135} and Sm^{149} generated by direct fission. The remaining fission products are condensed into four pseudo fission products, in accordance with their saturation characteristics. The nuclide chains assumed, are shown in Figure 8.2.1.

The study leading to the choice of fission product model, and the methods of generating cross-sections and effective yield data for the fission products, is described in References 20 and 46, and only the essence of that study will be discussed here. The work involved the study of different reduced representations of fission products and comparing these against a more exact scheme, where all fission products in explicit chains are followed during burnup.

A general fission product code, FISSION (Ref. 46), was first developed, where all known fission products of significance are incorporated, and where a complete analytic method similar to that of CINDER (Ref. 47) is used to solve the linear burnup differential equations. The general nuclide decay chains are split into linear sub-chains and, after discarding negligible components, the detailed fission product representation consisted of 69 sub-chains containing 370 components of 179 different nuclides. A study of the individual nuclide contribution to the total poisoning for a typical BWR fuel, showed that about 20 fission products were responsible for approximately 85 - 90% of the total poison, excluding that due to Xe^{135} and Sm^{149} .

A number of different fission product aggregates were now constructed and tested against the complete analytical method. From six to 26 fission products were treated explicitly in these models, together with one to four pseudo fission products. Concentrations and thermal and epithermal absorp-

tion cross-sections for all nuclides, including the pseudo fission products, were calculated and compared for a variety of reactor states as function of burnup (or time). An example of such a comparison is shown in Figure 8.2.2.

The choice of fission product model is made on a judgement of (a) accuracy, in comparison with exact method and computer limitations; (b) respect to detail that can be handled in the pinwise treatment of fuel burnup in RECORD; and (c) the implication on computing time in solving the burnup differential equations in each of a large number of fuel pins in a general fuel assembly calculation. The model finally incorporated in RECORD, altogether consisting of 12 fission products in six chains, and four pseudo fission products, showed good agreement with exact representation for burnups up to about 30 000 MWD/TU.

The fission products not given explicit treatment are combined into the four pseudo fission products, depending on their saturation properties which, in turn, are mainly dependent on their effective absorption cross-sections. The nuclides in the pseudo fission products are grouped according to their resonance integrals, being in the range 0 - 100, 100 - 500, 500 - 1200, and 1200 - 3400 barns for the four pseudo elements, respectively.

8.3 Solution of Burnup Equations

The general system of differential equations describing fuel depletion and fission product buildup as function of neutron irradiation, is given by

$$\frac{dN_i(t)}{dt} = Y_i + Y_{i-1}N_{i-1}(t) - A_i N_i(t) \quad (8.3.1)$$

where

$N_i(t)$ = concentration of isotope i at time t

A_i = $\int_0^{\infty} \sigma_a^i(E) \phi(E) dE + \lambda_i$

λ_i = decay constant

γ_{i-1} = either (a) decay constant,
 or (b) capture rate, $\int_0^\infty \sigma_c^{i-1}(E) \phi(E) dE$
 of precursor isotope

$\sigma_a^i(E)$ = absorption (fission + capture) cross-section

$\sigma_c^i(E)$ = capture cross-section

$\phi(E)$ = flux

E = energy

and where the yield term is given by

$$Y_i = \sum_k Y_i^k \int_0^t N_k(t) \int_0^\infty \sigma_f^k(E) \phi(E) dE dt \quad (8.3.2)$$

where

Y_i^k = fractional yield for fission product i
 per fission in fissile isotope k

The summation is taken over all the fissile isotopes k .

Assuming constant flux and cross-sections during a time interval t , and assuming the isotope chains to be resolved into single-path or linear chains with no branching, Equation (8.3.1) can be solved analytically to give:

$$N_i(t) = \sum_{k=1}^i \frac{1}{Y_i} \prod_{n=k}^i \gamma_n \left[N_k(0) \sum_{\substack{j=k \\ \neq j}}^i \frac{e^{-A_j t}}{\pi (A_l - A_j)} \right] + \quad (8.3.3)$$

$$+ \bar{Y}_k \left(\frac{1}{\prod_{\ell=k}^i A_\ell} - \sum_{j=k}^i \frac{e^{-A_j t}}{A_j \prod_{\substack{\ell=k \\ \ell \neq j}}^i (A_\ell - A_j)} \right) \quad (8.3.3)$$

(Cont'd)

where

$N_k(0)$ = initial concentration of isotope k
(i.e. at beginning of time interval), and

Y_k = time-averaged direct yield rate to nuclide k
from all fissile nuclides in the time interval

For small values of t , rounding errors may occur in the summations within the main brackets of Equation (8.3.3). The exponential terms cannot be evaluated to more than N significant digits in double precision on the computer and, hence, the summations cannot be correctly calculated if they are smaller than $\sim |X_j| * 10^{-N}$, where $|X_j|$ is the largest term of the summation. Accordingly, following the method of England (Ref. 47), the following test is incorporated into the code:

$$|X_j| * 10^{-N} > \sum_{j=k}^i X_j \quad (8.3.4)$$

where X_j are the terms of the summation. If Equation (8.3.4) is true, all terms with $j \leq k$ are neglected, being insignificant contributions from far-away isotopes in the chain on the isotope i .

Using recurrence relations between the different terms in the expansion of Equation (8.3.3) and England's method of discarding insignificant terms, the concentrations of isotopes in the linear burnup chains can be calculated accurately on the computer with very short computing times.

The poisoning due to Xenon-135 formation is treated at all burnup states with the assumption of equilibrium xenon concentration. This equilibrium concentration is given by (in the same notation as before):

$$N_{Xe} = \frac{\sum_k \gamma_{Xe}^k N_k \sum_g \bar{\sigma}_{f,g}^k \bar{\phi}_g}{\lambda_{Xe} + \sum_g \bar{\sigma}_{a,g}^{Xe} \bar{\phi}_g} \quad (8.3.5)$$

where

$$\gamma_{Xe}^k = \text{effective yield for Xe per fission in fissile isotope } k.$$

The energy generated in each burnup interval is calculated from the fission rate in each fissile nuclide. If ϵ_k is the energy release (in MeV) per fission of nuclide k , the total energy (MeV/cm³) generated in time step t sec. is given by

$$P = \sum_k \epsilon_k \int_0^t N_k(t) \int_0^\infty \sigma_f^k(E) \phi(E) dE dt \quad (8.3.6)$$

where the summation is taken over all fissile nuclides k .

Using average group cross-sections and fluxes, and a conversion factor to convert the power density to the usual units, Megawatt-days per initial tonne heavy metal, the above expression, applied to all fuel pins of a fuel assembly, determines the burnup distribution at any given time.

In RECORD, the isotopic concentrations of each nuclide (uranium, plutonium, trans-plutonium and fission product nuclides) in each fuel pin of a fuel assembly, are followed as function of burnup, using Equation (8.3.3) where the fluxes and effective cross-sections in each fuel pin will be functions of the isotopic concentration reached at any given burnup. Within each burnup interval, the burnup equations are solved for each fuel pin; during which, the spectrum, fluxes and cross-sections in each pin cell are held

constant at the values evaluated at the beginning of the burnup interval. The code iterates to precise burnup values by iterating the burnup calculations (seldom using more than two or three steps) over the assembly unit until the average burnup of the fuel is within 1/2 MWD/TU of the required, specified average fuel burnup at the end of a given burnup interval as given in the code input.

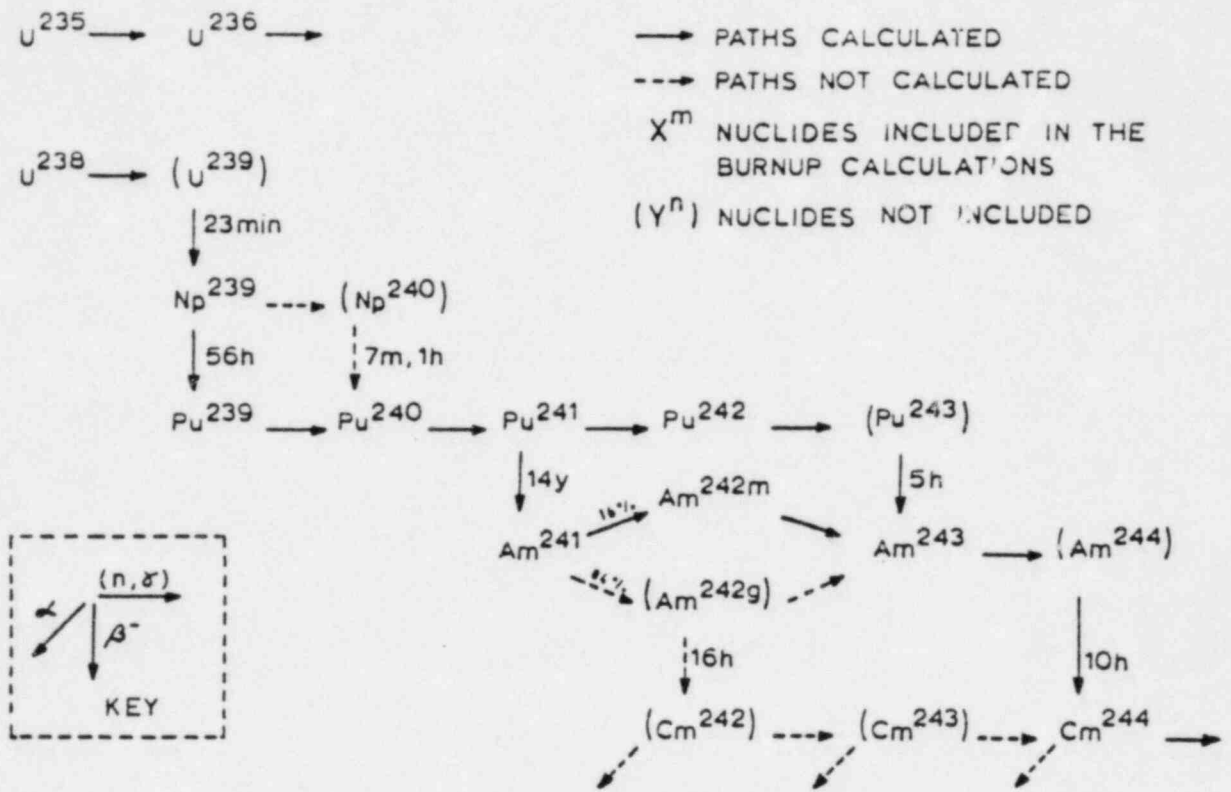


FIGURE 8.1.1 Fuel Burnup Chains in RECORD

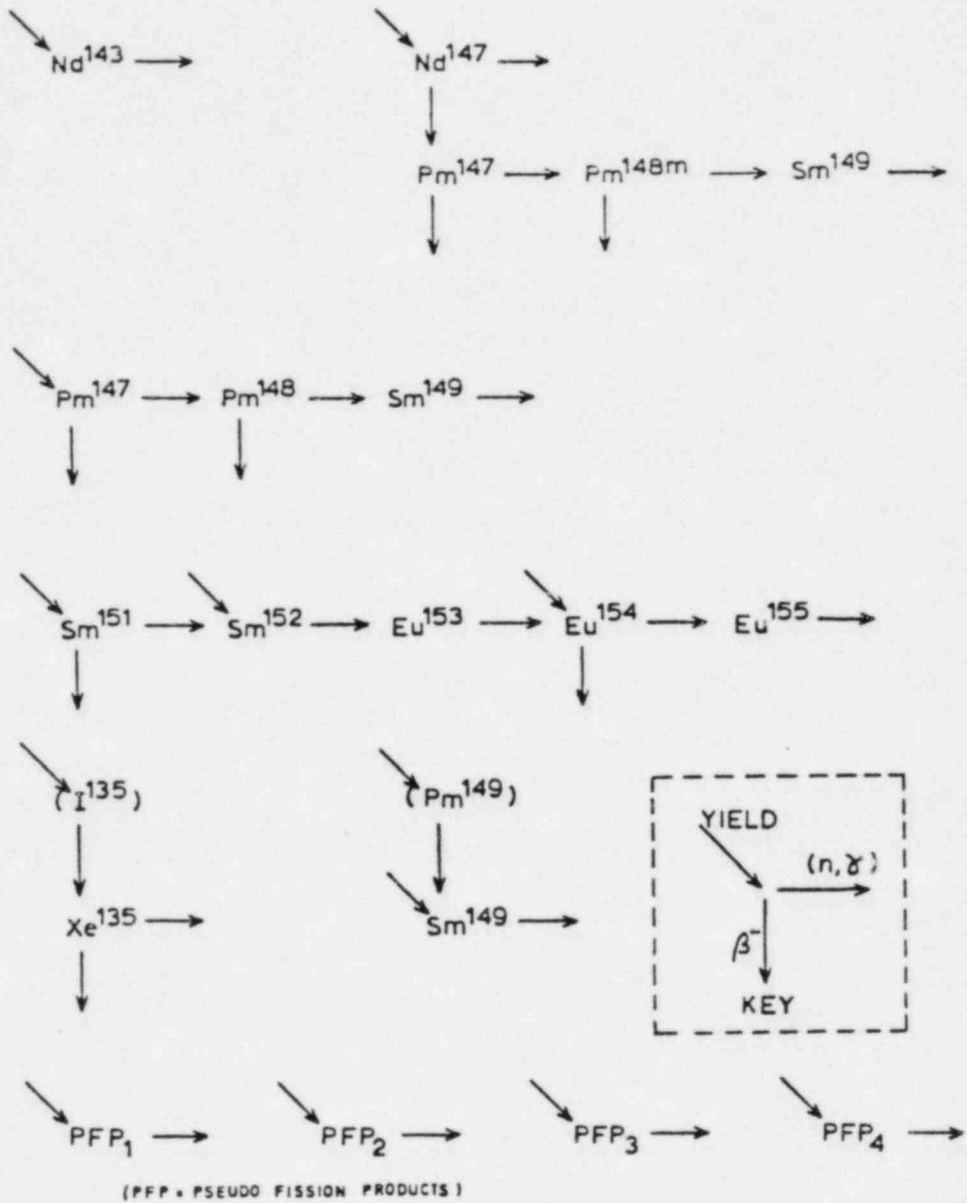
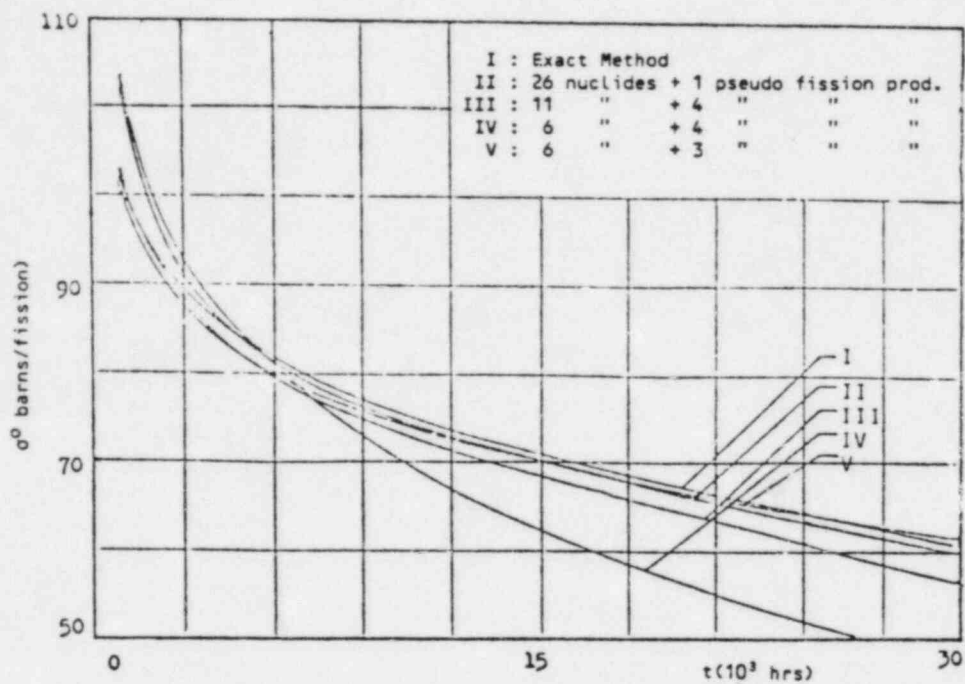


FIGURE 8.2.1 Fission Product Chains in RECORD

Thermal (2200 m/s):



Epithermal:

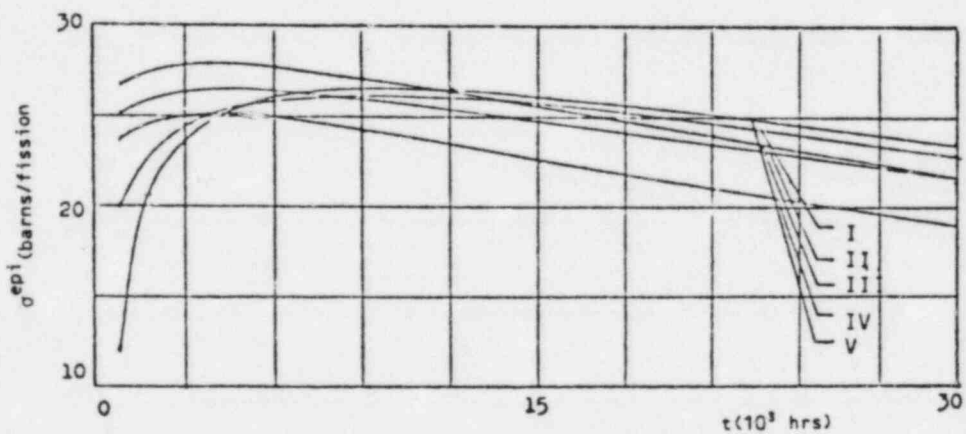


FIGURE 8.2.2 Effective Macroscopic Fission Product Absorption Cross-Sections for a Typical BWR (40% void)

9. OTHER FEATURES OF RECORD

9.1 TIP Instrumentation Factors

The relative power levels in different regions of a BWR core is often determined from measurements from a travelling-in-core detector, inserted in the narrow-narrow water gap corner region outside the fuel assemblies. For proper interpretation of the power levels, it is necessary to relate the detector readings to the average power level of the surrounding fuel assemblies.

In the calculation of the reaction rate in the narrow-narrow water gap region, the so-called TIP-region, the influence from the spectrum variations in the surrounding fuel assemblies must be taken into account. Of particular importance in this respect, is the influence on the TIP-region spectrum due to void variations in the moderator within the adjacent fuel assemblies.

In modelling the TIP-region reaction rate, RECORD assumes the TIP-detector to be a fission chamber where the detector signal R is proportional to the fission rate in U^{235} :

$$R \propto \int_0^E \sigma_f^{235}(E) \phi(E) dE \quad (9.1.1)$$

where

$\sigma_f^{235}(E)$ = fission cross-section for U^{235} at energy E , and

$\phi(E)$ = flux spectrum in the detector region

The detector region is assumed to be the quadratic region in the narrow-narrow water gap corner outside the assembly flow box (see Fig. 2.1.4). It is assumed that the amount of U^{235} present in the detector is sufficiently small so as not to influence the spectrum or flux level in that region.

A detailed study has been made on typical BWR assembly cells to determine the void dependence of the TIP-region reaction rates, where the void is the average void in the surrounding fuel assemblies. From this work, it has been possible to establish a correlation that relates the effective two-group U^{235} thermal fission cross-sections to the average void within the assembly flow box. This correlation is incorporated in RECORD and, in standard BWR applications, is used in calculating the TIP-region fission rate according to Equation (9.1.1). In non-standard applications of RECORD, or in cases where the User so wishes, the calculation of detector fission rate from the established correlations is replaced by applying group data and effective detector fission cross-sections for the TIP-region, as defined in the code input.

The application of instrumentation factors in PRESTO is described in Reference 3. The instrumentation factors derived from the standard calculation method in RECORD, is routinely used in PRESTO reactor simulation studies, and extensive verification of PRESTO-calculated axial TIP-traces in comparison with measured data (Refs. 3, 4) testifies to the soundness of the established calculation procedures.

9.2 Delayed Neutron Parameters

Kinetic parameters, represented by effective delayed neutron fractions and associated decay constants, are calculated for applications in neutron kinetics codes.

The fraction of neutrons being delayed (β) varies considerably between the fissionable isotopes. The value of β will vary from pin-to-pin in the lattice and is a relatively strong function of irradiation. The delayed neutron fission spectrum differs from that of the prompt neutrons, and is reflected in the calculation of the effective delayed neutron fraction, β_{eff} .

Due to the specific fission spectrum of the delayed neutrons, a detailed calculation of β_{eff} would be complicated and time-consuming. To avoid this, the following approximations are introduced in RECORD to calculate the

delayed neutron parameters : Neutron spectra and reaction rates from the conventional prompt neutron calculation is used, but the neutron events at energies above the delayed neutron fission spectrum are excluded in the calculation of β_{eff} . However, the effects on the neutron spectrum at lower energies, caused by the fast neutron events, are neglected.

Delayed neutrons are grouped together into the conventional six groups. The following expression (for nomenclature, see end of section) is used in the calculation of the effective delayed neutron fraction, $\beta_{\text{eff},\ell}^i$, for isotope ℓ in delayed neutron group i (cf. Ref. 13) :

$$\beta_{\text{eff},\ell}^i = \frac{k_D}{k} \frac{\sum_{j=1}^J \beta_{\ell}^i \cdot \text{PROD}_{\ell,j}}{\sum_{\ell} \sum_j \text{PROD}_{\ell,j}} \quad (9.2.1)$$

with the multiplication factor, k , from

$$k = \frac{\sum_{\ell} \sum_{j=1}^J \text{PROD}_{\ell,j}}{\sum_{\ell} \sum_{j=1}^J (\text{ABS}_{\ell,j} + \text{LEAK}_{\ell,j})} \quad (9.2.2)$$

and the "delayed" multiplication factor, k_D , from

$$k_D = \frac{\sum_{\ell} \sum_{j=J_D}^J \text{PROD}_{\ell,j}}{\sum_{\ell} \sum_{j=J_D}^J (\text{ABS}_{\ell,j} + \text{LEAK}_{\ell,j})} \quad (9.2.3)$$

where the energy group index j runs from 1 (highest group) to J (total no. of energy groups) in the calculation of k , but from J_D , the highest group containing delayed fission neutrons, to J in the calculation of k_D .

The basic, isotopic delayed neutron fractions, β_{ℓ}^i , are calculated from data on yields, γ_{ℓ} , and group fractions, a_{ℓ}^i :

$$\beta_{\ell}^i = \frac{\gamma_{\ell} \cdot a_{\ell}^i}{\nu_{\ell}} \quad (9.2.4)$$

Average delayed neutron fractions are calculated by summation over the fissile isotopes :

$$\beta_{\text{eff}}^i = \sum_{\ell} \beta_{\text{eff},\ell}^i \quad (9.2.5)$$

The total delayed neutron fraction is given by

$$\beta_{\text{eff}}^{\text{TOT}} = \sum_{i=1}^6 \beta_{\text{eff}}^i \quad (9.2.6)$$

and average data for each isotope expressed as

$$\beta_{\text{eff},\ell} = \sum_{i=1}^6 \beta_{\text{eff},\ell}^i \quad (9.2.7)$$

The average group decay constants are given by

$$\bar{\lambda}^i = \frac{\sum_{\ell} a_{\ell}^i \cdot \frac{\beta_{\text{eff},\ell}}{\beta_{\text{eff}}^{\text{TOT}}}}{\sum_{\ell} \frac{a_{\ell}^i}{\lambda_{\ell}^i} \cdot \frac{\beta_{\text{eff},\ell}}{\beta_{\text{eff}}^{\text{TOT}}}} \quad (9.2.8)$$

Fundamental data on group yields and decay constants are those recommended in Reference 48 and given in Table 9.2.1.

All calculations of kinetics parameters in RECORD are performed in the five-group scheme, i.e., $J=5$, and with the delayed fission neutrons introduced in Group 2, i.e., $J_D=2$. The accuracy of the approximative expression (Eq. 9.2.3) for the delayed neutron multiplication factor, k_D , under these assumptions, has been investigated by comparing it with the exact value of k_D calculated with a detailed delayed neutron fission spectrum. For a typical BWR fuel design, the approximation was found to introduce an error in β_{eff} of only 0.2%.

The following nomenclature is used in this section :

i = delayed neutron group index

j = energy group index

l = isotopic index

J = total no. of energy groups (=5)

J_D = highest energy group with delayed fission neutrons (=2)

$PROD_{l,j}$ = production rate of isotope l in group j

$ABS_{l,j}$ = absorption rate of isotope l in group j

$LEAK_{l,j}$ = leakage rate of isotope l in group j

γ_l = absolute delayed neutron yield

a_l^i = fractional delayed neutron yield

λ_l^i = decay constant

$\bar{\nu}_l$ = average no. neutrons per fission

TABLE 9.2.1 Delayed Neutron Data (Ref. 48)

ISOTOPE	ABSOLUTE DELAYED NEUTRON YIELD	GROUP i	FRACTIONAL GROUP YIELD a_i	DECAY CONSTANT λ_i (sec ⁻¹)
U ²³⁵	0.01697 ± 0.00020 ± 1.2%	1	0.038 ± 0.004	0.0127 ± 0.0003
		2	0.213 ± 0.007	0.0317 ± 0.0012
		3	0.118 ± 0.024	0.115 ± 0.004
		4	0.407 ± 0.010	0.311 ± 0.012
		5	0.128 ± 0.012	1.40 ± 0.12
		6	0.026 ± 0.004	3.87 ± 0.55
U ²³⁸	0.04508 ± 0.00060 ± 1.3%	1	0.013 ± 0.001	0.0132 ± 0.0004
		2	0.137 ± 0.003	0.0321 ± 0.0009
		3	0.162 ± 0.030	0.139 ± 0.007
		4	0.388 ± 0.018	0.358 ± 0.021
		5	0.225 ± 0.019	1.41 ± 0.10
		6	0.075 ± 0.007	4.02 ± 0.32
Pu ²³⁹	0.00655 ± 0.00012 ± 1.8%	1	0.038 ± 0.004	0.0129 ± 0.0003
		2	0.280 ± 0.006	0.0311 ± 0.0007
		3	0.216 ± 0.027	0.134 ± 0.004
		4	0.328 ± 0.015	0.331 ± 0.018
		5	0.103 ± 0.013	1.26 ± 0.17
		6	0.035 ± 0.007	3.21 ± 0.38
Pu ²⁴⁰	0.0096 ± 0.0011 ± 11.5%	1	0.028 ± 0.004	0.0129 ± 0.0006
		2	0.273 ± 0.006	0.0313 ± 0.0007
		3	0.192 ± 0.078	0.135 ± 0.016
		4	0.350 ± 0.030	0.333 ± 0.046
		5	0.128 ± 0.027	1.36 ± 0.30
		6	0.029 ± 0.009	4.04 ± 1.16
Pu ²⁴¹	0.0160 ± 0.0016 ± 10.0%	1	0.010 ± 0.003	0.0128 ± 0.0002
		2	0.229 ± 0.006	0.0299 ± 0.0006
		3	0.173 ± 0.025	0.124 ± 0.013
		4	0.390 ± 0.050	0.352 ± 0.018
		5	0.182 ± 0.019	1.61 ± 0.15
		6	0.016 ± 0.005	3.47 ± 1.7
Pu ²⁴² *	0.0228 ± 0.0025 ± 11.0%	1	0.004 ± 0.001	0.0128 ± 0.0003
		2	0.195 ± 0.032	0.0314 ± 0.0013
		3	0.161 ± 0.048	0.128 ± 0.009
		4	0.412 ± 0.153	0.325 ± 0.020
		5	0.218 ± 0.087	1.35 ± 0.09
		6	0.010 ± 0.003	3.70 ± 0.44

*Same data used for the other fissionable trans-plutonium isotopes not included in the Table.

10. CODE QUALIFICATION

The RECORD code is founded on the accumulated experiences from the reactor physics development work at the Institute for Atomic Energy (Institute for Energy Technology since 1980), Kjeller, Norway, during the 1960's and early 1970's. Some of the component modules of RECORD are based on codes developed during this period, and initially tested during the experimental activity also taking place at this time; in particular, in conjunction with the international NORA Project. Initial confidence in some of the basic reactor physics methods later incorporated in RECORD, was therefore established during this time. This reactor physics development work at the Institute is well summarized in IAEA reports (Refs. 27, 49 and 50).

The reactor physics models in RECORD have undergone extensive modifications and improvements, during the years of code development. New features have been incorporated and new computational techniques in the solution methods have been introduced. The code qualification work described in this chapter pertains, unless otherwise stated, to that performed with the latest (1981) version of RECORD and associated codes.

This chapter first recapitulates the RECORD analyses of altogether 55 cold, clean critical uranium and plutonium lattice configurations, as measured at different laboratories. These analyses constitute the basic integral verification of the fundamental reactor physics methods of RECORD and the adequacy of basic cross-sections used. The further integral verification of basic methods at hot operating conditions, and of the code's Nuclear Data Library, is provided by the analyses of the uranium and plutonium isotopics as function of fuel burnup, as measured during the Yankee-Rowe Core Evaluation Program.

The ability of RECORD to predict local power distributions within a fuel assembly has been investigated in some detail, and a discussion is given of the results of comparisons with gamma scan measurements on different assemblies from Quad Cities-1. Of particular importance in this and other analyses is the ability to demonstrate that the power in gadolinium-

contained fuel rods is predicted with an accuracy consistent with that of other rods.

A code's qualification can finally be stated to depend on how the code is to be applied. From the Utility's or reactor operator's point-of-view, the main qualification of a reactor code can be said to be its proven performance in actual reactor fuel and core calculations. The RECORD code has its main applications in the generation of data banks containing few-group cross-sections, and other data, such as differential effects due to control rod absorbers, Xenon, Doppler, voids, etc., which are relevant for describing LWR fuel as function of fuel exposure. These data form the basic data sets used by the reactor simulator, PRESTO. The main integral qualification of RECORD, therefore, can be considered to be the very positive experiences accumulated through many years in the application of RECORD - PRESTO in the accurate analyses of a large number of BWR and PWR operating cycles. This experience is reviewed in the final section of this chapter.

10.1 Analysis of Clean Critical UO_2 and UO_2/PuO_2 Lattices

A set of clean critical UO_2 and UO_2/PuO_2 lattices have been used to qualify the basic reactivity predictions of RECORD at room temperatures (in the region of 20 °C). The measurements have been made at different laboratories, and the lattice and experimental data are well documented.

The lattices have been analyzed using RECORD in single-pin option, in generating the standard RECORD five-group data for lattice regions and surrounding reflector. The leakage calculations were performed by representing the cylindrical core geometry of the critical configurations in a radial one-dimensional diffusion calculation with the code MD-1 (Ref. 51), using the RECORD calculated five-group data for each region. This analysis assumed a two-region, radial model of the reactor; i.e., a homogeneous core and a homogeneous reflector, and where the axial leakage was represented by the axial buckling.

10.1.1 Critical UO₂ Lattices

The UO₂ lattices analyzed are from Westinghouse (Refs. 52, 53, 54 and 55), Babcock & Wilcox (Refs. 56, 57), and NORA Project (Ref. 50). The enrichment in these lattices varied from approximately 1.3 to 4.0 weight per cent U²³⁵. Lattice pitches varied from 1.03 to 2.69 cm, and the water-to-fuel volume ratios varied from approximately 1 to 5. The configurations included both square and hexagonal lattices. The clad material is either aluminium or stainless steel. Tables 10.1.1 and 10.1.2 show the main characteristics of these critical lattices, together with the RECORD / MD-1 calculated k_{eff} -values. Figure 10.1.1 also shows the k_{eff} -values plotted as function of water-to-fuel volume ratio.

The mean k_{eff} -values and standard deviations obtained for lattices from the different laboratories are as follows :

Westinghouse : Mean k_{eff} = 0.9997 ± 0.0040

Babcock & Wilcox : Mean k_{eff} = 0.9990 ± 0.0038

NORA : Mean k_{eff} = 1.0046 ± 0.0041

The mean k_{eff} -value for the 25 UO₂ lattices analyzed is 1.0001 ± 0.0042 .

10.1.2 Critical UO₂/PuO₂ Lattices

The plutonium lattice experimental data from Battelle Pacific Northwest Laboratories (Ref. 58) have been analyzed with RECORD / MD-1 in the same manner as the UO₂ lattices. The critical lattice measurements were made on different UO₂/PuO₂ rods, ranging in PuO₂ enrichments from 1.5 to 4.0 weight per cent, and Pu²⁴⁰ content varying from 8 to 24%. The lattice measurements were made over a broad range of water-to-fuel volume ratios, varying from approximately 1.1 to 11.6. Details of the 30 lattices analyzed are given in Tables 10.1.3 and 10.1.4, together with the resulting k_{eff} -values from

RECORD / MD-1. The results are also shown in Figure 10.1.2, where k_{eff} is plotted against water-to-fuel volume ratio.

The mean k_{eff} -values and standard deviations obtained for the different UO_2 / PuO_2 lattices are given in Table 10.1.5. The mean value for all 30 lattices analyzed is 1.0071 ± 0.0046 .

Also shown in Figure 10.1.2 are the results of BNWL's own, detailed analysis of the critical lattices (Ref. 59). As can be observed, there is a consistent bias in the RECORD / MD-1 results in comparison with the BNWL calculated k_{eff} -values. For a broad range of lattices, a parallel displacement of the results, can be observed, reflecting that variations in the experimental conditions are similarly reproduced in the different calculation models. The results agree best for the more open lattices with larger critical core radii. There are many uncertainties involved in the theoretical predictions, and the BNWL Paper (Ref. 59) discusses the detailed analyses of some of these uncertainties related to calculation models, energy detail, lattice hardware, and reactivity effects due to particulate fuel and other heterogeneities.

It is not the intention here to further discuss at length the adequacy of the different models. Notice should be taken, however, of the small size of the critical assemblies, and the difficulty in calculating leakage accurately. It is most questionable if one-dimensional, five-group diffusion theory (four-group in the BNWL analysis) is adequate for such systems and, as stated in Reference 59, higher order calculations are necessary to ensure proper calculation of leakage for these assemblies. Analysis of these same assemblies with the WIMS and MURLI codes (Ref. 60) used 27-group, one-dimensional calculations for representing the critical systems in sufficient energy detail. There, four-group leakage calculations gave a bias of up to +1% in k_{eff} in comparison with the 27-group calculations, the difference being highest for the lower critical core radii and tighter lattices.

The direct results of the analysis indicates that RECORD / MD-1 tend to overpredict the reactivity of plutonium lattices, in the order of 700 pcm, compared with clean UO_2 lattices. Including corrections for reactivity

effects of lattice grid plates, PuO_2 particle size and more detailed leakage calculations will reduce the apparent overprediction considerably.

10.2 Fuel Depletion Isotopic Analysis Comparisons

RECORD calculated uranium and plutonium isotopics as function of fuel burnup have been compared to the isotopic measurements made during different phases of the Yankee-Rowe Core Evaluation Program (Refs. 61, 62). The experimental data represent detailed isotopics of fuel rods in perturbed, intermediate and asymptotic reactor neutron spectra, measured over a broad range of fuel burnups up to approximately 31 000 MWD/TU.

The analysis of the data was made with RECORD for a single-pin in an asymptotic spectrum. The calculated plutonium-to-uranium mass ratio, and isotopic concentrations for U^{235} , U^{236} , U^{238} , Pu^{239} , Pu^{240} , Pu^{241} , and Pu^{242} , in comparison with the experimental data, are shown in Figures 10.2.1 through 10.2.8.

The agreement between RECORD-calculated isotopic concentrations and measured data is generally quite good, except for Pu^{240} which tends to be underestimated at higher burnups. There is also a tendency for overprediction of Pu^{239} isotopics at burnups greater than about 25 000 MWD/TU.

The general good agreements constitute an integral verification of the basic unit cell model in RECORD under hot operating conditions. In addition, the results verify the adequacy of the Nuclear Data Library and the treatment for temperature-dependence of cross-sections and resonance integrals, as well as verifying the burnup calculation method.

10.3 Gamma-Scan Comparisons of BWR Assembly Pin-Power Distributions

The local power distribution within the fuel assembly, as generated by RECORD, was compared with the experimental data from the 1976 Quad Cities-1 gamma scan measurements (Ref. 63). In those experiments, five fuel assemblies were removed from the reactor at the end of Cycle 2, disassembled and pinwise gamma-scanned for the La^{140} isotope intensity. Before the shutdown,

the reactor had been operated with all control rods out for a period of 1-1/2 months, and with a total core power-level change of only 12% during the same period (Ref. 64). The measured isotope distribution is therefore proportional to the power distribution over the assembly at noncontrolled, rated conditions. Since the gamma scans were taken at several axial elevations, a wide range of exposure and void levels were covered. The quoted accuracy in the reported rod-to-rod La^{140} intensities is approximately 3%.

Out of the five measured assemblies, two were of the mixed oxide (MO_2) type and three of standard UO_2 design. The three UO_2 -bundles were selected for the RECORD benchmark analysis and have the characteristics given in Table 10.3.1. (The MO_2 -bundles were excluded from this analysis due to lack of data on isotopic content.) A detailed description of the fuel design is found in Reference 64. Each fuel bundle was measured at eight axial elevations (15, 21, 51, 56, 87, 93, 123 and 129 inches above the bottom of the active fuel). Data at the pair-wise close positions were merged together in order to reduce the experimental uncertainty, and the RECORD data analysis was therefore done at four axial levels. The nodal distributions of exposure and exposure-weighted void of Quad Cities-2 had been generated in a core-follow analysis, using the 3-D BWR simulator CORE, and were obtained from Reference 65.

The RECORD data were generated in depletion calculations performed at three different void levels: 0, 40 and 70% void. The actual, local power distributions used in the benchmarking, were derived by interpolation between the void levels, as well as the discrete burnup points in the depletion calculation.

Figures 10.3.1 through 10.3.6 compare the calculated and measured local power distributions. The main results, represented by the root-mean-square (RMS) power differences, are listed in Table 10.3.2. The total RMS difference of 540 pins is 3.1%, which is in the same order of magnitude as the measurement uncertainty.

The RECORD calculations were performed with reflective boundary conditions, and assuming diagonal symmetry within the assembly, and will therefore not account for possible flux tilts over the fuel bundle. In an attempt to reduce this inconsistency between measurements and calculations, the experimental data were also reflected and averaged with respect to the symmetry line (the diagonal). This resulted in a reduced, total RMS power difference of 2.9%.

The local pin power-peaking factor is, in RECORD, overpredicted by an average of $2.4\% \pm 2.3\%$, relative to the gamma scan. All the analyzed cases show conservatism (overprediction) in the calculated peaking factor.

RECORD systematically overpredicts the power somewhat on the boundary along the narrow water gap. It is, however, difficult to draw any definite conclusions as to the modelling in RECORD based on this observation, because of both the uncertainty in the measurements ($\pm 3\%$) and the limitations of the "cell" approach of the RECORD calculations. The cell calculations will neglect effects like:

- influence of neighboring assemblies
- macroscopic flux tilts
- control rod history
- nonuniform void distribution within the assembly
- void variations during burnup
- influence of detector tubes and sources.

These effects will mostly influence the peripheral row of pins; e.g., the presence of a detector tube will reduce the power in the narrow-narrow corner pin by approximately 2%. (Of the analyzed fuel bundles, CX-214 is located next to a detector string and GEH-002 next to a source.)

The power in the gadolinia-bearing fuel rods is predicted with an accuracy consistent with the other rods.

10.4 Historical Review of LWR Analysis with RECORD - PRESTO

The core simulator PRESTO, with nuclear data from RECORD, has been applied in core-follow calculations and other applications for LWRs, where a systematic comparison with operating data has been possible. Feedback from these applications has played an important role in the evaluation and further development of RECORD over the past ten years. Substantial parts of the basic methodology employed in RECORD was evaluated in a core-follow study for the Dodewaard BWR in 1971 (Ref. 66). Following the completion of the first version of RECORD in 1972 (Ref. 1), ScP has systematically tested the RECORD - PRESTO system in the analysis of more than 20 BWR and PWR operating cycles. A summary of this experience is reported in Reference 4. Core-follow analyses with RECORD - PRESTO on Mühleberg (BWR), Quad Cities (BWR), and the Yankee (PWR) reactors, are described in References 67 and 68.

Table 10.4.1 gives an overview of the reactors and operating cycles which have provided the main basis for evaluations of RECORD - PRESTO by ScP's own staff. The average k_{eff} and its standard deviation at critical states through each cycle, are also given. In addition, the Users of FMS have independently conducted their own qualification of the programs (Refs. 69 and 70).

The procedures used for the analyses of gadolinium poisoned fuel were first tested against critical measurements in Dodewaard (Ref. 16) and, later, against gamma scan results from Mühleberg. Figure 10.4.1 shows the results of the analysis on the Dodewaard gadolinium-containing assembly at the cold, initial state. Results from comparison with proprietary data on low burnup gadolinium fuel is shown in Figure 10.4.2.

These gamma scan results from KKM were particularly important, as they confirmed the ability of the model to properly predict the burnup of the gadolinium pins. This assembly was located close to the core boundary, such that there was considerable flux-tilting across the assembly. This does not measurably affect the comparison of peaking factors in the gadolinium pins relative to its neighbors, however.

TABLE 10.1.1 WESTINGHOUSE UO₂ Critical Lattices

CATALOG NO.	U ²³⁵ ENRICHMENT (wt%)	LATTICE PITCH		H ₂ O / FUEL	BUCKLING (m ⁻²)		CORE RADIUS (cm)	k _{eff} RECORD & MD-1
		CM	SQUARE OR HEXAGONAL		TOTAL	AXIAL		
W1	2.70	1.029	SQ.	1.049	40.7 ± 0.4	5.4	32.01	0.9966
W2	"	1.062	"	1.200	47.1 ± 0.3	12.4	32.79	0.9990
W3	"	1.105	"	1.405	53.2 ± 0.7	5.4	26.82	0.9974
W4	"	1.194	"	1.853	63.3 ± 0.4	5.4	24.27	0.9974
W5	"	1.252	"	2.164	68.8 ± 0.5	10.96	25.12	0.9995
W6	"	1.455	"	3.369	65.64 ± 0.6	5.53	23.60	0.9949
W7	"	1.562	"	4.077	60.07 ± 0.8	5.48	24.77	0.9931
W8	"	1.689	"	4.983	52.92 ± 0.5	5.41	27.17	0.9905
W9	1.311	1.558	HEX.	1.430	32.59 ± 0.15	5.24	38.13	1.0045
W10	"	1.652	"	1.782	35.47 ± 0.18	5.29	36.34	1.0039
W11	"	1.806	"	2.402	34.22 ± 0.13	5.30	37.63	1.0025
W12	"	2.205	"	1.073	28.37 ± 0.06	5.05	41.24	1.0040
W13	"	2.359	"	1.405	30.17 ± 0.06	5.13	39.69	1.0037
W14	"	2.512	"	1.758	29.06 ± 0.07	5.20	41.44	1.0021
W15	"	1.558	"	1.393	25.28 ± 0.10	5.11	45.14	1.0016
W16	"	1.652	"	1.735	25.21 ± 0.10	5.24	45.77	1.0008
W17	3.70	1.062	SQ	1.225	68.30 ± 0.3	18.6	26.36	1.0027
W18	"	1.252	"	2.210	95.10 ± 0.7	8.86	19.01	0.9997

TABLE 10.1.2 B&W and NORA UO₂ Critical Lattices

CATALOG NO.	U ²³⁵ ENRICHMENT (wt%)	LATTICE PITCH SQ. (cm)	H ₂ O/FUEL	BUCKLING (m ⁻²)		CORE RADIUS (cm)	k _{eff} RECORD & MD-1
				TOTAL	AXIAL		
BW5	4.02	1.511	1.136	88.0	3.60	18.75	0.9977
BW13	4.02	1.450	0.955	79.0	3.95	20.18	0.9953
BW16	2.46	1.511	1.370	70.1	4.07	20.82	1.0042
BW27	4.02	1.511	1.139	87.1	-14.58	16.36	0.9988
NH18	3.41	2.687	4.505	86.4 ± 1.0	22.12	23.49	0.9999
NH19	"	2.314	3.032	98.8 ± 1.2	21.22	20.56	1.0072
NH20	"	1.900	1.655	91.8 ± 1.7	20.08	21.01	1.0068

10-10

TABLE 10.1.3 BNWL UO₂-2 wt% PuO₂ Critical Lattices

CATALOG NO. BNWL-	PU ENRICHMENT		HEXAGONAL LATTICE PITCH (cm)	H ₂ O/FUEL	BUCKLING (m ⁻²)		CORE RADIUS (cm)	k _{eff} RECORD & MD-1
	wt% PuO ₂	% Pu ²⁴⁰			TOTAL	AXIAL		
2.1	2.0	8	2.032	1.515	93.7	8.86	19.08	1.0084
2.2	"	"	2.362	2.489	103.3	8.70	17.20	1.0141
2.3	"	"	2.667	3.515	101.3	8.65	17.27	1.0090
2.4	"	"	2.903	4.397	97.0	8.84	18.51	1.0126
2.5	"	"	3.353	6.282	75.6	8.89	22.48	1.0079
2.6	"	"	3.520	7.054	68.9	9.10	24.76	1.0028
2.7	2.0	16	2.362	2.489	86.3	8.60	19.44	1.0135
2.8	"	"	2.667	3.515	85.4	8.58	19.52	1.0096
2.9	"	"	2.903	4.397	81.5	8.77	20.87	1.0092
2.10	"	"	3.353	6.282	61.6	8.89	26.17	1.0045
2.11	"	"	3.520	7.054	55.6	9.28	29.49	0.9987
2.12	2.0	24	2.032	1.515	63.1	8.48	24.32	1.0007
2.13	"	"	2.362	2.488	79.4	8.67	20.98	1.0053
2.14	"	"	2.667	3.515	77.6	8.71	21.38	1.0060
2.15	"	"	2.903	4.397	72.2	8.88	23.22	1.0075
2.16	"	"	3.353	6.282	53.7	9.30	30.30	1.0014
2.17	"	"	3.520	7.054	44.3	9.43	35.33	0.9979

TABLE 10.1.4 BNWL UO₂-4 & 1.5 wt% PuO₂ Critical Lattices

CATALOG NO. BNWL-	PU ENRICHMENT		HEXAGONAL LATTICE PITCH (cm)	H ₂ O/FUEL	BUCKLING (m ⁻²)		CORE RADIUS (cm)	k _{eff} RECORD & MD-1
	wt% PuO ₂	% Pu ²⁴⁰			TOTAL	AXIAL		
4.1	4.0	18	2.159	1.929	94.7	8.59	18.02	1.0019
4.2	"	"	2.362	2.563	107.9	8.70	16.59	1.0029
4.3	"	"	2.667	3.622	108.7	8.70	16.50	1.0139
4.4	"	"	2.903	4.531	107.9	8.78	16.86	1.0130
4.5	"	"	3.520	7.268	88.4	9.06	20.55	1.0135
4.6	"	"	4.064	10.115	59.5	9.48	28.70	1.0066
4.7	"	"	4.318	11.585	41.1	9.46	37.38	1.0019
1.1	1.5	8	1.397	1.099	48.0	5.04	28.28	1.0112
1.2	"	"	1.524	1.557	65.1	5.10	23.04	1.0096
1.3	"	"	1.803	2.705	78.5	5.20	20.83	1.0102
1.4	"	"	2.032	3.788	74.9	5.26	21.86	1.0072
1.5	"	"	2.286	5.143	60.9	5.28	25.52	1.0063
1.6	"	"	2.362	5.580	55.2	5.30	27.40	1.0070

TABLE 10.1.5 RECORD/MD-1 Calculated k_{eff} -Values for UO_2/PuO_2 Lattices

% PuO_2	% Pu^{240}	NO. OF LATTICES	MEAN k_{eff}
2	8	6	1.0091 ± 0.0040
	16	5	1.0071 ± 0.0057
	24	6	1.0031 ± 0.0037
4	18	7	1.0077 ± 0.0057
1.5	8	6	1.0086 ± 0.0020
Mean k_{eff} for 30 lattices :			1.0071 ± 0.0046

TABLE 10.3.1 Characteristics of the Gamma Scanned Fuel Bundles in Quad Cities-1

IDENTIFICATION	CORE LOCATION	FUEL DESIGN	AVERAGE EXPOSURE
GEH-002	13 - 36	8 x 8 Reload , 2.50%	8 933 MWD/TU
CX-672	15 - 36	7 x 7 Initial, 2.12%	17 150 MWD/TU
CX-214	33 - 34	7 x 7 Initial, 2.12%	17 328 MWD/TU

IDENTIFICATION	GADOLINIUM LOADING		
	NO.	INITIAL Gd_2O_3	LATTICE POSITIONS
GEH-002	4	1.5 %	C3, G3, C7, G7
CX-672	2	3.0 %	F4, D6
CX-214	2	3.0 %	F4, D6
	1	0.5 %	C3

TABLE 10.3.2 Summary of Comparison Between RECORD and Fuel Bundle Gamma Scan Data in Quad Cities-1

AXIAL ELEVATION (Inches from Bottom)	GEH-002			CX-672			CX-214		
	EXPOSURE (MWD/TU)	EXP.W. VOID (%)	RMS DIFF. (%)	EXPOSURE (MWD/TU)	EXP.W. VOID (%)	RMS DIFF. (%)	EXPOSURE (MWD/TU)	EXP.W. VOID (%)	RMS DIFF. (%)
18	10.948	11.1	1.8	16.885	4.4	4.2	17.207	6.1	3.1
53.5	10.231	45.2	2.1	20.592	34.5	3.9	20.636	36.0	2.9
90	9.548	61.6	2.6	19.530	54.0	3.8	19.753	54.5	3.1
126	6.798	69.9	2.2	14.584	63.5	3.4	14.203	63.8	2.9
TOTAL			2.2			3.8			3.0

TABLE 10.4.1 Overview of the Main Reactor Cycles Used for Evaluation of RECORD - PRESTO by ScP

REACTOR	CYCLE	TYPE	YEAR OF ANALYSIS	AVERAGE k_{eff}	REFERENCE
MÜHLEBERG (KKM)	1	BWR	1974	1.0097 ± 0.0025	(67)
"	2	"	1975	1.0011 ± 0.024	"
"	3	"	1977	1.0062 ± 0.0014	-
QUAD CITIES	1	"	1976	0.9947 ± 0.0034	(68)
"	2	"	1976	0.9901 ± 0.0020	"
SANTA MARIA de GAROÑA (NUCLENOR)	7	"	1978	1.0015 ± 0.0010	-
BRUNSBÜTTEL (KKB)	1A	"	1979	0.9992 ± 0.0033	-
	1B	"	1982	1.0035 ± 0.0012	-
HATCH	1	"	1982	0.9972 ± 0.0025	(3)
MAINE YANKEE	1	PWR	1976	$.9848 \pm .0029$	(68)
	1A	"	1976	$.9919 \pm .0015$	"
BEAVER VALLEY	1	"	1980	0.9951 ± 0.0020	-

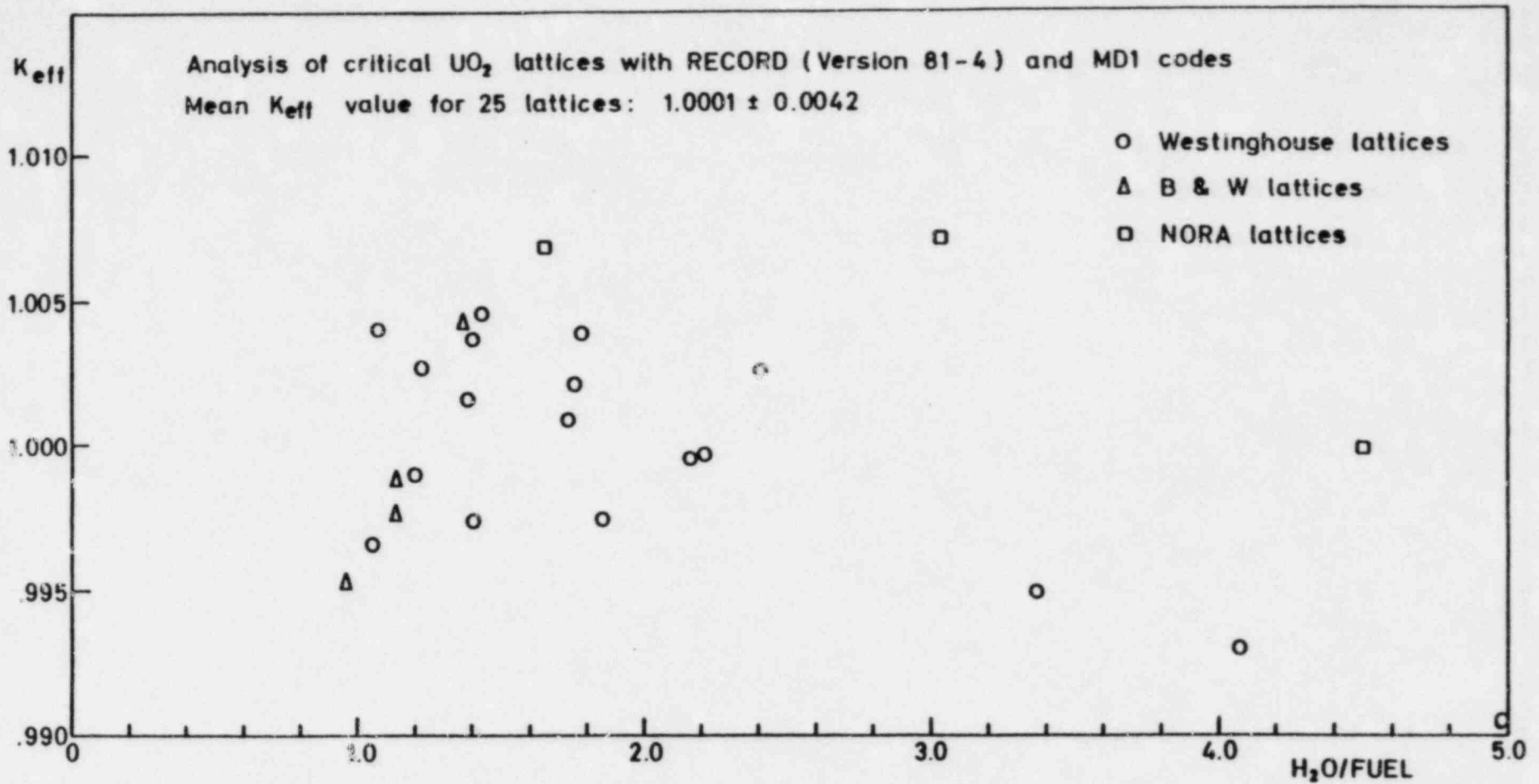
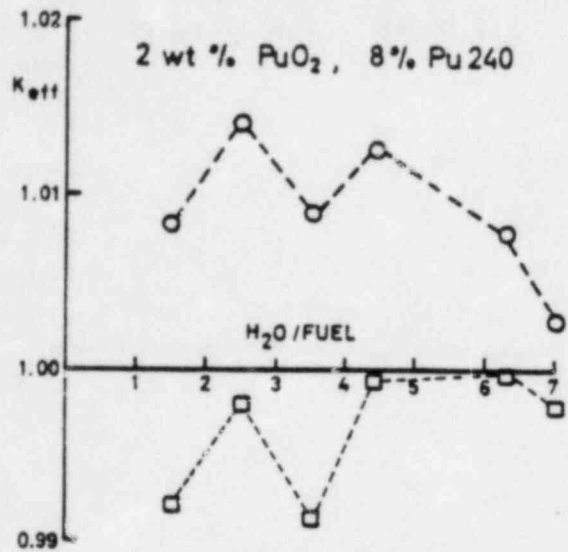


FIGURE 10.1.1 Calculated k_{eff} -values for Critical UO_2 Lattices at 20 °C



Analysis of BNWL critical UO₂-PuO₂ lattices at 22 - 25°C.

—○— Results from RECORD (Version 81-4) and MD1 codes.

—□— Result from BNWL analysis (1972): Codes HRG3, BRT-I and HFN.

Mean k_{eff} value for 30 lattices:

RECORD + MD1: 1.0071 ± 0.0046

BNWL analysis: 0.9985 ± 0.0036

(No corrections for reactivity effect of particulate fuel, or lattice grid plates)

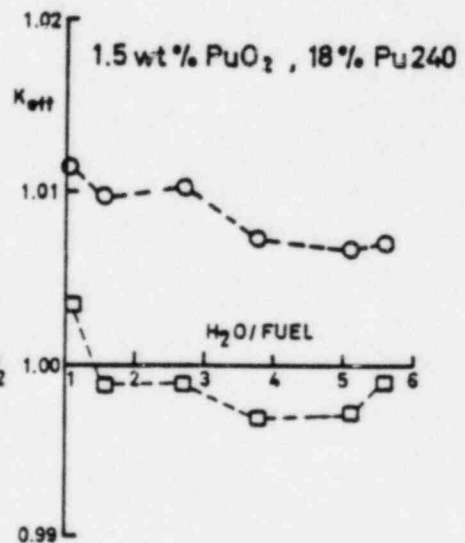
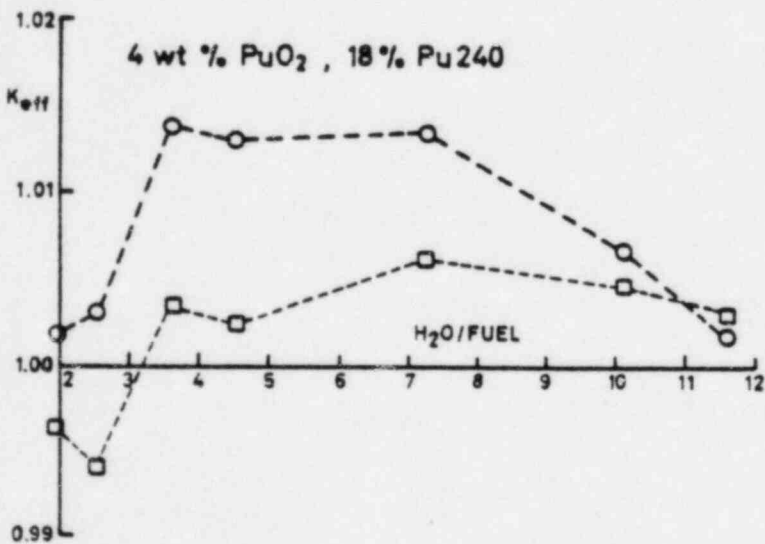
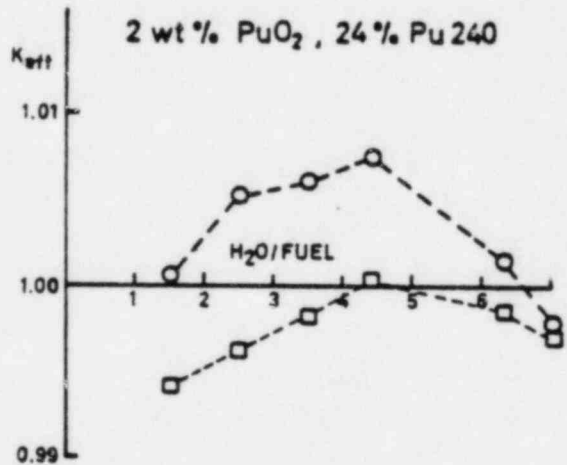
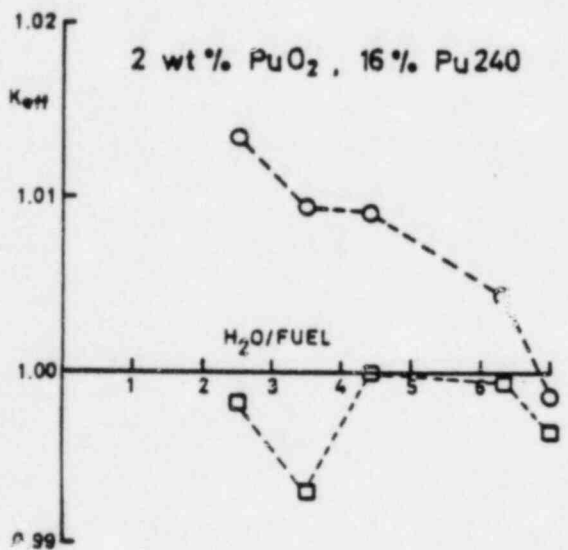


FIGURE 10.1.2 Calculated K_{eff} -values for Critical UO₂ - PuO₂ Lattices

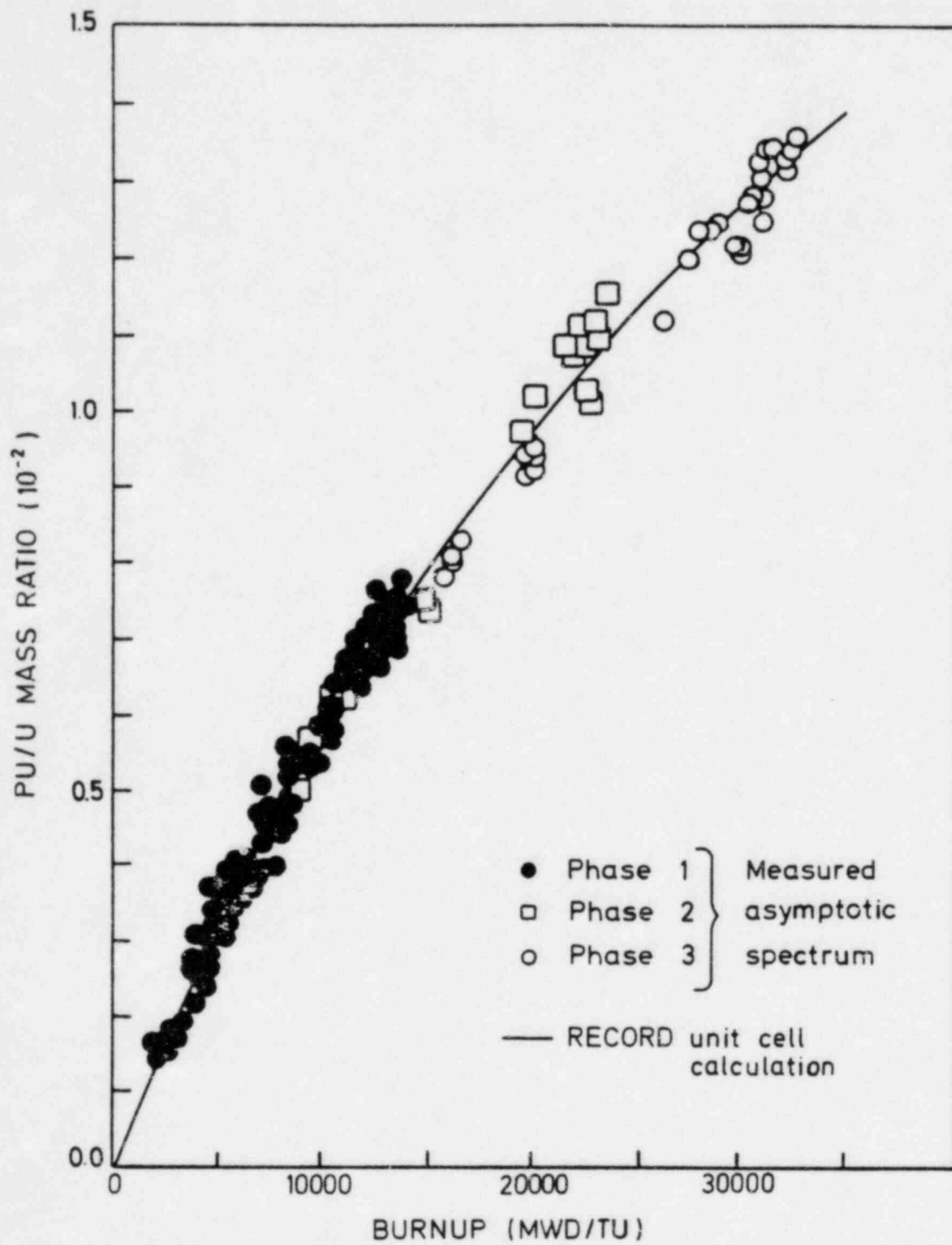


FIGURE 10.2.1 Plutonium-to-Uranium Mass Ratio vs. Burnup, Maine Yankee, Core 1

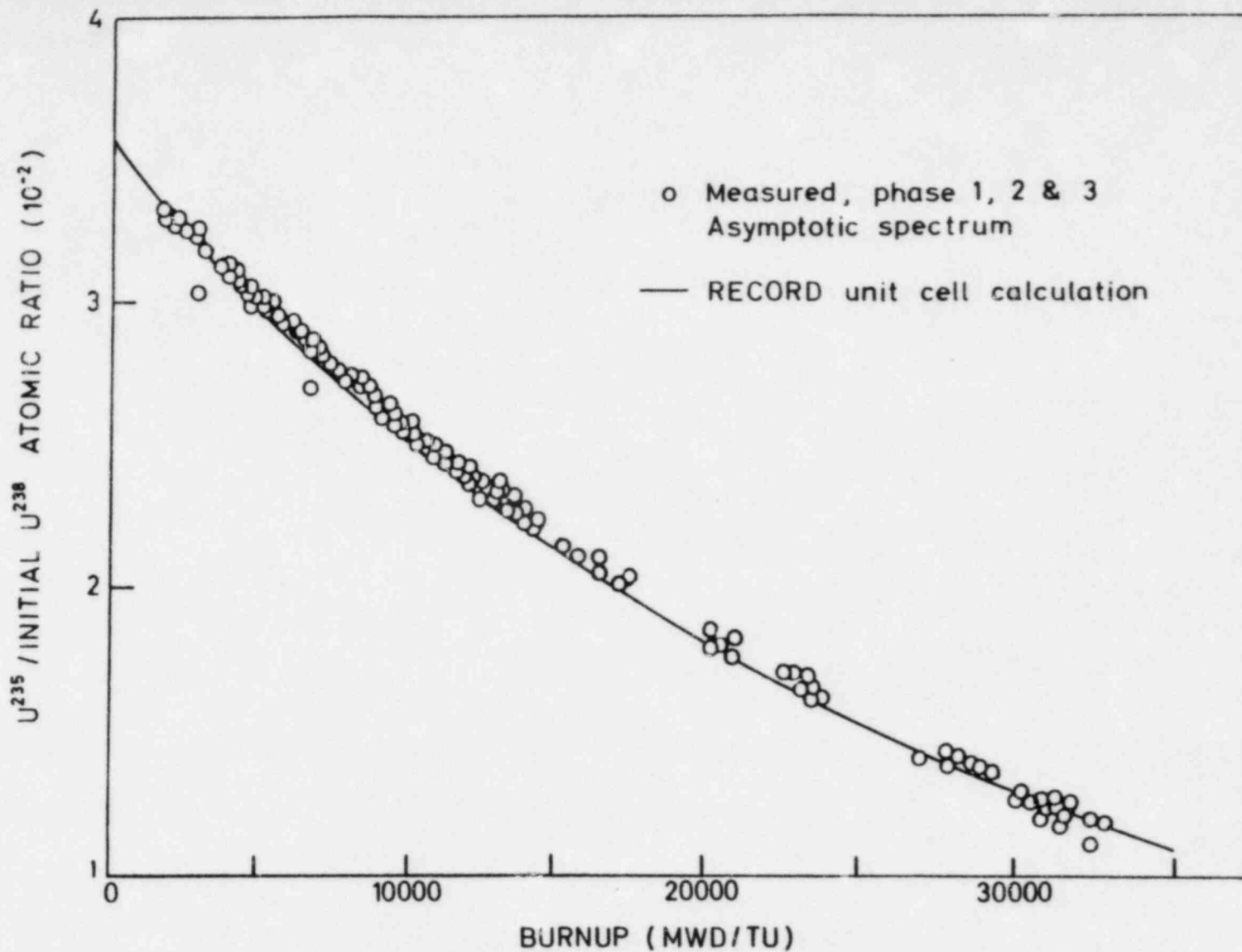


FIGURE 10.2.2 U^{235} Concentrations vs. Burnup, Maine Yankee, Core 1

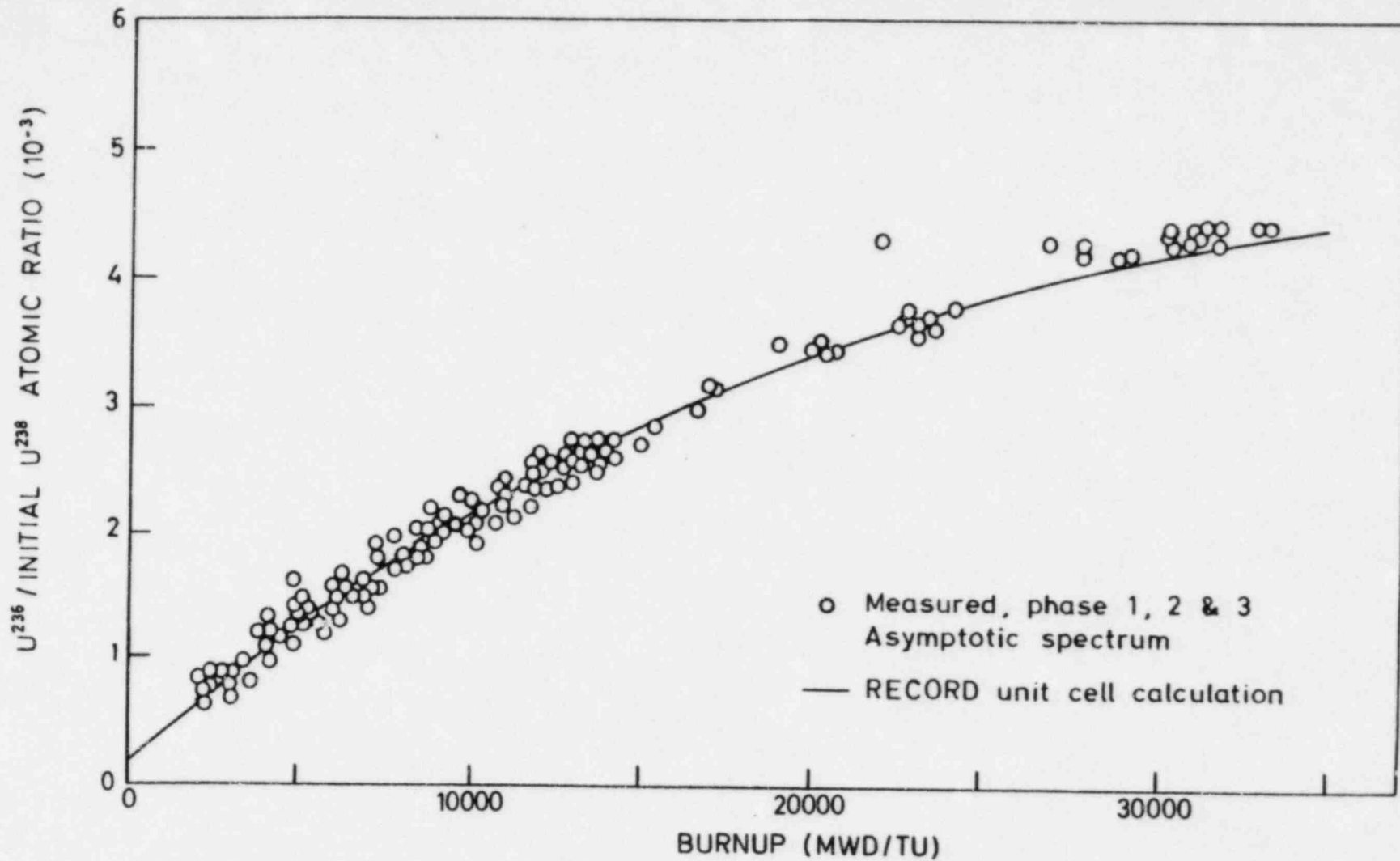
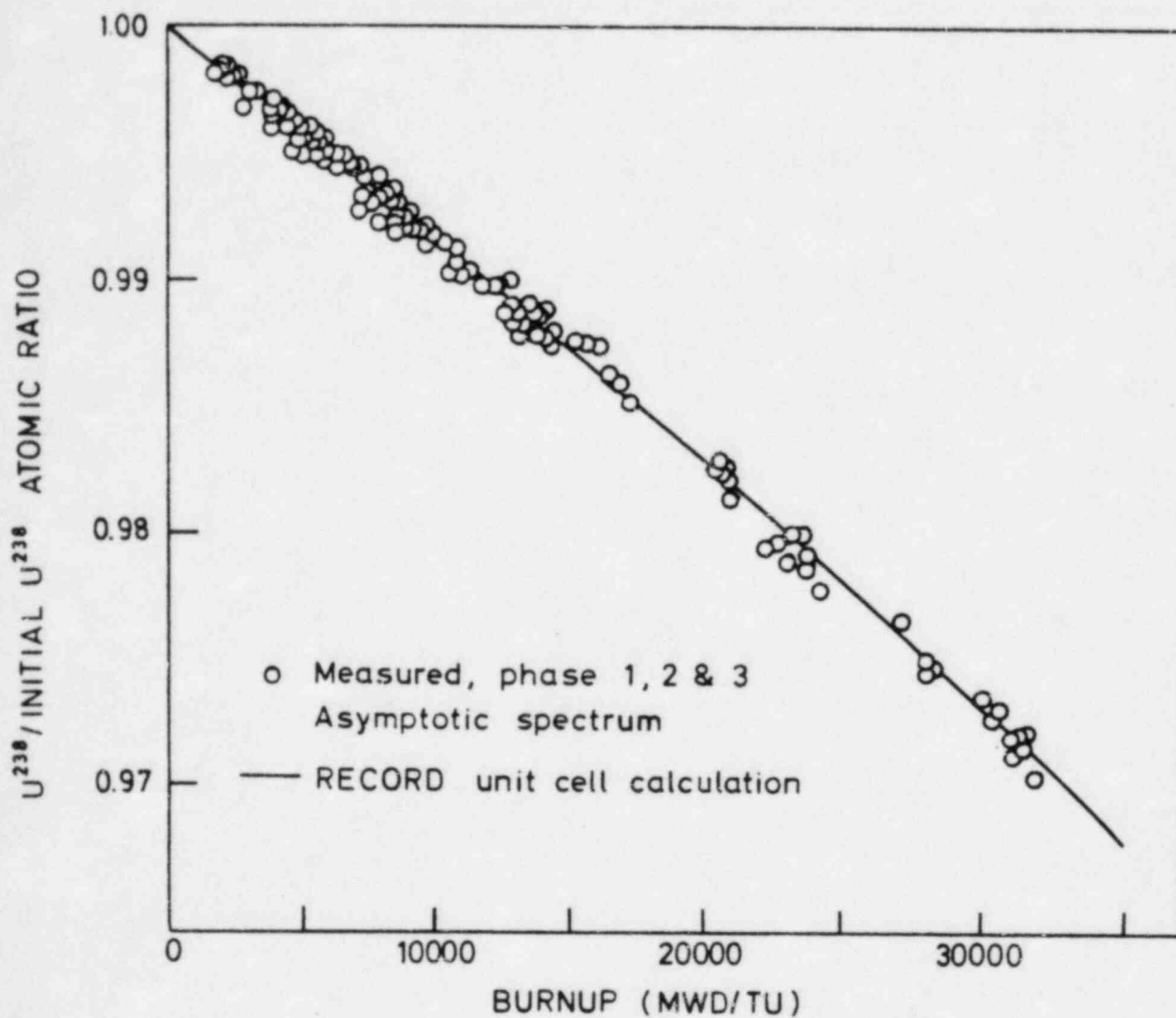


FIGURE 10.2.3 U^{236} Concentrations vs. Burnup, Maine Yankee, Core 1

FIGURE 10.2.4 U^{238} Concentrations vs. Burnup, Maine Yankee, Core 1

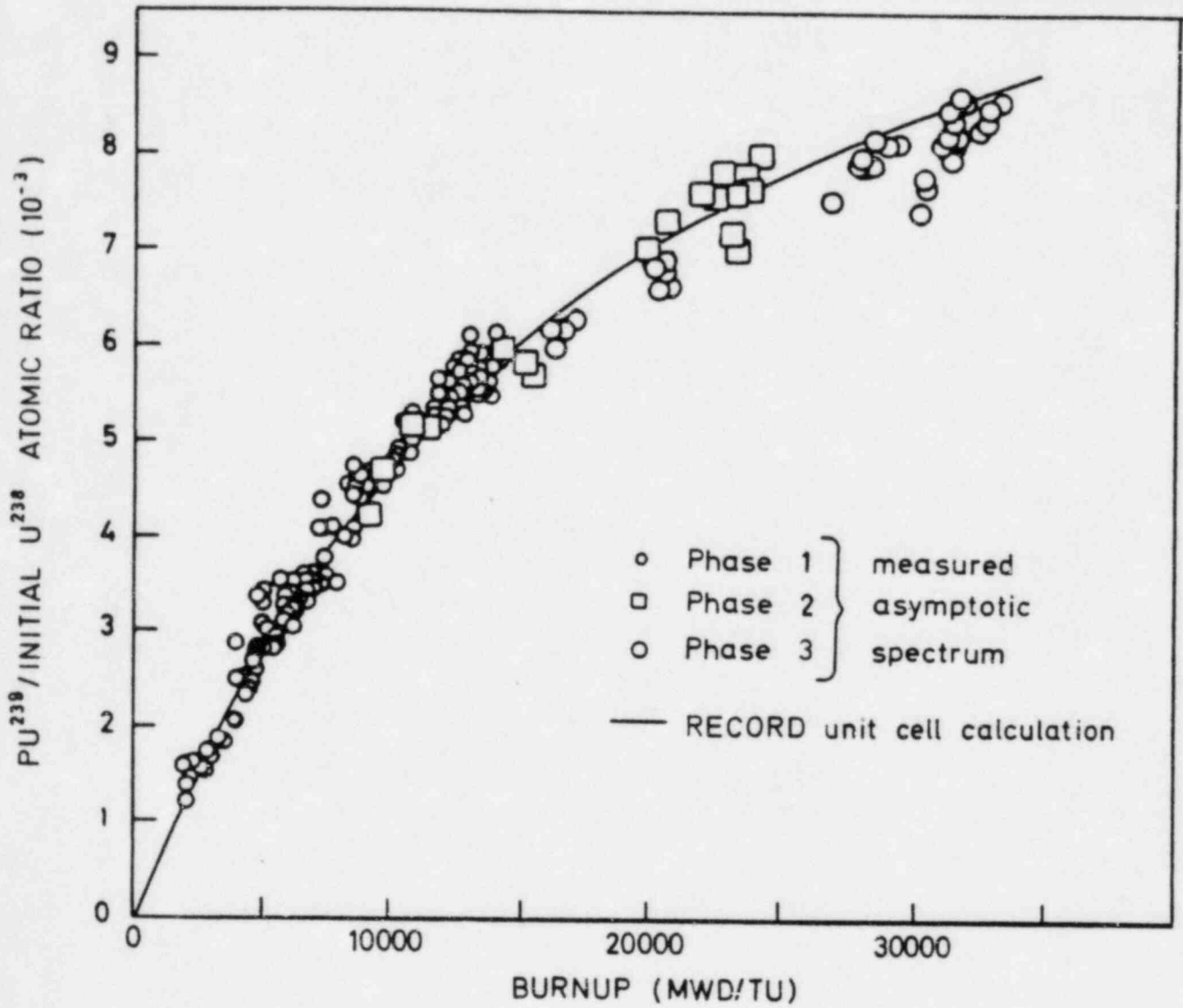


FIGURE 10.2.5 Pu²³⁹ Concentrations vs. Burnup, Maine Yankee, Core 1

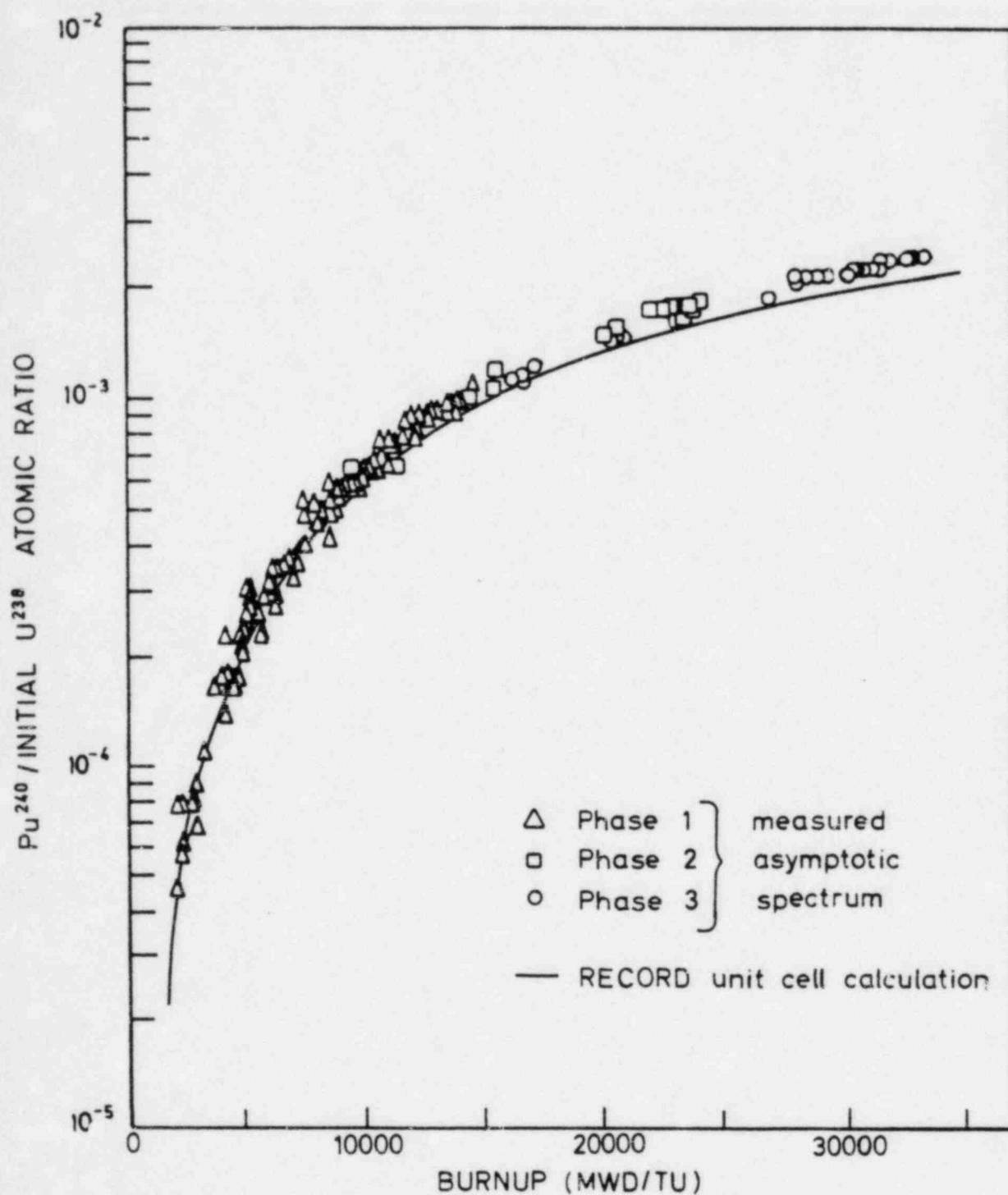


FIGURE 10.2.6 Pu^{240} Concentrations vs. Burnup, Maine Yankee, Core 1

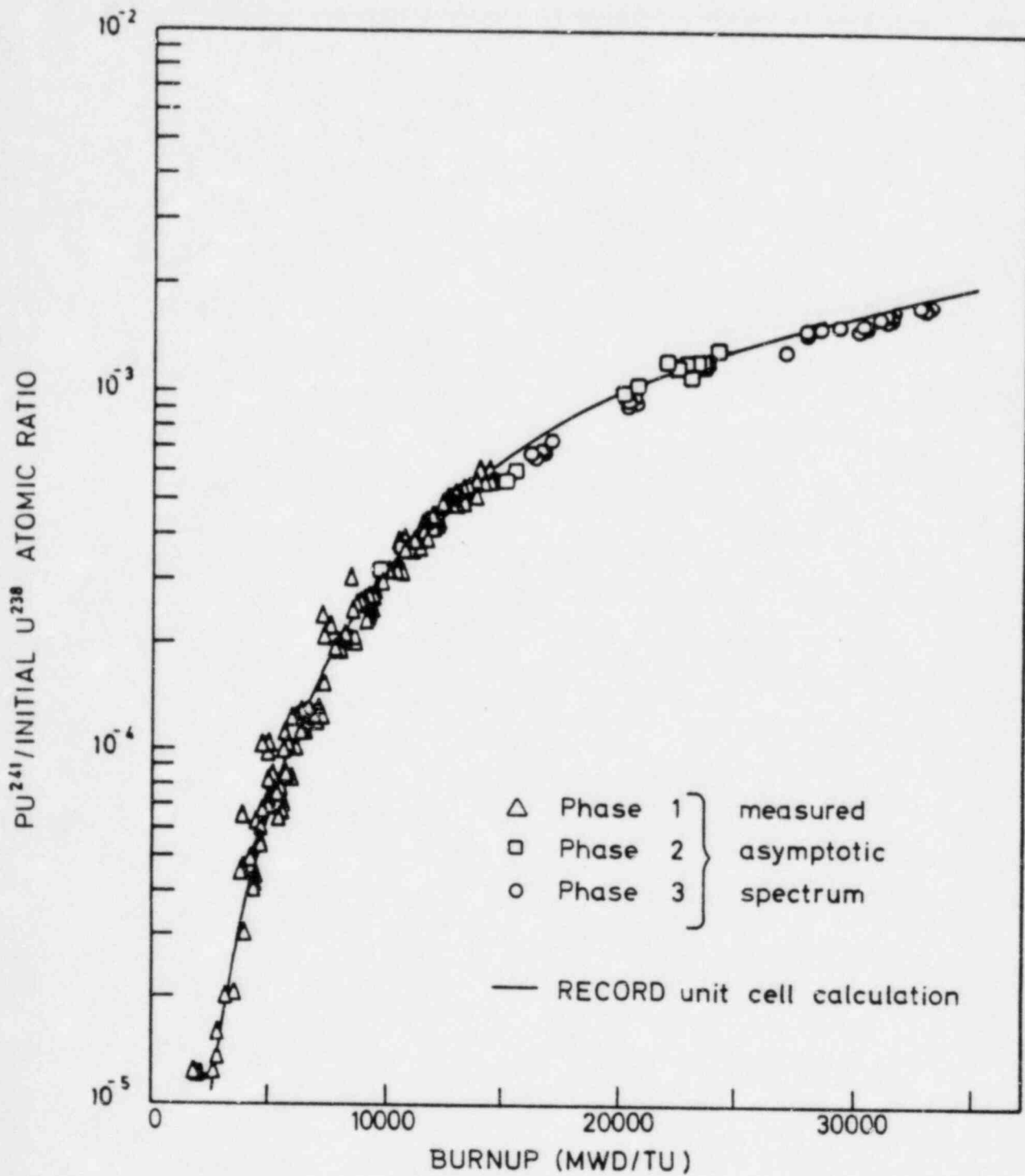


FIGURE 10.2.7 Pu^{241} Concentrations vs. Burnup, Maine Yankee, Core 1

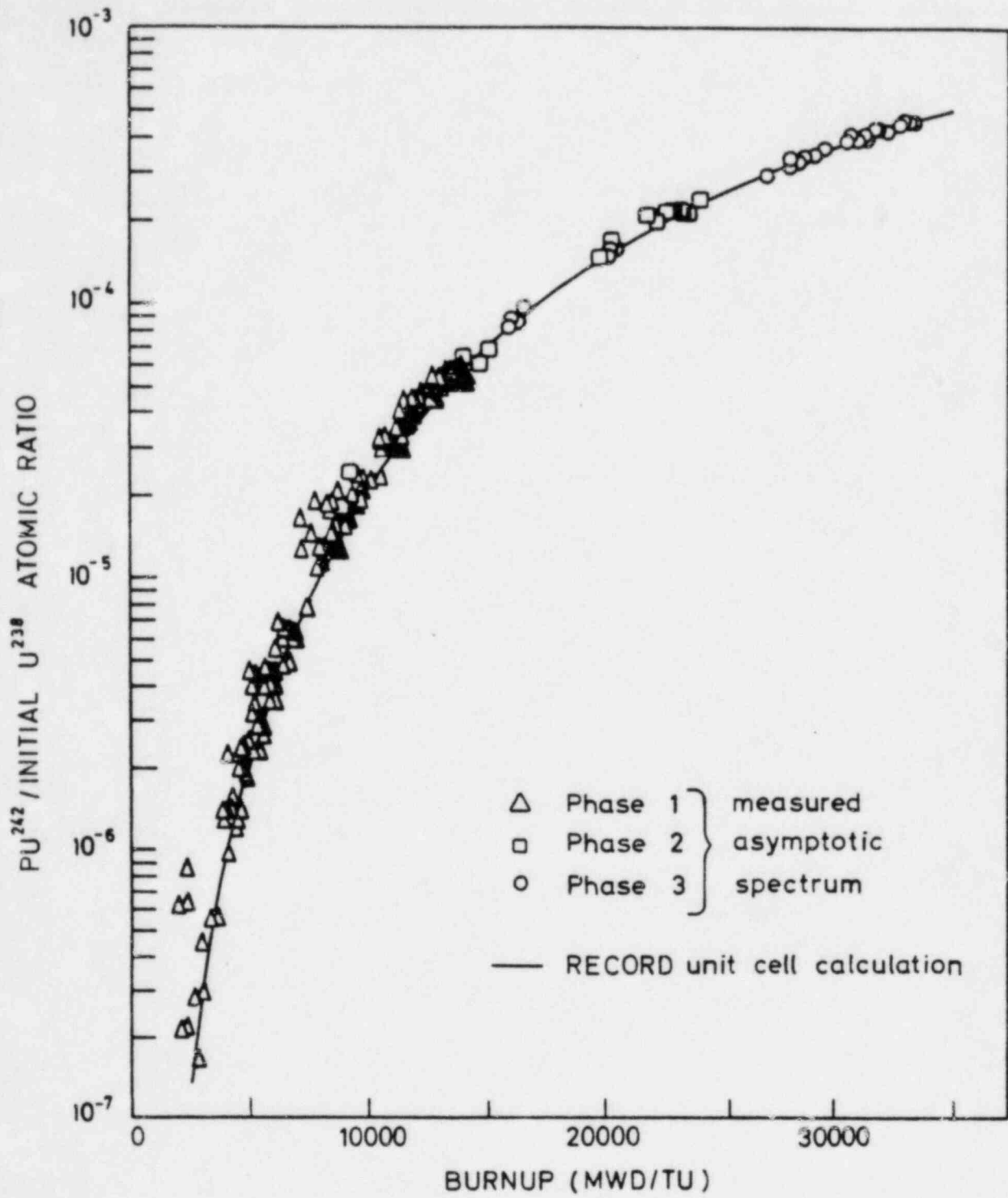


FIGURE 10.2.8 Pu^{242} Concentrations vs. Burnup, Maine Yankee, Core 1

WIDE CITIES-1 EOC2
BENCHMARK GAMMA SCAN
WIDE
WIDE
GAP
RECORD RESULTS COMPARED WITH
MEASUREMENTS
BUNDLE SERIAL NUMBER GEH-002
ROD BY ROD PLANAR LAY4C DISTRIBUTION
16.6 INCHES ABOVE BOTTOM OF FUEL
LEGEND:

I CALC.I : NCRP. POWER CALC BY RECORD
I MEAS.I : NCRP. LAY4C INTENSITY
I DIFF.I : CALC. - MEAS.

AVERAGE OF 55 RODS = 1.0
RMS POWER DIFFERENCE : 1.8 %

	A	B	C	D	E	F	G	H
1	1.997	1.014	1.000	1.010	1.000	1.000	1.000	1.007
1	1.002	1.043	1.000	1.027	1.000	1.000	1.000	1.043
1	-0.005	-0.014	1.000	-0.021	-0.002	1.000	-0.000	0.004
2	1.029	0.982	1.005	1.023	1.012	1.029	1.076	1.012
2	1.023	0.993	1.073	1.040	1.016	1.029	1.094	1.000
2	0.006	-0.011	-0.000	-0.017	-0.004	0.000	-0.016	0.012
3	1.000	1.005	0.982	0.941	0.931	0.948	0.997	1.000
3	1.000	1.066	0.990	0.954	0.921	0.959	1.000	1.000
3	1.000	0.000	0.000	0.000	0.000	0.000	0.000	0.000
4	1.000	1.000	0.941	0.918	0.919	0.920	0.957	1.007
4	1.000	1.034	0.947	0.918	0.920	0.927	0.965	1.001
4	0.000	0.000	0.000	0.000	0.000	0.000	0.000	0.000
5	1.000	1.012	0.921	0.921	0.930	0.930	0.947	1.000
5	1.000	1.030	0.927	0.945	0.934	0.934	0.944	1.000
5	0.000	0.000	0.000	0.000	0.000	0.000	0.000	0.000
6	1.000	1.029	0.942	0.926	0.930	0.934	0.904	1.000
6	1.000	1.043	0.957	0.924	0.929	0.922	0.955	1.000
6	1.000	0.000	0.000	0.000	0.000	0.000	0.000	0.000
7	1.000	1.078	0.997	0.957	0.947	0.964	1.012	1.118
7	1.000	1.065	0.997	0.955	0.929	0.940	0.989	1.095
7	0.000	0.007	0.000	0.002	0.018	0.024	0.023	0.023
8	1.047	1.012	1.000	1.067	1.056	1.000	1.116	1.031
8	1.000	0.998	1.000	1.035	1.006	1.000	1.080	0.962
8	0.012	0.014	1.000	0.028	0.042	1.000	0.038	0.069

WIDE CITIES-1 EOC2
BENCHMARK GAMMA SCAN
WIDE
WIDE
GAP
RECORD RESULTS COMPARED WITH
MEASUREMENTS
BUNDLE SERIAL NUMBER GEH-002
ROD BY ROD PLANAR LAY4C DISTRIBUTION
53.5 INCHES ABOVE BOTTOM OF FUEL
LEGEND:

I CALC.I : NCRP. POWER CALC BY RECORD
I MEAS.I : NCRP. LAY4C INTENSITY
I DIFF.I : CALC. - MEAS.

AVERAGE OF 55 RODS = 1.0
RMS POWER DIFFERENCE : 2.1 %

	A	B	C	D	E	F	G	H
1	1.073	1.003	1.000	1.047	1.035	1.000	1.003	1.093
1	1.001	1.066	1.000	1.055	1.057	1.000	1.080	1.094
1	0.012	0.017	1.000	-0.008	-0.022	1.000	0.003	-0.001
2	1.003	1.015	1.001	1.029	1.012	1.028	1.079	1.030
2	1.070	1.010	1.102	1.048	1.029	1.060	1.089	1.000
2	0.013	0.005	-0.021	-0.019	-0.017	-0.032	-0.010	0.022
3	1.000	1.001	0.997	0.932	0.916	0.932	0.997	1.000
3	1.000	1.005	1.010	0.966	0.921	0.942	0.989	1.000
3	1.000	0.004	-0.013	-0.034	-0.005	-0.010	0.008	1.000
4	1.047	1.029	0.932	0.902	0.898	0.903	0.931	1.052
4	1.052	1.035	0.942	0.917	0.933	0.911	0.933	1.003
4	0.005	0.006	-0.010	-0.015	-0.035	-0.000	-0.002	-0.031
5	1.000	1.012	0.916	0.898	0.899	0.915	0.915	1.035
5	1.037	1.012	0.916	0.934	0.931	0.921	0.920	1.052
5	0.002	0.000	0.000	-0.036	0.000	-0.032	-0.005	-0.017
6	1.000	1.028	0.932	0.903	0.899	0.903	0.931	1.000
6	1.000	1.030	0.939	0.896	0.912	0.896	0.930	1.000
6	1.000	0.002	-0.007	0.007	-0.013	0.005	0.001	1.000
7	1.003	1.079	0.997	0.931	0.915	0.931	0.997	1.099
7	1.072	1.079	0.972	0.933	0.900	0.915	0.949	1.098
7	0.011	0.000	0.025	-0.002	-0.009	0.016	0.048	0.001
8	1.004	1.030	1.000	1.052	1.035	1.000	1.099	1.036
8	1.075	0.983	1.000	1.027	0.999	1.000	1.051	0.986
8	0.019	0.047	1.000	0.025	0.036	1.000	0.048	0.050

FIGURE 10.3.1 RECORD Results Compared with Quad Cities Gamma Scan, Fuel Bundle GEH-002

		A	B	C	D	E	F	G	H
QUAD CITIES-1 EOC2 BENCHMARK GAMMA SCAN	WIDE	1 1.117	1 1.115	1 x x x	1 1.064	1 1.045	1 x x x	1 1.092	1 1.119
	WIDE GAP	1 1.074	1 1.100	1 x x x	1 1.050	1 1.060	1 x x x	1 1.107	1 1.110
RECORD RESULTS COMPARED WITH MEASUREMENTS	1	1	1	1	1	1	1	1	1
		1 -.043	1 .015	1 x x x	1 -.026	1 -.011	1 x x x	1 -.009	1 .009
BUNDLE SERIAL NUMBER GEH-002 ROD BY ROD PLANNER LA14C DISTRIBUTION 90.0 INCHES ABOVE BOTTOM OF FUEL	2	1 1.115	1 1.033	1 1.091	1 1.033	1 1.012	1 1.027	1 1.079	1 1.037
		1 1.057	1 1.021	1 1.120	1 1.068	1 1.068	1 1.053	1 1.086	1 1.026
	2	1	1	1	1	1	1	1	1
		1 -.018	1 -.012	1 -.029	1 -.035	1 -.036	1 -.026	1 -.007	1 -.011
LEGENDS:		1 x x x	1 1.091	1 1.014	1 .927	1 .909	1 .922	1 1.003	1 x x x
		1 x x x	1 1.100	1 1.010	1 .960	1 .934	1 .937	1 .986	1 x x x
1 CALC.1 : NCRP. POWER CALC BY RECORD 1 MEAS.1 : NCRP. LA140 INTENSITY 1 DIFF.1 : CALC. - MEAS.	3	1	1	1	1	1	1	1	1
		1 x x x	1 -.009	1 .004	1 -.033	1 -.025	1 -.015	1 .017	1 x x x
AVERAGE OF 55 RODS = 1.0 RMS POWER DIFFERENCE : 2.6 %		1 1.064	1 1.033	1 .927	1 .896	1 .887	1 .851	1 .916	1 1.040
		1 1.074	1 1.058	1 .945	1 .913	1 .917	1 .914	1 .936	1 1.061
	4	1	1	1	1	1	1	1	1
		1 -.010	1 -.025	1 -.018	1 -.017	1 -.030	1 -.023	1 -.022	1 -.021
		1 1.049	1 1.012	1 .909	1 .887	1 w w w	1 .823	1 .897	1 1.020
		1 1.049	1 1.007	1 .914	1 .911	1 w w w	1 .905	1 .914	1 1.016
	5	1	1	1	1	1	1	1	1
		1 .000	1 .005	1 -.005	1 -.024	1 w w w	1 -.022	1 -.017	1 .004
		1 x x x	1 1.028	1 .922	1 .851	1 .883	1 .817	1 .911	1 x x x
		1 x x x	1 1.047	1 .937	1 .901	1 .912	1 .875	1 .910	1 x x x
	6	1	1	1	1	1	1	1	1
		1 x x x	1 -.019	1 -.015	1 -.010	1 -.029	1 .012	1 .001	1 x x x
		1 1.096	1 1.079	1 1.003	1 .914	1 .897	1 .911	1 .992	1 1.084
		1 1.092	1 1.071	1 .966	1 .905	1 .864	1 .899	1 .922	1 1.041
	7	1	1	1	1	1	1	1	1
		1 .006	1 .008	1 .037	1 .011	1 .013	1 .012	1 .070	1 .043
		1 1.119	1 1.037	1 x x x	1 1.040	1 1.020	1 x x x	1 1.084	1 1.034
		1 1.091	1 1.001	1 x x x	1 1.029	1 1.001	1 x x x	1 1.038	1 .956
	8	1	1	1	1	1	1	1	1
		1 .028	1 .036	1 x x x	1 .011	1 .019	1 x x x	1 .047	1 .078

		A	B	C	D	E	F	G	H
QUAD CITIES-1 EOC2 BENCHMARK GAMMA SCAN	WIDE	1 1.137	1 1.139	1 x x x	1 1.073	1 1.054	1 x x x	1 1.109	1 1.132
	WIDE GAP	1 1.104	1 1.120	1 x x x	1 1.088	1 1.058	1 x x x	1 1.121	1 1.103
RECORD RESULTS COMPARED WITH MEASUREMENTS	1	1	1	1	1	1	1	1	1
		1 .033	1 .019	1 x x x	1 -.015	1 -.004	1 x x x	1 -.012	1 .028
BUNDLE SERIAL NUMBER GEH-002 ROD BY ROD PLANNER LA14C DISTRIBUTION 120.0 INCHES ABOVE BOTTOM OF FUEL	2	1 1.139	1 1.048	1 1.105	1 1.039	1 1.015	1 1.030	1 1.086	1 1.037
		1 1.133	1 1.045	1 1.125	1 1.058	1 1.037	1 1.037	1 1.116	1 1.022
	2	1	1	1	1	1	1	1	1
		1 .006	1 .002	1 -.020	1 -.019	1 -.022	1 -.007	1 -.030	1 .015
LEGENDS:		1 x x x	1 1.106	1 1.036	1 .922	1 .901	1 .914	1 1.017	1 x x x
		1 x x x	1 1.122	1 .999	1 .943	1 .906	1 .922	1 .980	1 x x x
1 CALC.1 : NCRP. POWER CALC BY RECORD 1 MEAS.1 : NCRP. LA140 INTENSITY 1 DIFF.1 : CALC. - MEAS.	3	1	1	1	1	1	1	1	1
		1 x x x	1 -.017	1 .037	1 -.021	1 -.007	1 -.008	1 .037	1 x x x
AVERAGE OF 55 RODS = 1.0 RMS POWER DIFFERENCE : 2.2 %		1 1.073	1 1.039	1 .922	1 .888	1 .876	1 .880	1 .904	1 1.033
		1 1.083	1 1.053	1 .941	1 .903	1 .898	1 .890	1 .924	1 1.044
	4	1	1	1	1	1	1	1	1
		1 -.010	1 -.014	1 -.019	1 -.015	1 -.022	1 -.010	1 -.021	1 -.011
		1 1.054	1 1.015	1 .901	1 .876	1 w w w	1 .869	1 .882	1 1.009
		1 1.058	1 1.021	1 .906	1 .896	1 w w w	1 .886	1 .888	1 1.002
	5	1	1	1	1	1	1	1	1
		1 -.004	1 -.006	1 -.007	1 -.020	1 w w w	1 -.017	1 -.006	1 .001
		1 x x x	1 1.030	1 .914	1 .880	1 .869	1 .872	1 .895	1 x x x
		1 x x x	1 1.052	1 .929	1 .883	1 .894	1 .854	1 .895	1 x x x
	6	1	1	1	1	1	1	1	1
		1 x x x	1 -.022	1 -.015	1 -.003	1 -.025	1 .016	1 -.000	1 x x x
		1 1.109	1 1.086	1 1.017	1 .904	1 .882	1 .855	1 .996	1 1.078
		1 1.109	1 1.092	1 .969	1 .912	1 .884	1 .885	1 .927	1 1.048
	7	1	1	1	1	1	1	1	1
		1 -.010	1 -.012	1 .048	1 -.006	1 -.002	1 .010	1 .069	1 .030
		1 1.132	1 1.036	1 x x x	1 1.033	1 1.009	1 x x x	1 1.078	1 1.023
		1 1.123	1 1.023	1 x x x	1 1.044	1 1.010	1 x x x	1 1.039	1 .977
	8	1	1	1	1	1	1	1	1
		1 .009	1 .014	1 x x x	1 -.011	1 -.001	1 x x x	1 .039	1 .046

Figure 10.3.2 RECORD Results Compared with Quad Cities Gamma Scan, Fuel Bundle GEH-002

WUAD CITIES-1 EOC2
BENCHMARK GAMMA SCAN
RECORD RESULTS COMPARED WITH
MEASUREMENTS

WIDE
WIDE
GAP

BUNDLE SERIAL NUMBER CX-672
ROD BY ROD PLANAR LAY40 DISTRIBUTION
30.0 INCHES ABOVE BOTTOM OF FUEL

LEGEND:

I CALC_1 : NORM. POWER CALC BY RECORD
I MEAS_1 : NORM. LA140 INTENSITY
I DIFF_1 : CALC. - MEAS.

AVERAGE OF 40 RODS = 1.0
RMS POWER DIFFERENCE = 4.351 %

	A	B	C	D	E	F	G
1	1.001	.939	X X X	.987	X X X	1.004	.965
1	1.031	.982	X X X	1.003	X X X	1.049	.933
11	1	1	1	1	1	1	1
1	-.031	-.043	X X X	-.036	X X X	-.040	-.032
1	.939	.948	.908	1.032	1.036	1.063	.983
1	.983	.998	.905	1.075	1.063	1.043	.991
21	1	1	1	1	1	1	1
1	-.044	-.050	.003	-.043	-.027	.024	-.008
1	X X X	.908	.997	.972	.978	1.014	X X X
1	X X X	.943	1.046	.989	.983	1.023	X X X
31	1	1	1	1	1	1	1
1	X X X	-.035	-.049	-.017	-.005	-.019	X X X
1	.987	1.032	.972	X X X	.955	1.011	1.075
1	1.049	1.060	.989	X X X	.972	1.023	1.090
41	1	1	1	1	1	1	1
1	-.062	-.028	-.017	X X X	-.017	-.012	.085
1	X X X	1.036	.978	.955	.960	.956	X X X
1	X X X	1.093	.968	.966	.919	1.023	X X X
51	1	1	1	1	1	1	1
1	X X X	-.057	.010	-.013	.041	-.016	X X X
1	1.010	1.063	1.014	1.031	.997	1.026	1.104
1	1.031	1.072	1.027	.996	.976	1.005	1.045
61	1	1	1	1	1	1	1
1	-.021	-.009	-.013	.015	.026	.021	.059
1	.965	.983	X X X	1.025	X X X	1.104	1.010
1	.911	.915	X X X	1.019	X X X	1.015	.920
71	1	1	1	1	1	1	1
1	.054	.068	X X X	.066	X X X	.089	.090

WUAD CITIES-1 EOC2
BENCHMARK GAMMA SCAN
RECORD RESULTS COMPARED WITH
MEASUREMENTS

WIDE
WIDE
GAP

BUNDLE SERIAL NUMBER CX-672
ROD BY ROD PLANAR LA140 DISTRIBUTION
53.5 INCHES ABOVE BOTTOM OF FUEL

LEGEND:

I CALC_1 : NORM. POWER CALC BY RECORD
I MEAS_1 : NORM. LA140 INTENSITY
I DIFF_1 : CALC. - MEAS.

AVERAGE OF 40 RODS = 1.0
RMS POWER DIFFERENCE = 3.863 %

	A	B	C	D	E	F	G
1	1.070	.994	X X X	1.012	X X X	1.032	1.021
1	1.015	.951	X X X	.977	X X X	.994	.958
11	1	1	1	1	1	1	1
1	.055	.043	X X X	.035	X X X	.038	.063
1	.994	.967	.926	1.018	1.021	1.046	1.001
1	.934	.958	.919	1.069	1.038	1.040	.942
21	1	1	1	1	1	1	1
1	.060	.009	.007	-.051	-.017	.006	.059
1	X X X	.926	.984	.957	.961	.955	X X X
1	X X X	.917	1.035	1.010	.999	1.038	X X X
31	1	1	1	1	1	1	1
1	X X X	.009	-.051	-.053	-.038	-.043	X X X
1	1.012	1.018	.957	X X X	.933	.985	1.056
1	1.015	1.075	.952	X X X	.977	1.021	1.018
41	1	1	1	1	1	1	1
1	-.063	-.057	-.035	X X X	-.044	-.036	.038
1	X X X	1.021	.961	.933	.936	.971	X X X
1	X X X	1.087	.974	.982	.928	.950	X X X
51	1	1	1	1	1	1	1
1	X X X	-.066	-.013	-.049	.008	-.019	X X X
1	1.032	1.046	.955	.985	.971	.959	1.081
1	1.004	1.084	1.032	.956	.957	1.013	1.056
61	1	1	1	1	1	1	1
1	.028	-.038	-.037	-.011	.014	-.014	.025
1	1.021	1.001	X X X	1.056	X X X	1.081	1.027
1	1.000	.967	X X X	1.013	X X X	1.016	1.001
71	1	1	1	1	1	1	1
1	.013	.034	X X X	.043	X X X	.065	.026

FIGURE 10.3.3 RECORD Results Compared with Quad Cities Gamma Scan, Fuel Bundle CX-672

		A	B	C	D	E	F	G
NUCLEONIC-1 ECC2 BENCHMARK GAMMA SCAN	WIDE	1 1.145	1 1.030	1 X X X	1 1.037	1 X X X	1 1.058	1 1.056
	WIDE	1 1.002	1 .960	1 X X X	1 .928	1 X X X	1 1.041	1 .996
	GAP	11 1	1 1	1 1	1 1	1 1	1 1	1 1
RECORD RESULTS COMPARED WITH MEASUREMENTS		1 .062	1 .042	1 X X X	1 .049	1 X X X	1 .017	1 .058
		1 1.030	1 .988	1 .936	1 1.019	1 1.020	1 1.048	1 1.016
		1 1.009	1 .984	1 .917	1 1.067	1 1.057	1 1.017	1 .992
BUNDLE SERIAL NUMBER CX-672 RCD BY ROD PLANNER LA140 DISTRIBUTION 96.0 INCHES ABOVE BOTTOM OF FUEL	21	1	1	1	1	1	1	1
		1 .021	1 .004	1 .019	1 -.048	1 -.037	1 .021	1 .024
		1 X X X	1 .936	1 .978	1 .942	1 .943	1 .981	1 X X X
LEGEND:		1 X X X	1 .936	1 1.028	1 .971	1 .977	1 1.020	1 X X X
		31 1	1 1	1 1	1 1	1 1	1 1	1 1
		1 X X X	1 -.000	1 -.050	1 -.029	1 -.034	1 -.039	1 X X X
I CALC.1 : NCRP. POWER CALC BY RECORD I MEAS.1 : NCRP. LA140 INTENSITY I DIFF.1 : CALC. - MEAS.		1 1.037	1 1.119	1 .942	1 X X X	1 .905	1 .934	1 1.047
		1 1.016	1 1.052	1 .973	1 X X X	1 .954	1 .964	1 1.041
	41	1	1	1	1	1	1	1
AVERAGE OF 40 RODS = 1.0 RMS POWER DIFFERENCE = 3.752 %		1 .021	1 -.033	1 -.031	1 X X X	1 -.049	1 -.060	1 .006
		1 X X X	1 1.020	1 .943	1 .905	1 .906	1 .945	1 X X X
		1 X X X	1 1.009	1 .940	1 .946	1 .896	1 1.001	1 X X X
I CALC.1 : NCRP. POWER CALC BY RECORD I MEAS.1 : NCRP. LA140 INTENSITY I DIFF.1 : CALC. - MEAS.	51	1	1	1	1	1	1	1
		1 X X X	1 -.049	1 .003	1 -.041	1 .014	1 -.056	1 X X X
		1 1.059	1 1.049	1 .981	1 .934	1 .945	1 .978	1 1.075
LEGEND:		1 1.024	1 1.038	1 .957	1 .974	1 .957	1 .968	1 1.076
	61	1	1	1	1	1	1	1
		1 .037	1 .011	1 -.016	1 -.040	1 -.012	1 -.020	1 -.001
AVERAGE OF 40 RODS = 1.0 RMS POWER DIFFERENCE = 3.752 %		1 1.056	1 1.016	1 X X X	1 1.047	1 X X X	1 1.075	1 1.038
		1 .986	1 .951	1 X X X	1 1.022	1 X X X	1 1.017	1 1.022
	71	1	1	1	1	1	1	1
	1 .070	1 .065	1 X X X	1 .025	1 X X X	1 .058	1 .016	

		A	B	C	D	E	F	G
NUCLEONIC-1 ECC2 BENCHMARK GAMMA SCAN	WIDE	1 1.146	1 1.037	1 X X X	1 1.050	1 X X X	1 1.075	1 1.058
	WIDE	1 1.053	1 1.013	1 X X X	1 1.006	1 X X X	1 1.048	1 1.015
	GAP	11 1	1 1	1 1	1 1	1 1	1 1	1 1
RECORD RESULTS COMPARED WITH MEASUREMENTS		1 .094	1 .024	1 X X X	1 .044	1 X X X	1 .027	1 .043
		1 1.036	1 1.002	1 .932	1 1.029	1 1.027	1 1.064	1 1.019
		1 .973	1 .985	1 .897	1 1.073	1 1.046	1 1.066	1 1.009
BUNDLE SERIAL NUMBER CX-672 RCD BY ROD PLANNER LA140 DISTRIBUTION 126.0 INCHES ABOVE BOTTOM OF FUEL	21	1	1	1	1	1	1	1
		1 .064	1 .016	1 .035	1 -.044	1 -.019	1 -.002	1 .010
		1 X X X	1 .932	1 .978	1 .930	1 .929	1 .974	1 X X X
LEGEND:		1 X X X	1 .943	1 1.018	1 .960	1 .948	1 1.018	1 X X X
		31 1	1 1	1 1	1 1	1 1	1 1	1 1
		1 X X X	1 -.011	1 -.040	1 -.030	1 -.019	1 -.044	1 X X X
I CALC.1 : NCRP. POWER CALC BY RECORD I MEAS.1 : NCRP. LA140 INTENSITY I DIFF.1 : CALC. - MEAS.		1 1.050	1 1.029	1 .930	1 X X X	1 .882	1 .942	1 1.046
		1 1.033	1 1.052	1 .951	1 X X X	1 .904	1 .983	1 1.054
	41	1	1	1	1	1	1	1
AVERAGE OF 40 RODS = 1.0 RMS POWER DIFFERENCE = 3.410 %		1 .017	1 -.023	1 -.021	1 X X X	1 -.022	1 -.041	1 -.008
		1 X X X	1 1.027	1 .929	1 .882	1 .881	1 .925	1 X X X
		1 X X X	1 1.056	1 .940	1 .905	1 .880	1 .979	1 X X X
I CALC.1 : NCRP. POWER CALC BY RECORD I MEAS.1 : NCRP. LA140 INTENSITY I DIFF.1 : CALC. - MEAS.	51	1	1	1	1	1	1	1
		1 X X X	1 -.029	1 -.011	1 -.023	1 .001	1 -.054	1 X X X
		1 1.076	1 1.064	1 .974	1 .942	1 .925	1 .963	1 1.079
LEGEND:		1 1.055	1 1.074	1 1.015	1 .962	1 .926	1 .980	1 1.091
	61	1	1	1	1	1	1	1
		1 .020	1 -.010	1 -.049	1 -.020	1 -.001	1 -.017	1 -.012
AVERAGE OF 40 RODS = 1.0 RMS POWER DIFFERENCE = 3.410 %		1 1.058	1 1.019	1 X X X	1 1.046	1 X X X	1 1.079	1 1.032
		1 .996	1 .958	1 X X X	1 1.038	1 X X X	1 1.051	1 1.045
	71	1	1	1	1	1	1	1
	1 .062	1 .061	1 X X X	1 .008	1 X X X	1 .028	1 -.013	

FIGURE 10.3.4 RECORD Results Compared with Quad Cities Gamma Scan, Fuel Bundle CX-672

QUAD CITIES-1 EOC2
BENCHMARK GAMMA SCAN
WIDE WIDE GAP
RECORD RESULTS COMPARED WITH MEASUREMENTS
BUNDLE SERIAL NUMBER CX-214
ROD BY ROD PLANAR LA140 DISTRIBUTION
18.0 INCHES ABOVE BOTTOM OF FUEL

	A	B	C	D	E	F	G
I	1.004	.942	X X X	.988	X X X	1.010	.968
I	1.040	.973	X X X	1.043	X X X	1.023	.933
11	I	I	I	I	I	I	I
I	-.036	-.041	X X X	-.055	X X X	-.013	.035
I	.942	.949	.910	1.031	1.035	1.062	.984
I	.972	.991	.925	1.070	1.054	1.051	.919
21	I	I	I	I	I	I	I
I	-.030	-.042	-.015	-.039	-.019	.011	.064
I	X X X	.910	.996	.972	.978	1.013	X X X
I	X X X	.912	1.022	.974	.984	1.007	X X X
31	I	I	I	I	I	I	I
I	X X X	-.002	-.026	-.002	-.007	.006	X X X
I	.988	1.031	.972	X X X	.954	1.010	1.074
I	1.010	1.090	.988	X X X	.960	.950	1.044
41	I	I	I	I	I	I	I
I	-.022	-.059	-.016	X X X	-.006	.020	.030
I	X X X	1.035	.976	.954	.960	.956	X X X
I	X X X	1.075	.987	.936	.968	.953	X X X
51	I	I	I	I	I	I	I
I	X X X	-.040	-.009	.018	-.008	.003	X X X
I	1.010	1.062	1.013	1.010	.996	1.025	1.102
I	1.036	1.045	.987	1.015	.942	.968	1.059
61	I	I	I	I	I	I	I
I	-.026	.017	.026	-.005	.054	.057	.043
I	.968	.984	X X X	1.074	X X X	1.102	1.011
I	.955	.966	X X X	1.048	X X X	1.079	.955
71	I	I	I	I	I	I	I
I	.013	.018	X X X	.026	X X X	.023	.056

LEGEND:

I CALC. I : NCRP. POWER CALC BY RECORD
I MEAS. I : NCRP. LA140 INTENSITY
I DIFF. I : CALC. - MEAS.

AVERAGE OF 40 RODS = 1.0
RMS POWER DIFFERENCE : 3.143 %

QUAD CITIES-1 EOC2
BENCHMARK GAMMA SCAN
WIDE WIDE GAP
RECORD RESULTS COMPARED WITH MEASUREMENTS
BUNDLE SERIAL NUMBER CX-214
ROD BY ROD PLANAR LA140 DISTRIBUTION
53.5 INCHES ABOVE BOTTOM OF FUEL

	A	B	C	D	E	F	G
I	1.074	.996	X X X	1.013	X X X	1.033	1.023
I	1.057	.991	X X X	1.027	X X X	1.026	.984
11	I	I	I	I	I	I	I
I	-.017	-.005	X X X	-.054	X X X	-.007	.039
I	.996	.967	.926	1.017	1.020	1.045	1.002
I	.984	.990	.932	1.060	1.051	1.056	.948
21	I	I	I	I	I	I	I
I	-.012	-.023	-.006	-.043	-.031	-.011	.054
I	X X X	.926	1.000	.956	.959	.993	X X X
I	X X X	.940	1.021	.995	.979	1.007	X X X
31	I	I	I	I	I	I	I
I	X X X	-.014	-.021	-.039	-.020	-.014	X X X
I	1.013	1.017	.956	X X X	.930	.981	1.059
I	1.005	1.055	.983	X X X	.951	1.009	1.022
41	I	I	I	I	I	I	I
I	.006	-.038	-.027	X X X	-.021	-.028	.033
I	X X X	1.020	.959	.931	.933	.969	X X X
I	X X X	1.031	.980	.980	.941	.954	X X X
51	I	I	I	I	I	I	I
I	X X X	-.011	-.021	-.050	-.008	.015	X X X
I	1.034	1.045	.993	.921	.969	.957	1.080
I	.996	1.031	.989	.995	.958	1.012	1.074
61	I	I	I	I	I	I	I
I	-.036	.014	-.004	-.015	.011	-.083	.006
I	1.024	1.002	X X X	1.055	X X X	1.080	1.028
I	.972	.946	X X X	1.057	X X X	1.058	.953
71	I	I	I	I	I	I	I
I	.051	-.056	X X X	-.002	X X X	.022	.075

LEGEND:

I CALC. I : NCRP. POWER CALC BY RECORD
I MEAS. I : NCRP. LA140 INTENSITY
I DIFF. I : CALC. - MEAS.

AVERAGE OF 40 RODS = 1.0
RMS POWER DIFFERENCE : 2.876 %

FIGURE 10.3.5 RECORD Results Compared with Quad Cities Gamma Scan, Fuel Bundle CX-214

QUAD CITIES-1 EOC2
BENCHMARK GAMMA SCAN
RECORD RESULTS COMPARED WITH
MEASUREMENTS

WIDE
WIDE
GAP

BUNDLE SERIAL NUMBER CX-214
ROD BY ROD PLANAR LATAO DISTRIBUTION
96.6 INCHES ABOVE BOTTOM OF FUEL

LEGEND:

1 CALC.I : NORM. POWER CALC BY RECORD
1 MEAS.I : NORM. LATAO INTENSITY
1 DIFF.I : CALC. - MEAS.

AVERAGE OF 40 RODS = 1.0
RMS POWER DIFFERENCE = 3.065 %

	A	B	C	D	E	F	G
1	1.126	1.031	X X X	1.037	X X X	1.058	1.058
1	1.124	1.032	X X X	1.063	X X X	1.031	1.018
11	1	1	1	1	1	1	1
1	.000	-.001	X X X	-.026	X X X	.028	.040
1	1.039	.987	.936	1.019	1.019	1.047	1.016
1	1.023	.986	.949	1.023	1.063	1.027	.959
21	1	1	1	1	1	1	1
1	.008	.001	-.013	-.064	-.044	.026	.057
1	X X X	.936	.928	.942	.943	.980	X X X
1	X X X	.943	1.012	.991	.954	.942	X X X
31	1	1	1	1	1	1	1
1	X X X	-.007	-.024	-.049	-.011	.018	X X X
1	1.037	1.019	.942	X X X	.905	.932	1.046
1	1.045	1.064	.961	X X X	.908	.956	.997
41	1	1	1	1	1	1	1
1	-.028	-.045	-.019	X X X	-.003	-.074	.049
1	X X X	1.019	.943	.905	.905	.944	X X X
1	X X X	1.054	.950	.920	.907	.936	X X X
51	1	1	1	1	1	1	1
1	X X X	-.035	-.007	-.015	-.002	.008	X X X
1	1.059	1.047	.980	.932	.944	.977	1.074
1	1.030	1.033	.965	.965	.969	.974	1.036
61	1	1	1	1	1	1	1
1	.029	.014	.015	-.033	-.025	.003	.038
1	1.058	1.016	X X X	1.046	X X X	1.074	1.039
1	1.016	.967	X X X	1.065	X X X	1.064	.974
71	1	1	1	1	1	1	1
1	.042	.049	X X X	-.023	X X X	.010	.065

QUAD CITIES-1 EOC2
BENCHMARK GAMMA SCAN
RECORD RESULTS COMPARED WITH
MEASUREMENTS

WIDE
WIDE
GAP

BUNDLE SERIAL NUMBER CX-214
ROD BY ROD PLANAR LATAO DISTRIBUTION
146.6 INCHES ABOVE BOTTOM OF FUEL

LEGEND:

1 CALC.I : NORM. POWER CALC BY RECORD
1 MEAS.I : NORM. LATAO INTENSITY
1 DIFF.I : CALC. - MEAS.

AVERAGE OF 40 RODS = 1.0
RMS POWER DIFFERENCE = 2.944 %

	A	B	C	D	E	F	G
1	1.142	1.037	X X X	1.050	X X X	1.076	1.057
1	1.122	1.040	X X X	1.023	X X X	1.055	1.033
11	1	1	1	1	1	1	1
1	.026	-.003	X X X	-.033	X X X	.021	.024
1	1.037	1.002	.932	1.030	1.026	1.065	1.019
1	1.021	1.029	.950	1.061	1.049	1.055	.994
21	1	1	1	1	1	1	1
1	.016	-.027	.001	-.031	-.021	.010	.025
1	X X X	.932	.976	.930	.928	.973	X X X
1	X X X	.968	.999	.938	.940	.976	X X X
31	1	1	1	1	1	1	1
1	X X X	-.037	-.021	-.009	-.012	-.003	X X X
1	1.050	1.030	.930	X X X	.881	.944	1.046
1	1.074	1.064	.945	X X X	.905	.956	1.046
41	1	1	1	1	1	1	1
1	-.024	-.034	-.016	X X X	-.024	-.010	-.000
1	X X X	1.028	.928	.881	.880	.924	X X X
1	X X X	1.083	.943	.911	.894	.923	X X X
51	1	1	1	1	1	1	1
1	X X X	-.055	-.015	-.030	-.015	.001	X X X
1	1.076	1.065	.973	.944	.924	.962	1.079
1	1.074	1.037	.939	.962	.929	.963	1.004
61	1	1	1	1	1	1	1
1	.002	.028	.034	-.018	-.005	-.001	.075
1	1.057	1.019	X X X	1.046	X X X	1.079	1.031
1	1.039	.983	X X X	1.062	X X X	1.010	.959
71	1	1	1	1	1	1	1
1	.018	.036	X X X	-.016	X X X	.069	.072

FIGURE 10.3.6 RECORD Results Compared with Quad Cities Gamma Scan, Fuel Bundle CX-214

1.162					
1.168					
0.5	Thermal absorption rates in DODEWAARD Gd-assembly, initial, hot, voided, Gd pin hatched.				
1.032	0.891				
1.043	0.888				
1.1	-0.3				
0.993	0.831	0.773			
1.001	0.827	0.753			
0.8	-0.5	-2.6			
1.004	0.819	0.730	0.730	THERMOGENE RECORD % Dev.	
1.006	0.804	0.710	0.694		
0.2	-1.8	-2.7	-4.9		
1.086	0.840	2.016	0.759	0.838	
1.082	0.841	2.006	0.743	0.840	
-0.4	0.1	-0.5	-21	0.2	
1.260	1.023	0.918	0.925	0.995	1.146
1.260	1.034	0.939	0.937	1.009	1.150
C.	1.1	2.3	1.3	1.4	1.2

1.186					
1.170					
-1.3	Power distribution in DODEWAARD Gd-assembly, cold, initial.				
1.095	0.939				
1.074	0.936				
-1.9	-0.3				
1.070	0.898	0.835			
1.061	0.897	0.843			
-0.8	-0.1	1.0			
1.097	0.885	0.779	0.813	EXPERIMENT RECORD % Dev.	
1.084	0.877	0.795	0.794		
-1.2	-0.9	2.1	-2.3		
1.221	0.903	0.241	0.850	0.965	
1.187	0.900	0.236	0.837	0.963	
-2.8	-0.3	-2.1	-1.5	-0.2	
1.425	1.180	1.050	1.103	1.191	1.310
1.447	1.172	1.079	1.102	1.194	1.402
1.5	-0.7	2.8	-0.1	0.2	7.0

FIGURE 10.4.1 Comparisons of Power Distributions and Absorption Rates in a Dodewaard Assembly Containing Gadolinium (From Ref. 16)

FIGURE 10.4.2 Power Distribution in Mühleberg
Gd-Assembly GED-01, End-of Cycle 1C

11. REFERENCES

- (1) T.O. Sauar, S. Børresen, J. Haugen, E. Nitteberg, H.K. Næss, T. Skardhamar: "A Multilevel Data-Based Computer Code System for In-Core Management in Light Water Reactors"; Proc. 4th UN Int. Conf. IAEA, A/Conf. 49/P/293, 2, 645 (1972).
- (2) S. Børresen: "A Simplified, Coarse Mesh, Three-Dimensional Diffusion Scheme for Calculating the Gross Power Distribution in a Boiling Water Reactor"; Nucl. Sci. Eng., 44, 37 (1971).
- (3) S. Børresen, L. Moberg, J. Rasmussen: "Methods of PRESTO, A Three-Dimensional BWR Core Simulation Code"; Topical Report to NRC (1982).
- (4) S. Børresen, T. Skardhamar, S.E. Wennemo-Hanssen: "Applications of FMS-RECORD/PRESTO for Analysis and Simulation of Operating LWR Cores"; Proceedings NEACRP Specialists' Meeting on Calculation of 3-Dimensional Rating Distributions in Operating Reactors, Paris Nov. 1979, NEA-OECD publication (1980).
- (5) L. Moberg, J. Rasmussen, T.O. Sauar, O. Øye: "RAMONA Analysis of the Peach Bottom-2 Turbine Trip Transients"; EPRI-NP-1869, (Research Project 1119-2), Final Report (June 1981).
- (6) T. Skardhamar, et al: "RECORD Program Description"; FMS Documentation System, Vol. 2 (User Manual), (1972 - present).
- (7) T. Skardhamar: "Summary Description and Main Features of the RECORD Code"; IFA Internal Report, PP-363 (1977).
- (8) T. Skardhamar: "RECORD Program Description, Its Overlays and Segments, and General Flow Charts"; IFA Internal Report (Confidential) (1978).
- (9) M. Hron: "Calculations of Thermal Neutron Group Constants during Burnup of Light-Water-Moderated Lattices"; Nucl. Sci. Eng. 45, 230 (1971).
- (10) B. Fredin, T. Boševski, M. Mataušek: "Discrete Energy Representation of Thermal-Neutron Spectra in Uranium-Plutonium Lattices"; Nucl. Sci. Eng. 36, 315 (1969).
- (11) H. Nelkin: "Scattering of Slow Neutrons by Water"; Phys. Rev. 119, 741 (1960).
- (12) R.J.J. Stamm'ler, O.P. Tverbakk, Z. Weiss, J.M. Døderlein: "DATAPREP-II. A Reactor Lattice Homogenization and BIGG-II Data Preparation Computer Code"; Kjeller Report, KR-78 (1964).
- (13) O.P. Tverbakk, J.M. Døderlein: "BIGG-II. A Multigroup Neutron Spectrum and Criticality Code"; Kjeller Report, KR-75 (1965).
- (14) H.C. Honeck: "The Distribution of Thermal Neutrons in Space and Energy in Reactor Lattices. Part I. Theory"; Nucl. Sci. Eng., 8, 193 (1960).

- (15) R.J.J. Stamm'ler: "K-7 THERMOS, Neutron Thermalization in a Heterogeneous Cylindrically Symmetric Reactor Cell"; Kjeller Report, KR-47 (1963).
- (16) K. Haugset, H.K. Næss, T. Skardhamar, P. Brand: "Analysis of BWR Fuel Assemblies Containing Gadolinium as Burnable Poison"; Trans. Am. Nucl. Soc., 16, 283 (1973).
- (17) S. Børresen: "Application of Effective Boundary Conditions to B₄C Cluster Control Calculations"; Nukleonik 12, 124 (1969), and later extensions of method described in internal reports.
- (18) K. Bendiksen: "Treatment of Ag-In-Cd Cluster Control Rods in the Code ALFA"; IFA Work Report, PP-353 (1976).
- (19) G.E. Fladmark: "MD-2 Specification. Mathematical and Numerical Techniques"; IFA Work Report, PM-151 (1970).
- (20) K. Bendiksen, T. Skardhamar: "Processing Effective Fission Product Data from the ENDF/B Data File"; Seminar on Nuclear Data Processing Codes, Ispra, Dec. 1973, NEA Computer Program Library, Newsletter No. 16 (1974).
- (21) W.K. Bertram, et al: "A Fission Product Group Cross-Section Library"; AAEC/E214 (1971).
- (22) E. Patrakka, R. Terasvirta: "ETOF, A Program to Process Data from ENDF/B to FORM"; Technical Research Center of Finland, Nuc. Eng. Lab., Report 5 (1973).
- (23) R. Dannels, D. Kusner: "ETOM-1 - A FORTRAN-IV Program to Process Data from the ENDF/B File to the MUFT Format"; WCAP-3688-1 (1968).
- (24) H.D. Brown, D.S. St. John: "Neutron Energy Spectrum in D₂O"; DP-33 (1954).
- (25) A. Tas, A.W. den Houting: "A Programme for the Calculation of Thermal Group Constants by Means of Converting the Energy and Space Dependent Integral Transport Equation into an Energy Dependent One"; RCN Report, RCN-95 (1968).
- (26) R.J.J. Stamm'ler: "Fast Methods for Computing Thermal Neutron Group Constants in Single-Pin Lattice Cells"; Dr. Thesis (1968).
- (27) R.J.J. Stamm'ler, S.M. Takač, Z.J. Weiss: "Neutron Thermalization in Reactor Lattice Cells: An NPY-Project Report"; Tech. Report Series No. 68, IAEA, Vienna (1966).
- (28) M. Mataušek: "Calculation of Multipoint Data for Thermal Neutron Spectra Determination"; IBK-714, Boris Kidric Institute of Nuclear Sciences, Beograd-Vinča (1968).
- (29) M.M. Levine: "Resonance Integral Calculations for U²³⁸ Lattices"; Nucl. Sci. Eng. 16, 271 (1963).
- (30) G.A.G. de Coulon, L.D. Gates, W.R. Worley: "SSCR Basic Physics Program - Theoretical Analysis, Part II, BPG Computer Program Report". BAW-1230, Babcock & Wilcox Co. (1962).

- (31) Brown Ferry Nuclear Power Station, Units 1, 2, and 3. Final Safety Analysis Report, Amendment 21; Docket-50259-38, Tennessee Valley Authority (1972).
- (32) E. Hellstrand: "Measurements of the Effective Resonance Integral in Uranium Metal and Oxide in Different Geometries"; Journ. Appl. Physics, 28, 1493 (1957).
- (33) A Sauer: "Approximate Escape Probabilities"; Nucl. Sci. Eng. 16, 329 (1963).
- (34) A. Mockel: "Reflection and Transmission by a Strongly Absorbing Slab"; Nucl. Sci. Eng. 22, 339 (1965).
- (35) D. Schiff, S. Stein: "Escape Probability and Capture Fraction for Gray Slabs"; WAPD-149 (1956).
- (36) A.F. Henry: "A Theoretical Method for Determining the Worth of Control Rods"; WAPD-218 (1959).
- (37) S. Børresen: "Cylindrical Absorbers in the Code ALFA"; IFA Work Report, PP-324 (1969).
- (38) G.W. Stuart, R.W. Woodruff: "Methods of Successive Generations"; Nucl. Sci. Eng. 3, 339 (1958).
- (39) W.J. Eich, H.T. Williams, H. Aisu: "The Analytic Representation of Rod Cluster Control Elements in Nuclear Design Calculations"; WCAP-3269-38 (1964).
- (40) B.W. Crawford, et al: "Flux Depression in a Parallel Array of Cylindrical Absorbers"; KAPL-P-3460 (1968).
- (41) K. Bendiksen: "Current-to-Flux Ratios for Slab Absorbers with Clad"; IFA Work Report, PP-348 (1975).
- (42) S. Stein: "Resonance Capture in a Heterogeneous System"; WAPD-139 (1955).
- (43) R.S. Varga: "Matrix Iteration Analysis"; Englewood Cliffs, New Jersey, Prentice-Hall, Inc. (1962).
- (44) E.L. Wachspress: "Iterative Solution of Elliptic Systems"; Englewood Cliffs, New Jersey, Prentice-Hall, Inc. (1966).
- (45) R. Froehlich: "A Theoretical Foundation for Coarse Mesh Variational Techniques"; General Atomic Division, General Dynamics, GA-7870 (1967).
- (46) K. Bendiksen: "Fission Product Poisoning in Thermal Reactors"; IFA Work Report, PP-318 (1973).
- (47) T.R. England: "CINDER - A One Point Depletion and Fission Product Program"; WAPD-TM-334 (Revised), (1964).
- (48) R.J. Tuttle: "Delayed-Neutron Data for Reactor Physics Analyses"; Nucl. Sci. Eng. 56, 37 (1975).

- (49) E. Andersen, J.O. Berg, J.M. Døderlein: "Reactor Physics Studies of H₂O/D₂O-moderated UO₂ Cores: A NORA Project Report"; Tech. Report Series No. 67, IAEA, Vienna (1966).
- (50) E. Andersen, et al: "Topics in Light Water Reactor Physics: Final Report of the NORA Project"; Tech. Report Series No. 113, IAEA, Vienna (1970).
- (51) H. Finnvik, et al: "Program MD-1, a One-Dimensional Multigroup Diffusion Code"; IFA Work Report, PM-154 (1970).
- (52) P.W. Davison, et al: "Yankee Critical Experiments - Measurements on Lattices of Stainless Steel Clad Slightly Enriched Uranium Dioxide Fuel Rods in Light Water"; YAEC-94 (1959).
- (53) W.J. Eich, et al: "Reactivity and Neutron Flux Studies in Multi-region Loaded Cores"; WCAP-1433 (1961).
- (54) V.E. Grob, et al: "Multi-Region Reactor Lattice Studies. Results of Critical Experiments in Loose Lattices of UO₂ Rods in H₂O"; WCAP-1412 (1960).
- (55) J.R. Brown, et al: "Kinetic and Buckling Measurements on Lattices of Slightly Enriched Uranium and UO₂ Rods in Light Water"; WAPD-176 (1958).
- (56) T.C. Engelder, et al: "Measurements and Analysis of Uniform Lattices of Slightly Enriched UO₂ Moderated by D₂O - H₂O Mixtures"; BAW-1273 (1963).
- (57) L.G. Barrett, et al: "Exponential Experiments at Elevated Temperatures on Lattices Moderated by D₂O - H₂O Mixtures"; BAW-1233 (1962).
- (58) V.O. Uotinen, et al: "Lattices of Plutonium-Enriched Rods in Light Water - Part I: Experimental Results"; Nucl. Technol., 15, 257 (1972).
- (59) R.C. Liikala, et al: "Lattices of Plutonium-Enriched Rods in Light Water - Part II: Theoretical Analysis of Plutonium-Fueled Systems"; Nucl. Technol., 15, 272 (1972).
- (60) P. Mohanakrishnan, H.C. Huria: "Reactivity Prediction of Uniform PuO₂-UO₂-Fueled Lattices and Pu(NO₃)₄ Solutions in Light Water"; Nucl. Sci. Eng., 68, 2 (1978).
- (61) R.J. Nodvik: "Evaluation of Mass Spectrometric and Radiochemical Analysis of Yankee Core I Spent Fuel"; WCAP-6068 (1966).
- (62) R.J. Nodvik, et al: "Supplementary Report on Evaluation of Mass Spectrometric and Radiochemical Analysis of Yankee Core-I Spent Fuel, including Isotopes of Elements Thorium through Curium"; WCAP-6086 (1969).
- (63) M.B. Cutrone, G.F. Valby: "Gamma Scan Measurements at Quad Cities Nuclear Power Station, Unit 1, Following Cycle 2"; EPRI NP-214 (1976).
- (64) N.H. Larsen, G.R. Parkos, O. Raza: "Core Design and Operating Data

for Cycles 1 and 2 of Quad Cities 1", EPRI NP-240 (1976).

- (65) S.L. Forkner: Tennessee Valley Authority; Private Communication.
- (66) J. Nitteberg, J. Haugen, J. Rasmussen, T.O. Sauar: "A Core-Follow Study of the Dodewaard Reactor with the Three-Dimensional BWR Simulator, PRESTO"; Kjeller Report, KR-145 (1971).
- (67) S. Børresen, H.K. Næss, T.O. Sauar, T. Skardhamar, F. Grandchamp, J. Rognon, R. Wehrli, C. Weigel: "Core-Follow Study of the Mühleberg BWR with the Fuel Management System - FMS"; ENC, Paris (April 1975).
- (68) S. Børresen, D.L. Pomeroy, E. Rolstad, T.O. Sauar: "Nuclear Fuel Performance Evaluation"; EPRI NP-409, Final Report (June 1977).
- (69) H. Guyer, H. von Fellenberg, W. Wiest: "Core Simulation and Its Experimental Verification of the Mühleberg BWR"; ENC-79, Hamburg, TANSO 31, 225 (1979).
- (70) W. Wiest, H. Hofer, N. Naula, C. Weigel, R. Wehrli: "Gamma-Scanning im KKM und dessen Anwendung bei der Reaktorsimulation"; presented at Reaktortagung 1978, Deutsches Atomforum e.V., Hannover (1978).

A P P E N D I X A

Breit-Wigner Formula for Cross-Section Calculations

BREIT-WIGNER FORMULA FOR CROSS-SECTION CALCULATIONS

Cross-sections in the RECCRD Library are calculated, where appropriate, from resonance parameters in ENDF/B-III, applying the single-level Breit-Wigner formula:

$$\sigma_{n\gamma}^{\lambda}(E) = \sum_{\lambda} \sigma_{n\gamma}^{\lambda}(E), \quad (\text{A.1.1})$$

where

$$\sigma_{n\gamma}^{\lambda}(E) = \sum_J g_J \cdot \sum_r \sigma_{o,r} \left(\frac{\Gamma_{\gamma r}}{\Gamma_r} \right) \cdot \frac{1}{4(E'_r - E)^2 / \Gamma_r^2 + 1} \quad (\text{A.1.2})$$

without Doppler broadening, and

$$\sigma_{n\gamma}^{\lambda}(E) = \sum_J g_J \sum_r \sigma_{o,r} \left(\frac{\Gamma_{\gamma r}}{\Gamma_r} \right) \cdot \psi(\xi_r, X_r) \quad (\text{A.1.3})$$

when Doppler broadening is included, and where

$$\sigma_{o,r} = \frac{4\pi}{k^2} \cdot \frac{\Gamma_{nr}}{\Gamma_r} \quad (\text{A.1.4})$$

$$\Gamma_{nr} = \Gamma_{nr}(E) = \frac{P_{\lambda}(E) \Gamma_{nr}(|E_r|)}{P_{\lambda}(|E_r|)} \quad (\text{A.1.5})$$

$$\Gamma_r = \Gamma_{nr}(E) + \Gamma_{\gamma r} (+\Gamma_{fr}) \quad (\text{A.1.6})$$

$$E'_r = E_r + \left[\frac{S_{\lambda}(|E_r|) - S_{\lambda}(E)}{2P_{\lambda}(|E_r|)} \right] \Gamma_{nr}(|E_r|) \quad (\text{eV}) \quad (\text{A.1.7})$$

and

$\Gamma_{\gamma r}, \Gamma_{fr}$ are the capture and fission widths, assumed to be energy-independent.

The penetration factors S_ℓ and P_ℓ are given by

$$a \left[\frac{dW_\ell^{(+)} / dr}{W_\ell^{(+)}} \right]_{r=a} \equiv S_\ell + i P_\ell \quad (\text{A.1.8})$$

$$a \left[\frac{dW_\ell^{(-)} / dr}{W_\ell^{(-)}} \right]_{r=a} \equiv S_\ell - i P_\ell \quad (\text{A.1.9})$$

where

$W_\ell^{(-)}$, $W_\ell^{(+)}$ are the "incoming" and "outgoing" parts of the radial wavefunction; here

$$W_\ell^{(+)}(kr) = n_\ell(kr) + i j_\ell(kr) \quad (\text{A.1.10})$$

$$W_\ell^{(-)}(kr) = n_\ell(kr) - i j_\ell(kr) \quad (\text{A.1.11})$$

j_ℓ , n_ℓ are spherical Bessel functions of 1st and 2nd order, and

a is the channel radius, equal to the effective scattering radius in the calculation of phase shifts, ϕ_ℓ , otherwise given by

$$a = (1.23M^{1/3} + 0.8) * 10^{-1} \text{ (cm}^{-12}\text{)}$$

For positive energy channels

$$S_0 = 0, S_1 = \frac{-1}{1 + (ka)^2}, \dots$$

$$P_0 = ka, P_1 = \frac{(ka)^3}{1 + (ka)^2}, \dots$$

$$k = 2.19685 \cdot 10^{-3} \left(\frac{M}{M+1.00867} \right) \sqrt{E} \text{ (barns)}^{-\frac{1}{2}}$$

E = neutron energy (eV) in the lab. system.

M = atomic weight of the isotope in the $C^{12}=12$ scale.

$$g_J = \frac{2J + 1}{2(2I + 1)}$$

Line shape Doppler functions are defined by:

$$\psi(\xi_r, X_r) = \frac{\xi_r}{\sqrt{4\pi}} \int_{-\infty}^{\infty} \frac{\exp(-(x_r - y_r)^2 \cdot \xi_r^2/4)}{1 + y_r^2} dy_r \quad (\text{A.1.12})$$

$$\chi(\xi_r, X_r) = \frac{\xi_r}{\sqrt{4\pi}} \int_{-\infty}^{\infty} \frac{2y_r \cdot \exp(-(x_r - y_r)^2 \cdot \xi_r^2/4)}{1 + y_r^2} dy_r \quad (\text{A.1.13})$$

where

$$\xi_r^2 = \frac{\Gamma_r^2 \cdot M}{4 |E' - E_r^e| K \cdot T}$$

T = temperature (Kelvin)

K = Boltzmann's constant

$$X_r = 2(E' - E_r^e) / \Gamma_r$$

$$Y_r = 2(E' - E_r^i) / \Gamma_r$$

E' = the neutron energy in a system where the absorber nucleus is at rest.

For a resonance at a negative energy, E_r , the neutron width is specified at the energy $|E_r|$. A numerical method is used to solve Equations A.1.12 and A.1.13.

In calculating cross-sections from the Breit-Wigner formalism for the RECORD Library, the 220 m/s value for a given nuclide was compared with the recommended value given in the ENDF/B-file, and whenever an exact agreement was not obtained, a 1/v-correction compensating the difference was added.

Elastic Scattering:

If resonance parameters are given in the ENDF/B-III file, point values for scattering cross sections are calculated from the single-level Breit-Wigner formula:

$$\sigma_{nn}(E) = \sum_l \sigma_{nn}^l$$

(A.1.14)

$$\begin{aligned}
 \sigma_{\text{hn}}^{\ell}(E) = \sum_{\text{J}} g_{\text{J}} \sum_{\text{r}} \left[\frac{\Gamma_{\text{n,r}}}{P_{\text{r}}} \sigma_{\text{o,r}} \cdot \psi(\xi_{\text{r}}, X_{\text{r}}) + \left(\sigma_{\text{o,r}} \cdot \sigma_{\text{p}}^{\ell} \cdot \frac{\Gamma_{\text{n,r}}}{\Gamma_{\text{r}}} \right)^{\frac{1}{2}} \cdot \right. \\
 \left. \chi(\xi_{\text{r}}, X_{\text{r}}) \right] + \sigma_{\text{p}}^{\ell}
 \end{aligned}
 \tag{A.1.15}$$

where the potential scattering cross-section is given by:

$$\sigma_{\text{p}}^{\ell} = \frac{4\pi}{k^2} (2\ell + 1) \sin^2 \phi_{\ell}
 \tag{A.1.16}$$

and all other symbols have been defined before.

A P P E N D I X B

Output Options in the RECORD Code

OUTPUT OPTIONS IN THE RECORD CODE

1. Main fuel assembly data (need not be requested, is always obtained).
2. Burnup distribution in fuel assembly (for non-zero burnup).
3. Power map (pin-power relative to unit average power).
4. Power density distribution (for non-zero average power).
5. Thermal mesh point flux distribution.
6. Thermal absorption rates for all lattice cells.
7. Group absorption rates for all groups and regions.
8. Group production rates for all groups and lattice cells.
9. Regionwise macroscopic group constants for all groups and regions.
10. Water gap data, flow box data and alpha values for control absorber (if calculated by code).
11. Region division of fuel assembly cell, mesh point coordinates, and composition map.
12. Number densities of fuel isotopes in each fuel pin.
13. Fuel inventory (wt % U^{235} , U^{236} , Pu^{239} , Pu^{240} , Pu^{241} and Pu^{242} , in each fuel pin.)
14. Neutron balance (two-group scheme).
15. Thermal flux ratios in each burnable poison and surrounding lattice cells (for use in THERMOS - GADPOL).

A P P E N D I X C

Excerpts from RECORD Output

RECORD 01-4 OUTPUT RE-SA 1 0 UWR SAMPLE PROBLEM

AVERAGE BURNUP = 6000. MWD/TU 10.400 W/GM, VOID .400, FP POIS , BURN. POIS.

MAIN FUEL ASSEMBLY DATA

(<1 ITNS. IN DIFF. CALC.)

K-INFINITY = 1.17325 K-EFFECTIVE = 1.10663
POWER PEAKING FACTOR = 1.0891
MAXIMUM LINEAR LOADING = 141.956 WATTS/CM AT PIN NO. 41
MAXIMUM POWER DENSITY = 20.005 WATTS/GM-U AT PIN NO. 41
MAXIMUM BURNUP = 6873. MWD/TU AT PIN NO. 40
TIP REGION: FISSION RATE = .14128E-07
AV. THERMAL FLUX = .43609E+14
AV. FAST FLUX = .10457E+15

AVERAGE FUEL COMPOSITION:

Table with 2 columns: GM/CM FUEL ASSEMBLY and WEIGHT PER CENT. Rows include isotopes U235, U236, U238, NP239 and plutonium isotopes PU239, PU240, PU241, PU242.

ACCUMULATED FISSIONABLE PLUTONIUM = .1031E+01 GM/CM

AVERAGE MACROSCOPIC GROUP DATA AND FLUXES FOR FUEL ASSEMBLY CELL

Table with 7 columns: GROUP, DIFF, SIGR, SIGA, NY+SIGF, SIGF, FLUX. Rows include groups 1, 2, 3, 4, 5, FAST, and THERMAL.

AVERAGE THERMAL FLUX = .3613E+14 NEUTR/CM**2/SEC

Excerpt from RECORD Output Listing - Main Fuel Assembly Data

RECORD 81-4 OUTPUT RE-SA 1 0 BWR SAMPLE PROBLEM
 AVERAGE BURNUP = 6000. MWD/TU 18.460 W/GM, VOID .400, FP POIS , BURN. POIS.

BURNUP DISTRIBUTION IN FUEL ASSEMBLY (IN MWD/TU PER PIN)

MAXIMUM BURNUP = 6873. MWD/TU AT PIN NO. 48

1	0109	6511	6230	6198	6283	6048	6200	6637
1	6511	4057	5370	5456	5411	4181	6514	6764
1	6230	5370	5375	5505	5409	5488	6247	6502
1	6198	5456	5505	*****	5533	5539	6224	6440
1	6283	5411	5409	5533	5434	5518	6287	6543
1	6048	4181	5488	5539	5518	4239	6641	6873
1	6200	6514	6247	6224	6287	6641	6341	6804
1	6657	6704	6502	6440	6543	6873	6804	6365
1	0109	6511	6230	6198	6283	6048	6200	6637
1	6511	4057	5370	5456	5411	4181	6514	6764
1	6230	5370	5375	5505	5409	5488	6247	6502
1	6198	5456	5505	*****	5533	5539	6224	6440
1	6283	5411	5409	5533	5434	5518	6287	6543
1	6048	4181	5488	5539	5518	4239	6641	6873
1	6200	6514	6247	6224	6287	6641	6341	6804
1	6657	6704	6502	6440	6543	6873	6804	6365
1	0109	6511	6230	6198	6283	6048	6200	6637
1	6511	4057	5370	5456	5411	4181	6514	6764
1	6230	5370	5375	5505	5409	5488	6247	6502
1	6198	5456	5505	*****	5533	5539	6224	6440
1	6283	5411	5409	5533	5434	5518	6287	6543
1	6048	4181	5488	5539	5518	4239	6641	6873
1	6200	6514	6247	6224	6287	6641	6341	6804
1	6657	6704	6502	6440	6543	6873	6804	6365

PIN NOS. 1 TO 8
 PIN NOS. 9 TO 16
 PIN NOS. 17 TO 24
 PIN NOS. 25 TO 32
 PIN NOS. 33 TO 40
 PIN NOS. 41 TO 48
 PIN NOS. 49 TO 56
 PIN NOS. 57 TO 64

***** REMARKS WATER HOLE

Excerpt from RECORD Output Listing - Burnup Distribution

RECORD 81-4 OUTPUT RE-5A 1 1 BWR SAMPLE PROBLEM, RESTART AT 6000 MWD/TU

AVERAGE BURNUP = 6000. MWD/TU

18.460 W/GM, VOID .400, FP PGIS, C-ROD IN, BURN. PGIS.

NEUTRON BALANCE - TWO GROUP SCHEME, THERMAL CUT OFF AT 1.04 EV (NORMALISED TO TOTAL PRODUCTION = 100000)

REGION / MATERIAL	ABSORPTION RATE			SLOWING DOWN RATE	PRODUCTION RATE		
	THERMAL	EPITH.	TOTAL		THERMAL	EPITH.	TOTAL
FUEL:							
U235	29320	5481	34801	1	60036	8874	68910
U236	14	304	318	0			
U238	6344	21580	27924	54	0	8764	8764
PU239	10673	794	11467	0	20138	1371	21509
PU240	1382	116	1498	0	0	14	14
PU241	329	43	372	0	697	105	802
PU242	0	4	4	0	0	0	0
AM*CM	3	1	4	0	1	0	1
XE135	1723	0	1723	0			
SM149	636	2	638	0			
FISS.P	1070	1120	2190	0			
GAD.	255	15	270	0			
O16	1	186	187	657			
OTHER	4	0	4	0			
TOTAL FUEL	51754	29646	81400	712	80872	19128	100000
CLAD:	385	558	943	70			
MODERATOR (CHANNEL): H2O	2617	325	2942	47253			
WATER HOLES	119	13	132	1965			
WATER GAP:	1645	145	1790	21921			
FLOW BOX WALL:	323	329	652	44			
CONTROL ROD:	15071	12037	27108	0			
ASSEMBLY TOTAL:	71916	43053	114969	71966	80872	19128	100000
THERMAL/EPITH./TOTAL LEAKAGE:	43	593	636				

C-4

Excerpt from RECORD Output Listing - Neutron Balance